HAL open science

Cybernetic driver modeling for the realization of haptic shared control and the adaptation of the human-machine system

Yishen Zhao

To cite this version:

Yishen Zhao. Cybernetic driver modeling for the realization of haptic shared control and the adaptation of the human-machine system. Modeling and Simulation. Ecole nationale supérieure Mines-Télécom Atlantique, 2021. English. NNT : 2021IMTA0245 . tel-03542633v2

HAL Id: tel-03542633

https://hal.science/tel-03542633v2

Submitted on 22 Apr 2022

HAL is a multi-disciplinary open access archive for the deposit and dissemination of scientific research documents, whether they are published or not. The documents may come from teaching and research institutions in France or abroad, or from public or private research centers.

L'archive ouverte pluridisciplinaire **HAL**, est destinée au dépôt et à la diffusion de documents scientifiques de niveau recherche, publiés ou non, émanant des établissements d'enseignement et de recherche français ou étrangers, des laboratoires publics ou privés.

THÈSE DE DOCTORAT DE

L'ÉCOLE NATIONALE SUPERIEURE MINES-TELECOM ATLANTIQUE
BRETAGNE PAYS DE LA LOIRE - IMT ATLANTIQUE

ÉCOLE DOCTORALE N° 601
Mathématiques et Sciences et Technologies
de l'Information et de la Communication
Spécialité : *Automatique, productique et robotique*

Par
Yishen ZHAO

Cybernetic driver modeling for the realization of haptic shared control and the adaptation of the human-machine system

Thèse présentée et soutenue à Nantes, le 20/04/2021
Laboratoire des Sciences du Numérique de Nantes, UMR CNRS 6004
Thèse N° : 2021IMTA0245

Rapporteurs avant soutenance :

Mariana NETTO	Chargée de Recherche HDR, Université Gustave Eiffel
Jean-Christophe POPIEUL	Professeur, Université Polytechnique Hauts-de-France

Composition du Jury :

Président :	Jean-Christophe POPIEUL	Professeur, Université Polytechnique Hauts-de-France
Examinateurs :	David ABBINK	Professeur, Delft University of Technology
	Mariana NETTO	Chargée de Recherche HDR, Université Gustave Eiffel
Dir. de thèse :	Philippe CHEVREL	Professeur, IMT Atlantique
Co-encadrant de thèse :	Franck MARS	Directeur de Recherche, CNRS
	Fabien CLAVEAU	Maître-Assistant, IMT Atlantique

Acknowledgement

First of all, I would like to express my gratitude to my supervisors: Philippe Chevrel, Franck Mars and Fabien Claveau. I would have never accomplished this thesis without their guidance, insight, support and encouragement. It has been a great pleasure to work with them during the past few years. Philippe and Fabien were also my teachers when I was studying for the engineer diploma. Almost all my knowledge in control theory and signal processing comes from them. I would never forget that day when Phillipe and I were walking to the canteen in school, he told me why an extended Kalman filter is needed for identification, and I was shocked by this brilliant idea. Franck opened the gate of human factors for me. His knowledge contributed a lot to this multidisciplinary work. His researches fulfilled my curiosity and extended my vision. I like the monthly seminar organized by his team. Each time I was able to discover some new research topics or ideas.

Secondly, I would like to thank all my colleagues, in particular Béatrice Pano. She did a fascinating work in the development and implementation of haptic guidance system for her thesis and for my research. She helped me with the utilization of driving simulator as well. I enjoyed our occasional exchange about our thesis and problems. Besides, the French proverbs that she taught me were really amusing and relaxing. It is a pity that we are not able to meet in person due to the current pandemic issue. I wish her a great success in her thesis defense. I would also like to thank Denis Creusot for his help in solving problems of the simulator, Paul Loiseau for his advice in Latex writing, Chaouki Nacer Boultifat for his jokes during lunch time and Jeffery Petit for his help of ANOVA. I want to appreciate all the participants who took part in my experiments. It was their help that made this work possible. The Région Pays de la Loire should be appreciated as well for financial support.

Finally, a big thank you should go to my parents and my wife. My parents introduced me the world of science when I was young. I hope that now they are proud of my progress. My wife embraces me with enduring love and encouragement since I decided to do this thesis. She is like the sunshine that enlightens my path and makes my life delightful.

Table of Contents

I Introduction **1**

1 Haptic Shared Control **3**

1.1 Development of Automated Vehicles 3
1.2 Haptic Shared Control 5
1.3 Realization of Haptic Guidance System 7
1.4 Lay-out of Thesis 10
1.5 List of Publications 12
1.6 References 13

2 Driver Model and Adaptation **17**

2.1 State-of-the-art of Driver Steering Model 17
2.1.1 Driver Models Based on Compensation and Preview 18
2.1.2 Driver Models Including Neuromuscular System 21
2.1.3 Challenges and New Trends 25
2.2 Adaptation of Human-Machine System 27
2.3 Objective of Thesis 28
2.4 Main Contributions 30
2.5 References 30

II Methodology **35**

3 Experiment Platform **37**

3.1 Driving Simulator SCANeR 37
3.1.1 Hardware 37
3.1.2 Software 38
3.1.3 Vehicle Model 40
3.2 Haptic Guidance System 41
3.3 References 43

4 Parameter Identification I: Prediction Error Minimization 45
4.1 Introduction 45
4.2 General Procedure of Model Identification 45
4.3 Prediction Error Minimization Method 46
4.4 Practical Use of PEM 48
4.4.1 Identifiability 48
4.4.2 Model Validation 49
4.4.3 Distribution of Parameter Estimates 49
4.5 References 52

5 Parameter Identification II: Unscented Kalman Filter 53
5.1 Introduction 53
5.2 Full article 53
5.2.1 Abstract 53
5.2.2 Introduction 54
5.2.3 Cybernetic Driver Model 55
5.2.4 Parameter Identification 58
5.2.5 Practical Use of UKF 62
5.2.6 Experiments 65
5.2.7 Conclusion 69
5.3 References 71

III Experiments and Results 75

6 Experimental studies 77
6.1 References 85

7 Driving with a Haptic Guidance System in Degraded Visibility Conditions: Behavioral Analysis and Identification of a Two-Point Steering Control Model 87
7.1 Introduction 88
7.2 Experiment 90
7.2.1 Participants 90
7.2.2 Independent Variables 90
7.2.3 Haptic Guidance System 91

7.2.4 Apparatus . . . 93
7.2.5 Scenarios . . . 93
7.3 Data Analysis Methods . . . 94
7.3.1 Driving Metrics . . . 94
7.3.2 Model Identification . . . 95
7.3.3 Validation of Identified Model . . . 97
7.3.4 Summary Diagram . . . 99
7.4 Results . . . 100
7.4.1 Steering Performance . . . 100
7.4.2 Lane Keeping Performance . . . 101
7.4.3 Driver Control Effort . . . 101
7.4.4 Identified Model Validation . . . 103
7.4.5 Anticipatory and Compensatory Gain . . . 105
7.5 Discussion . . . 105
7.5.1 Effect of Fog . . . 106
7.5.2 Effect of Haptic Guidance . . . 107
7.5.3 Synthesis . . . 107
7.6 Conclusion . . . 108
7.7 References . . . 109

8 Towards a Driver Model to Clarify Cooperation Between Drivers and Haptic Guidance Systems 115
8.1 Introduction . . . 115
8.2 Driver Model with Haptic Feedback . . . 117
8.2.1 Two-point Visual Model . . . 118
8.2.2 Neuromuscular Action . . . 118
8.3 Data Acquisition . . . 121
8.3.1 Apparatus . . . 121
8.3.2 Haptic Guidance System . . . 121
8.3.3 Participants . . . 123
8.3.4 Scenarios . . . 123
8.4 Model Parameter Identification . . . 123
8.4.1 Visual Model Identification . . . 123
8.4.2 Driver Internal Model Identification . . . 125

8.4.3 Explicit Haptic Feedback Loop Identification 126
8.5 Results 127
8.5.1 Visual Model with Delay 127
8.5.2 Driver Internal Model 128
8.5.3 Explicit Haptic Feedback Loop 129
8.6 Conclusion 131
8.7 References 132

9 Driver Model Validation through Interaction with Varying Levels of Haptic Guidance 135
9.1 Introduction 135
9.2 Cybernetic Driver Model 137
9.2.1 Structure of the Proposed Cybernetic Model 137
9.2.2 Internal Model 139
9.2.3 Explicit Haptic Feedback Loop 139
9.3 Experiment Setting 140
9.3.1 Apparatus 140
9.3.2 Haptic Guidance System 140
9.4 Validation I: Driver Model Simulation 141
9.4.1 Objective 141
9.4.2 Experiment 141
9.4.3 Results 143
9.5 Validation II: Driver Model Identification 144
9.5.1 Objective 144
9.5.2 Experiment 144
9.5.3 Parameter Identification 145
9.5.4 Results 147
9.6 Conclusion 150
9.7 References 151

IV Conclusion and Perspective 155

10 General Conclusion and Perspectives 157
10.1 General Discussion 157

10.2 Synthesis of Experimental Investigations 158
10.3 Review of Methodology 160
10.3.1 Model-based Analysis 160
10.3.2 System Identification 161
10.3.3 Driving Simulator 161
10.4 Proposition of Future Works 162
10.5 References 164

List of Figures

1.1 Levels of driving automation defined by SAE International (J3016). 4
1.2 Shared control architecture proposed by M. Steele. 6
1.3 Design of haptic guidance system proposed by P. Griffiths. 8
1.4 Design of haptic guidance system proposed by C. Sentouh 8
1.5 Design of haptic guidance system proposed by M. Flad. 9

2.1 Topology of the driver/vehicle system combining open- and closed-loop precognitive, pursuit, and compensatory control structures by D. McRuer. 18
2.2 Block diagram of the two-level model of driver steering behavior by E. Donges. 19
2.3 The driver/vehicle model by R. Hess. 20
2.4 Structure for driver path-following model with neuromuscular dynamics incorporated by A. Pick. 22
2.5 The structure of the driver model by C. Sentouh. 23
2.6 State estimation using multiple models and Kalman filters by N. Kim. . . . 24
2.7 Cybernetic driver model for lane keeping maneuver by L. Saleh. 25
2.8 Proposed framework for understanding the learning and adaptive human controller by M. Mulder. 26

3.1 Fixed-based driving simulator. 37
3.2 SCANeR studio modules concept. 39
3.3 Variables in bicycle model. 40
3.4 Haptic shard control strategy by B. Pano. 42

4.1 Example of two confidence regions 51

5.1 Cybernetic driver model. 56
5.2 Multi-UKF schema. 65
5.3 First experiment in Simulink. 66
5.4 First experiment results. 67

5.5 Second experiment in SCANeR. 68
5.6 Second experiment results. 70

7.2 Design strategy of haptic guidance system. 92
7.3 Route used for experiment. 93
7.4 Inputs of the two point model. 96
7.5 Summary of data analysis methods. 99
7.6 $SWRR$ per minute with gap-size 2°. 100
7.7 Mean of adjusted deviation of the lateral position. 101
7.8 Standard deviation of the deviation of the lateral position. 102
7.9 Driver steering torque energy. 102
7.10 FIT for all participants. 103
7.11 Confidence regions of identified parameters for participant No. 3. 104
7.12 Identified anticipatory gain (K_p). 105
7.13 Identified compensatory gain (K_c). 106

8.1 Cybernetic driver model proposed in previous studies. 116
8.2 Structure of the proposed cybernetic driver model. 118
8.3 Experiment settings. 121
8.4 Design strategy of the haptic guidance system. 122
8.5 Visual model with delay for identification. 124
8.6 Approximation of the far point angle and the near point angle. 125
8.7 Residual of the driver internal model for P1. 129
8.8 Validation of the entire driver model for P1. 131

9.1 Shared control between the human driver and haptic guidance system. . . 136
9.2 Structure of the proposed cybernetic driver model. 137
9.3 Left: fixed-base driving simulator; Right: track used in the first experiment. 140
9.4 Driver model validation with the implemented driver model. 142
9.5 Driver model validation with the identified driver model. 144
9.6 Left: track used in the validation II; Right: variation of the sharing level in the experiment. 145
9.7 Left: measured vs. predicted driver torque of Participant 1; Right: estimated K_I variation of Participant 5. 149
9.8 Mean K_I variation with the three-sigma band of all participants. 150

List of Tables

3.1 Technical specifications of sensors 38
3.2 Description of symbols in the bicycle model. 41

5.1 Description of signals in driver model. 56
5.2 Description of parameters in driver model. 56

7.1 Description of parameters in the model. 96
7.2 Comparison of model parameter uncertainties. 104

8.1 Description of signals in Figure 8.2 119
8.2 Identified visual model. 127
8.3 Identified driver internal model. 128
8.4 Identified explicit haptic feedback model. 130

9.1 Description of signals in Figure 9.2. 138
9.2 Nominal parameter values used in validation I. 142
9.3 Standard deviation of the lateral position of all 16 scenarios. 143

List of Symbols

Vehicle model

β	Slip angle
δ_f	Tyre steering angle
C_f	Front tire stiffness
C_r	Rear tire stiffness
F_w	Wind force
J	Vehicle moment of inertia
l_f	Distance between center of gravity and front axle
l_r	Distance between center of gravity and rear axle
l_w	Distance between center of gravity and wind hit point on vehicle
m	Vehicle mass
r	Yaw rate
v	Vehicle speed
v_x	Vehicle longitudinal speed

Haptic guidance system

α_{ant}	Anticipatory sharing level
α_{comp}	Compensatory sharing level
$\Gamma_{a_{FB}}$	Haptic guidance torque generated by feedback controller
$\Gamma_{a_{FF}}$	Haptic guidance torque generated by feedforward controller

Γ_{ref}	Reference guidance torque generated by feedforward controller
$\rho_{previewed}$	Previewed road curvature in distance
K_{FB}	Static output feedback gain
K_{FF}	Closed-loop transfer function matrix of feedforward controller
Q_z	Weighting matrix used in H_2 criterion
S_{input}	Sensitivity function of the closed-loop driver-vehicle-road system
T_{zw}	Transfer function of the model for optimization
x_{ref}	Reference vehicle-road system states generated by feedforward controller
x_{vr}	Vehicle-road system states

Identification

$\hat{\Theta}_N$	Estimated parameter vector
$\hat{Q}_N$	Estimated parameter covariance matrix
$\hat{y}[k \mid \Theta]$	Predicted output of model parametrized with Θ
$\|x\|_2$	ℓ^2 (Euclidean) norm of sampled signal/vector x
$\mathbb{D}_{\mathcal{M}}$	Subspace of all possible parameter vectors
$\mathbb{R}^n$	Euclidian n-dimensional space
$\mathcal{M}$	Model structure
$\mathcal{Z}^N$	Set of experimental data with N data samples
Θ	Parameter vector
Θ^*	"True" parameter vector
$dim(\cdot)$	Dimension of vector
$e[k \mid \Theta]$	Prediction error of model parametrized with Θ

N	Number of data samples
Q_Θ	Parameter covariance matrix
$u(t)$	Input signal vector
$u[k], y[k]$	Sampled input and output signal vector
$x_n \sim As\chi^2(n)$	Sequence of random variables x_n converges in distribution to the χ^2 distribution with n degrees of freedom
$x_n \sim As\mathcal{N}(\mu, \sigma)$	Sequence of random variables x_n converges in distribution to the normal distribution with mean μ and (co)variance σ
$y(t \mid \Theta)$	Output signal vector depending on Θ

Driver model

δ_d	Target (driver intention) steering wheel angle
δ_{SW}	Steering wheel angle
Γ_a	Haptic guidance torque
Γ_d	Driver steering torque
Γ_{fb}	Haptic feedback torque
Γ_I	Predicted torque from internal model
Γ_s	Self-aligning torque
τ_p	Processing delay
θ_{far}	Far-point (visual anticipation) angle
θ_{near}	Near-point (visual compensation) angle
K_c	Visual compensatory gain
K_p	Visual anticipatory gain
K_r	Internal gain of steering column stiffness

K_t	Gain of stretch reflex
T_I, T_L	Compensation time constant
T_N	Neuromuscular time constant

Acronyms

ACC	Adaptive cruise control
ADAS	Advanced driver-assistance systems
ANOVA	Analysis of variance
ASWS	Active steering wheel system
CoG	Center of gravity
DVR	Driver-vehicle-road
EKF	Extended Kalman filter
EMG	Electromyography
LC-SW	Lateral control and steering-wheel system
LDA	Lane departure avoidance
LPV	Linear parameter varying
NMS	Neuromuscular system
PEM	Prediction error minimization
SAE	Society of automotive engineers
SDLP	Standard deviation of lateral position
SWRR	Steering-wheel reversal rate
UKF	Unscented Kalman filter
UT	Unscented transformation
VR	Vehicle-road

Résumé

Conduire un véhicule fait partie de la vie quotidienne. Pour améliorer la sécurité et le confort de conduite, le développement des systèmes d'assistance à la conduite (ADAS) fait l'objet de nombreuses études ces dernières années. Cette thèse s'inscrit dans le contexte général du développement des véhicules hautement automatisés, prélude aux véhicules autonomes. La problématique concerne plus spécifiquement le développement de systèmes de contrôle partagé du volant entre le conducteur et un automate embarqué.

Le contrôle partagé est une nouvelle modalité d'interaction humain-machine. Contrairement au contrôle traditionnel qui définit souvent l'humain comme un superviseur, le contrôle partagé demande une coopération entre humains et machines sur une interface commune. Cette interface est une façon pour les deux de communiquer leur intention réciproque en termes de contrôle notamment au travers d'un retour haptique. Dans des situations dangereuses ou extrêmes, l'humain peut prendre la décision soit de suivre la consigne proposée par la machine, soit de la négliger. Dans le cas de l'appliquer à la problématique du contrôle de trajectoire pour la conduite, le conducteur et un automate embarqué contrôlent simultanément un volant. Le dispositif aide au contrôle du véhicule en agissant comme un copilote dont l'action augmente graduellement lorsque le véhicule s'écarte de la trajectoire de référence ou de l'action préconisée par la loi de commande. Les bénéfices associés au contrôle partagé s'observent sur des indicateurs de la tâche primaire de conduite, comme le positionnement latéral et le contrôle du volant, mais aussi sur le temps de réaction ou la charge mentale associée à la réalisation de tâches secondaires. Il a aussi été avancé qu'en facilitant la réalisation de la tâche sans prendre totalement le contrôle de la direction, le contrôle partagé permet d'éviter le syndrome de l'humain hors de la boucle.

La réalisation du contrôle partagé haptique dans le contrôle latéral de véhicule demande une connaissance fine du comportement de conducteur. Les questions de recherche fondamentales associées concernent la façon dont l'action de l'automate s'insère de façon fluide dans les boucles sensorimotrices du conducteur. Les problématiques abordées concernent la modélisation du contrôle de la trajectoire chez l'humain comme élément structurant des lois de commande de l'automate, mais aussi l'évaluation de la qualité de

la coopération et les processus adaptatifs mis en jeu par le conducteur au fil de l'usage. Les recherches menées précédemment montrent que l'introduction d'un modèle cybernétique du conducteur dans la synthèse de la loi de commande permet de faire des prédictions sur les trajectoires adoptées spontanément par le conducteur et de les prendre en compte pour la réalisation de l'action.

La modélisation cybernétique du conducteur pour le contrôle latéral de véhicule a commencé dans les années 1950s. Les modèles proposés à cette période étaient hiérarchiques. Il était souvent supposé que la tâche de conduite soit réalisée par une boucle ouverte et une boucle fermée. La boucle ouverte représentait l'anticipation de l'humain, qui lui permet de percevoir et prédire la trajectoire à venir. La boucle fermée représentait la compensation, qui sert à maintenir la position latérale de véhicule dans une voie. La sortie des modèles était toujours l'angle de volant. Néanmoins, aucune évidence ne prouvait que l'humain contrôle un véhicule en angle. En effet, plusieurs recherches dans les années 2000s ont montré la nécessité d'inclure une analyse du système neuromusculaire (NMS) dans le modèle de conducteur pour rendre compte de l'interaction entre le conducteur et le volant. L'hypothèse était alors que le conducteur réalise le contrôle latéral de véhicule en deux étapes. Dans la première, le conducteur génère un angle de volant d'intention à partir de la perception de l'environnement de conduite. Dans la deuxième, il applique cet angle au système de direction via des efforts musculaires. Ces modèles ont contribué à comprendre le rôle du retour haptique dans le contrôle du volant. Pendant ces dernières années, de nouvelles recherches ont pointé plusieurs défauts dans ces voies traditionnelles de la modélisation cybernétique de conducteur. Un des problèmes était que le conducteur était souvent vu comme un système invariant dans le temps. Les modèles obtenus n'étaient valides que pour des cas particuliers. La nature d'apprentissage et d'adaptation de l'humain était négligée. Il a donc été proposé de considérer explicitement ces deux aspects dans la modélisation. Ceci devient l'objective de la nouvelle voie cybernétique à suivre à l'avenir.

Plusieurs études sur l'adaptation de conducteur à l'environnement de conduite, y compris à l'assistance de contrôle partagé, ont été effectuées ces dernières années. Une analyse comportementale était généralement la méthode adoptée dans ces études. Cette méthode statistique consiste à analyser la performance de contrôle latéral en calculant des indicateurs et finalement comparer la valeur moyenne des groupes de test par l'analyse de variance (ANOVA). L'inconvénient de la méthode est que les conclusions des expérimentations sont difficiles à intégrer dans la conception de l'assistance car les indicateurs sont

évalués *a posteriori*. Ils sont incapables de prédire les changements du comportement de conducteur.

En résumé, notre connaissance actuelle sur le comportement de conducteur n'est pas suffisante pour minimiser des conflits entre humaines et automates pendant l'utilisation d'une assistance de contrôle partagé. D'un côté, les modèles cybernétiques considèrent rarement l'adaptation du conducteur. De l'autre côté, les études de l'adaptation ne permettent pas de prédire le comportement du conducteur. Cette constatation a motivé la réalisation de cette thèse. Le travail proposé s'attaquera principalement à l'adaptation réciproque du conducteur et de l'automate au fil de l'usage. Il s'agit de comprendre comment les conducteurs adaptent leur conduite lorsqu'ils interagissent de façon prolongée avec l'assistance.

Deux méthodes ont été adoptées dans cette thèse pour atteindre ces objectifs. La première était l'analyse comportementale comme dans les recherches précédentes. La deuxième était l'analyse par modèle de conducteur, qui est la contribution principale de cette thèse. Cette méthode cherche à observer l'adaptation de conducteur au changement de la condition de conduite avec les modèles, sous la forme d'une variation paramétrique ou structurelle. Une variation structurelle peut être transformée à une variation paramétrique en reconsidérant la structure du modèle et représentant explicitement le processus d'adaptation par des paramètres. Finalement, une variation paramétrique peut être capturée en appliquant un algorithme d'identification de système. Avec cette méthode, il est possible d'alimenter la modélisation de conducteur avec les résultats issus de l'analyse comportementale. Il est aussi possible d'obtenir un modèle qui permet de prédire le comportement adaptatif de conducteur, et enfin de contribuer à la conception de l'assistance de contrôle partagé.

Pour réaliser les identifications, deux algorithmes ont été utilisés dans cette thèse. Pour un modèle linéaire invariant, la méthode de minimisation de l'erreur de prédiction (PEM) a été choisie. L'incertitude paramétrique a été notamment considérée pendant l'application de cet algorithme afin de s'assurer que la différence entre les paramètres identifiés était bien la conséquence de l'adaptation. Pour un modèle linéaire variant, la méthode du filtre de Kalman sans parfum a été choisie. L'idée principale de cet algorithme est d'utiliser le filtre de Kalman pour estimer en même temps les états du système et les paramètres à identifier. Il faut d'abord augmenter le système avec les paramètres en supposant une certaine dynamique paramétrique. Un filtre de Kalman sans parfum est ensuite appliqué au système augmenté qui devient non-linéaire à cause de la multiplication entre les pa-

ramètres et les états. Une stratégie pour la configuration du filtre a été proposée dans cette thèse. Un compromis sur l'estimation entre la rapidité et la précision est inévitable. Une approche alternative en mettant en place plusieurs filtres en parallèle avec différentes configurations a finalement été proposée afin de comparer l'estimation paramétrique obtenue. Ces résultats ont été publiés et communiqués dans la conférence internationale IFAC Linear Parameter Varying Systems (LPVS).

Les expérimentations dans cette thèse ont été réalisées sur le simulateur de conduite du laboratoire LS2N. Cette plateforme met à disposition plusieurs dispositifs à contrôler. La scène visuelle est restituée sur trois écrans LCD couvrant 115° d'angle visuel. Le volant est équipé d'un système de direction active qui permet la production de retours de force réalistes. Le logiciel SCANeR Studio a une architecture modulaire permettant le chargement d'environnements routiers variés et le développement et l'évaluation d'assistances à la conduite intervenant directement dans le contrôle du véhicule. De nombreuses données relatives au véhicule, à la situation de conduite et au comportement du conducteur peuvent être enregistrées.

Les investigations expérimentales ont été menées progressivement selon les résultats de l'analyse par modèle de conducteur. Ces résultats sont regroupés dans trois articles soumis ou publiés. Le point de départ était de vérifier la faisabilité de l'analyse par modèle de conducteur dans les conditions du guidage haptique et de la visibilité. Un modèle de deux points a été choisi dans l'analyse. La conclusion nous a indiqué la nécessite d'un système neuromusculaire dans le modèle de conducteur pour bien distinguer le comportement de l'humain et de l'automate. Néanmoins, le rôle du retour haptique n'est jamais pris en compte dans les modèles à disposition. Un nouveau modèle cybernétique a donc été proposé ensuite. Finalement, l'adaptation de l'humain à l'assistance de conduite au niveau de partage variant a été capturée par ce modèle après deux tests de validation.

Le premier article cherche à vérifier dans quelle mesure un modèle simple et robuste, tel que celui utilisé pour rendre compte du contrôle latéral de véhicule à base de vision (i.e., le modèle visuel à deux points), est susceptible d' « expliquer » au travers de ses paramètres, le comportement du système conducteur-assistance haptique en fonction du guidage haptique ou de la visibilité. Dans ce travail, nous avons choisi d'étudier le comportement du système « contrôle latéral - volant » (CL-volant). Précisément, et selon le cas de figure, le CL comprend le conducteur seul pour la conduite manuelle, le conducteur et l'assistance pour la conduite en mode contrôle partagé. La visibilité et l'assistance de conduite ont été choisies en tant que deux variables indépendantes à manipuler pendant

l'expérimentation. Un brouillard a été implémenté pour réduire la visibilité. 15 sujets ont participé à cet essai. Leur performance du contrôle de véhicule a été évaluée par les deux analyses proposées. Deux paramètres dans le modèle de deux points, le gain anticipatoire et le gain compensatoire, ont été choisis comme paramètres à identifier dans l'analyse par modèle. La synthèse sur le résultat des analyses montrait que le modèle identifié permet de rendre en compte l'effet cumulatif de la visibilité et l'assistance de conduite. Le gain anticipatoire est sensible à tous les changements dans le contexte routier qui impacte directement le profil du trajet. Le gain compensatoire est sensible à la réduction de la variation du positionnement latéral. Pourtant, ce modèle ne permet pas de spécifier l'origine de l'influence sur la variation trajectoire au niveau de l'action sur volant. Il est donc nécessaire d'introduire un modèle NMS. Ce papier a été soumis à la revue internationale IEEE Transactions on Human-Machine Systems (THMS).

Un nouveau modèle cybernétique de conducteur a été proposé dans le deuxième article après avoir constaté que les modèles développés dans la littérature ne prenaient pas en compte le retour haptique. Dans ce papier, il a été mis en évidence que dans la plupart des cas, un conducteur ne peut pas distinguer le couple d'auto-alignement et le couple d'assistance. C'est la combinaison des deux qui forme le retour haptique ressenti par conducteur. Le NMS du nouveau modèle prend ce retour haptique comme entrée. Le retour haptique intervient dans l'action neuromusculaire via une voie implicite et une voie explicite. La voie implicite se réfère à l'adaptation paramétrique du modèle interne. Le modèle interne est une estimation approximative de la dynamique du système de direction par humain, qui est représenté par un gain. Il s'agit d'un contrôle en boucle ouverte. La voie explicite est un contrôle en boucle fermée. Elle sert à stabiliser le volant en compensant la dynamique non-prédictible par le modèle interne dans le retour haptique. Le résultat de l'identification nous a montré qu'en changeant le gain du modèle interne, la prédiction du modèle de conducteur est toujours valide que la conduite soit assistée ou pas. Le modèle devenait donc un candidat pour l'étude de l'adaptation à l'assistance de conduite.

Le troisième article cherche à comprendre l'adaptation réciproque du conducteur et de l'automate au fil de l'usage. Nous avons choisi d'étudier l'adaptation de conducteur à une variation du niveau de partage. Le niveau de partage est un coefficient qui permet de régler l'effort total délivré par l'assistance. Deux expérimentations ont été effectuées dans ce papier. L'objectif du premier test était de vérifier si le gain de modèle interne varie suivant le niveau de partage de l'assistance, comme observé dans le deuxième article. Le

test consistait à simuler le nouveau modèle de conducteur en tant que « conducteur virtuel » pour contrôler un véhicule. Le gain de modèle interne et le niveau de partage étaient deux variables indépendantes manipulées. La performance du contrôle latéral réalisé par les conducteurs virtuels et l'assistance à différents niveaux de partage a été évaluée. Le résultat a montré que la meilleure performance est atteinte si et seulement si le gain de modèle interne correspond au niveau de partage. Cette conclusion correspond actuellement au sens donné à ce paramètre, car du point de vue de conducteur, c'est la dynamique du système de direction qui est changé. Le deuxième test a donc été réalisé sur cette base pour essayer de capturer au travers de ce paramètre l'adaptation aux variations du niveau de partage. L'assistance de conduite a été configurée avec une variation de niveau de partage de 0 à 100% puis de 100% à 0. 17 sujets ont participé à cet essai. La variation paramétrique a été identifiée en utilisant l'algorithme du filtre de Kalman sans parfum. Les données de tous les sujets montraient une tendance similaire : lorsque le niveau de partage augmente, le gain de modèle interne diminue, et vice versa. Ce résultat a indiqué que le conducteur s'adapte à la variation du couple d'assistance en ajustant sa représentation interne du système de direction. La conclusion finale était que cette adaptation doit généralement se passer dès que la dynamique du système de direction est modifiée. Le deuxième et troisième article ont été publiés et communiqués dans la conférence internationale IEEE System, Man and Cybernetics (SMC).

En conclusion, cette thèse est une étape intermédiaire dans le développement d'une assistance de conduite en contrôle partagé. Elle répond à la question de l'adaptation réciproque du conducteur et de l'automate au fil de l'usage. Ce travail a été réalisé par la méthode de l'analyse comportemental et des modèles cybernétiques de conducteur. En combinant l'analyse des deux méthodes, nous arrivons non seulement à comprendre le mécanisme de l'adaptation, mais aussi à prédire le comportement adaptatif de conducteur avec le modèle cybernétique proposé. La conclusion finale était que l'adaptation du modèle interne de conducteur entre en jeu lorsque la dynamique du système de direction est modifiée par l'assistance de conduite. Notre conclusion était cohérente avec la littérature, en plus elle a été confirmée et présentée par un modèle cybernétique de conducteur pour la première fois. Cette connaissance est indispensable pour minimiser les conflits pendant la coopération humain-machine. D'ailleurs, notre étude par la modélisation de conducteur et l'algorithme d'identification du système variant est aussi une implémentation réussie de la nouvelle théorie cybernétique.

Ce travail de thèse montre l'adaptation de conducteur lorsque l'effort d'assistance

change. L'assistance de conduite peut rendre en compte ce comportement en incluant le modèle de conducteur dans la synthèse de loi de commande. Il est donc intéressant de savoir la coadaptation entre le conducteur et l'assistance. Il s'agit de déterminer la manière dont l'action de conducteur et de l'assistance arrive à une convergence. Une autre question de recherche possible pour la suite est de modéliser l'apprentissage de conducteur. Ceci demande des expérimentations spécifiques, mais cette connaissance aiderait à profondément comprendre les différents types de processus adaptatifs de l'humain.

Part I

Introduction

Chapter 1

Haptic Shared Control

1.1 Development of Automated Vehicles

Driving has become an essential part of modern life. According to the data of the national institute of statistics and economic (INSEE) in 2017, about 81% of French families have at least one car. However, driving is still a dangerous task. In 2020, the world health organization revealed that approximately 1.35 million people die each year as a result of road traffic crashes in the world. Between 20 and 50 million more people suffer non-fatal injuries, with many incurring a disability as a result of their injury. Road traffic injuries are the leading cause of the death for children and young adults aged 5-29 years. Past researches have found out that human factors contributed to 93% of the crashes investigated[1]. Although the traditional occupant crash protection systems such as seat-belts and airbags can reduce a certain amount of traffic deaths, they are mainly passive and cannot avoid human errors. Based on these facts, development of driver-assisting or highly automated vehicles are getting increasingly studied to improve the security and comfort of driving.

Advanced driver-assistance systems (ADAS) is the key element in the development of automated driving. ADAS are electromechanical systems developed to automate, adapt and enhance vehicle for assisting the driver in multiple driving tasks. These systems offer the potential to significantly reduce or eliminate most vehicle crashes by perceiving a dangerous situation before the crash has occurred and taking action to avoid or mitigate the crash. For example, the adaptive cruise control (ACC) adjusts the vehicle speed; the lane departure avoidance (LDA) alerts the driver when the vehicle is going to leave the lane. In addition to the vehicle security improvement, automated vehicles can also bring other benefits, including a reduction in fuel consumption[2], a wide range of economic benefits[3] etc.

In 2014, the society of automotive engineers (SAE International) published a classification system for automated driving with six levels ranging from fully manual to fully

automated[4] (see Figure 1.1). This classification system is based on the amount of driver intervention and attentiveness. It defines that the human driver still needs to engage in the driving task for automated driving below level 4. At level 0, the driver must directly control the vehicle with the automation system. At level 1 or 2, for certain tasks the driver must constantly monitor the driving environment and supervise the automation system. At level 3, the driver must be prepared for takeover requests.

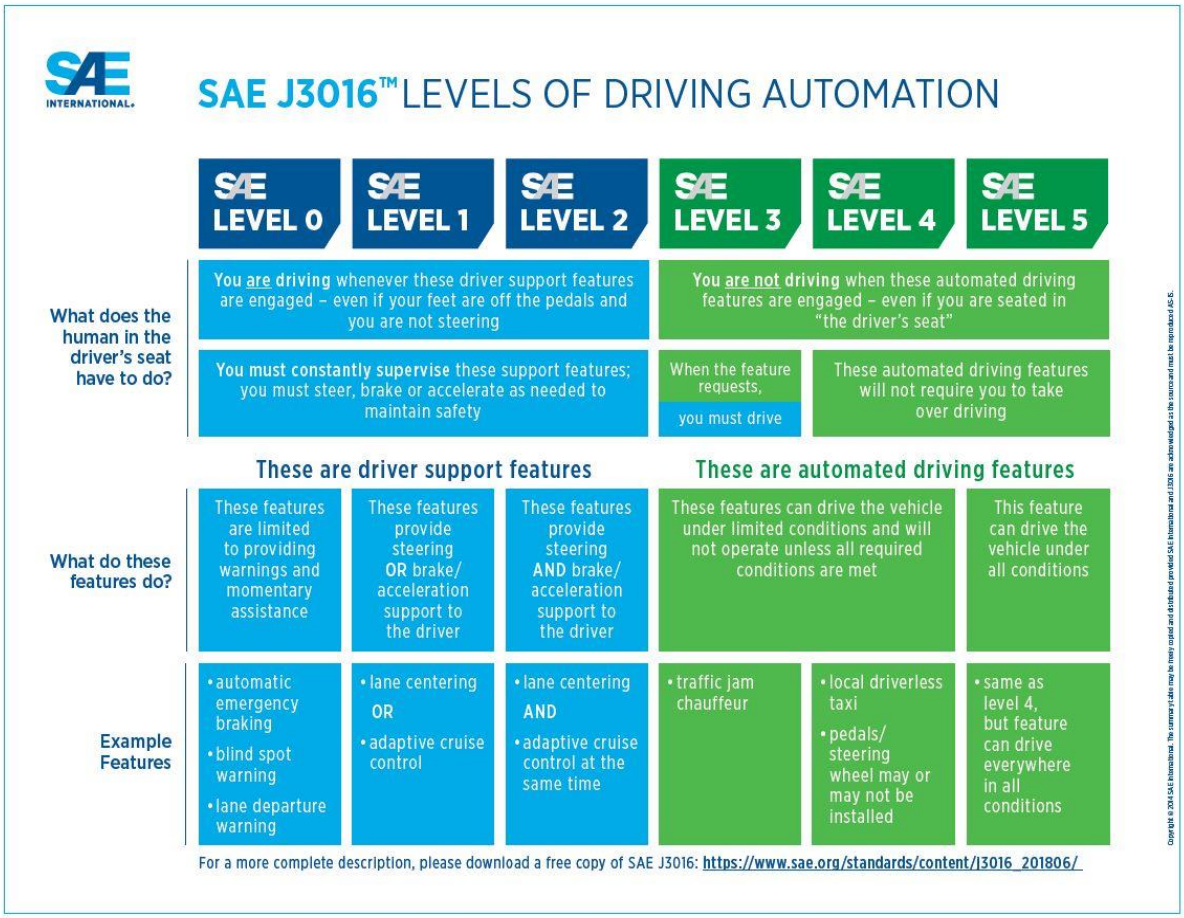

Figure 1.1 – Levels of driving automation defined by SAE International (J3016).

The last decade has witnessed the fast growing and commercialization of ADAS. In addition to academic researches, many vehicle manufacturers such as Renault, BMW and Ford have also proposed and implemented their own solutions. The focus of the ADAS development has moved from low level and driver engaged systems to highly automated and autonomous vehicles. As an example, the Autopilot system from Telsa company integrates a suit of ADAS features including lane centering, traffic-aware cruise control,

self-parking, automatic lane changes etc. It can realize self-driving in almost all conditions under the supervision of human driver. In general, more complex assistance and partly autonomous driving is expected to become a reality within the next few innovation cycles of high-end cars[5].

1.2 Haptic Shared Control

Despite the popularity and the impressive demonstrations of today's automated driving, highly automated and autonomous vehicles still demand time to be mature. A recent research estimates that the widespread deployment of fully automated driving systems that have no safety driver onboard will take at least a decade[6]. At current stage, human still have to stay in the driver's seat and at least supervise the state of ADAS. Apart from technical limitations, there are many other factors motivating the idea that human driver should always keep their hands on steering wheel. For example, there are ethical questions regarding the responsibility in critical situations[7]. From the perspective of human factors, concerns arose in the transitional phase during the human-automation interaction[8]–[10]. Besides, there are also people who claimed that they enjoy driving, and potentially they can drive better than automation[11].

To overcome these barriers and push forward the development of automated vehicles, the cooperative ADAS, which demands continuous interaction between human and automation, caught the attention of researchers. Among different system designs, a new human-machine interaction framework, called *shared control*, has been formulated and intensively studied in past few years. In 2001, Steele and Gillespie proposed a control architecture in which bi-directional information transfer occurs across a control interface, allowing the human to use the interface to simultaneously exert control and extract information[12]. Figure 1.2 shows a general structure of the architecture. Both human driver and controller can interact with the control interface, which could be the steering wheel or the pedals depending on the functionality of the automation system. In the meantime, the control interface provides the driver and the controller with haptic force/torque assistance. It acts as a real "interface" where human and automation system can exchange power with each other and communicate their intention. In addition, human driver is allowed to override the system or give way to it, if it is safe and necessary to do so.

A basic example of the proposed interaction mode can be found in horseback riding, which was introduced as the *H-Metaphor* by Flemisch in 2003[13]. During the riding,

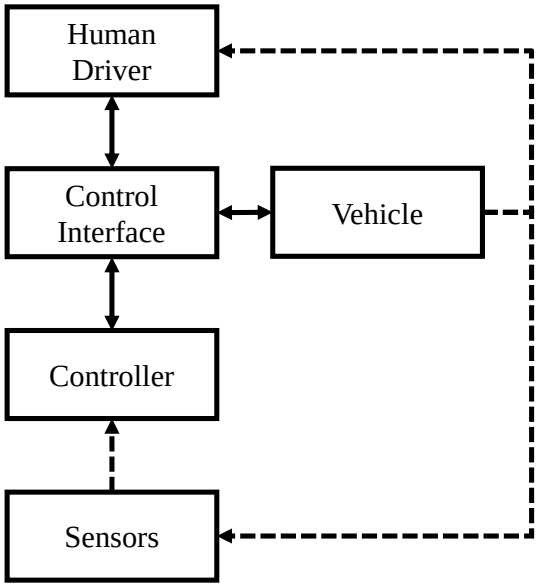

Figure 1.2 – Shared control architecture proposed in [12]. Solid line: power exchange; Dashed line: signal or information exchange.

the rider can execute a secondary task, such as looking around, without paying too much attention to obstacles because the horse instinctively avoids them. The rider has confidence because he or she is always aware of the action taken by the horse through haptic feedback from the saddle and the rein (the control interface). Meanwhile, the horse is also aware of the rider's intention and continuously adjusts its behavior. In a sudden critical situation, the rider can leave control to the horse and let it try to react before it is too late. When the rider aims at a certain destination, he or she can take control of the horse and give a direct command.

Shared control has given rise to a lot of work in recent years, with definitions that are not always homogeneous. The most consensual definition and topology of shared control at present is given in[14]:

> *In shared control, human(s) and robot(s) are interacting congruently in a perception-action cycle to perform a dynamic task, that either the human or the robot could execute individually under ideal circumstances.*

The manual control and fully automated control are not included in this definition because there is no human-machine interaction. Systems in which humans act as a supervisor or a fallback are also excluded because the interaction is not congruent in critical situations. Furthermore, an axiom for shared control is also given in that study:

> *Shared control should link the actions of the human(s) and the robot(s) by combining their efforts toward a final control action, decision, or plan, such that each agent directly perceives how its intent is shaped by the other agent, without having to wait for controlled system dynamics to reveal the outcome of their joint efforts.*

The complete field of shared control in automated vehicles including concepts, categories, algorithms and status of technology has been reviewed in [15] recently. The shared control could be classified in two main modalities: *haptic shared control* and *input-mix shared control*. In the haptic shared control, force feedback is provided on the actuator of a mechanically coupled system. Examples are torque assistance on steering wheel for lane keeping or force assistance on pedals for cruise control and vehicle following. In the input-mix shared control, the automated system complements the input from driver with an additional control signal if necessary. In this case the control interface and the actuator of system is not mechanically coupled. The assistance systems based on steer-by-wire belong to this category. This thesis mainly deals with the haptic shared control in lane keeping task. The driver interacts with the automation system through a motorized steering wheel which is directly connected with vehicle front tires by steering column and other mechanical components. The system applies torque through electric motor while the driver applies torque through the contraction of arm muscles in accordance with the perceived force[16].

1.3 Realization of Haptic Guidance System

The application of haptic shared control in vehicle steering is usually referred as *haptic guidance system* in literature. The design and realization of haptic guidance system have been explored in many researches. Some examples are introduced below.

Griffiths and Gillespie proposed a design for the haptic guidance system as shown in Figure 1.3[17]. A simple human driver model is considered in this design. The model firstly produces a target steering wheel angle θ_h and then converts it to a torque control τ_h on the steering wheel. A motor is used to simulate the self-aligning torque τ_{sa} perceived during driving. It also applies the torque from a controller, τ_c. Human subject experiment with this haptic guidance system revealed that mental workload was reduced and resources made available for secondary, simultaneous tasks. There were also significantly less visual demand and improved performance in a path following task.

Sentouh et al. proposed a two-level cooperative control structure in [18] (see Figure 1.4). In this structure, the control authority between human driver and the steering

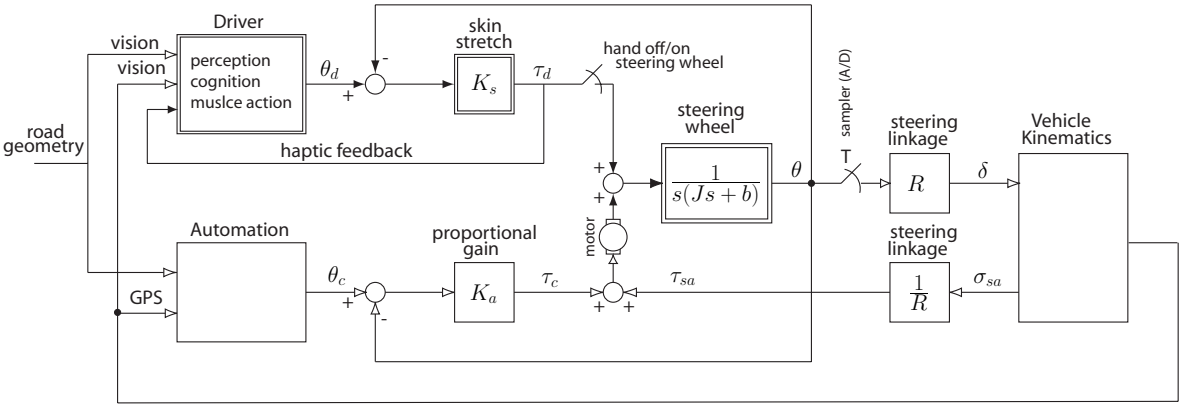

Figure 1.3 – Design of haptic guidance system proposed in [17] © 2004 IEEE. Equation numbers in the "Automation" and "Vehicle Kinematics" boxes are removed.

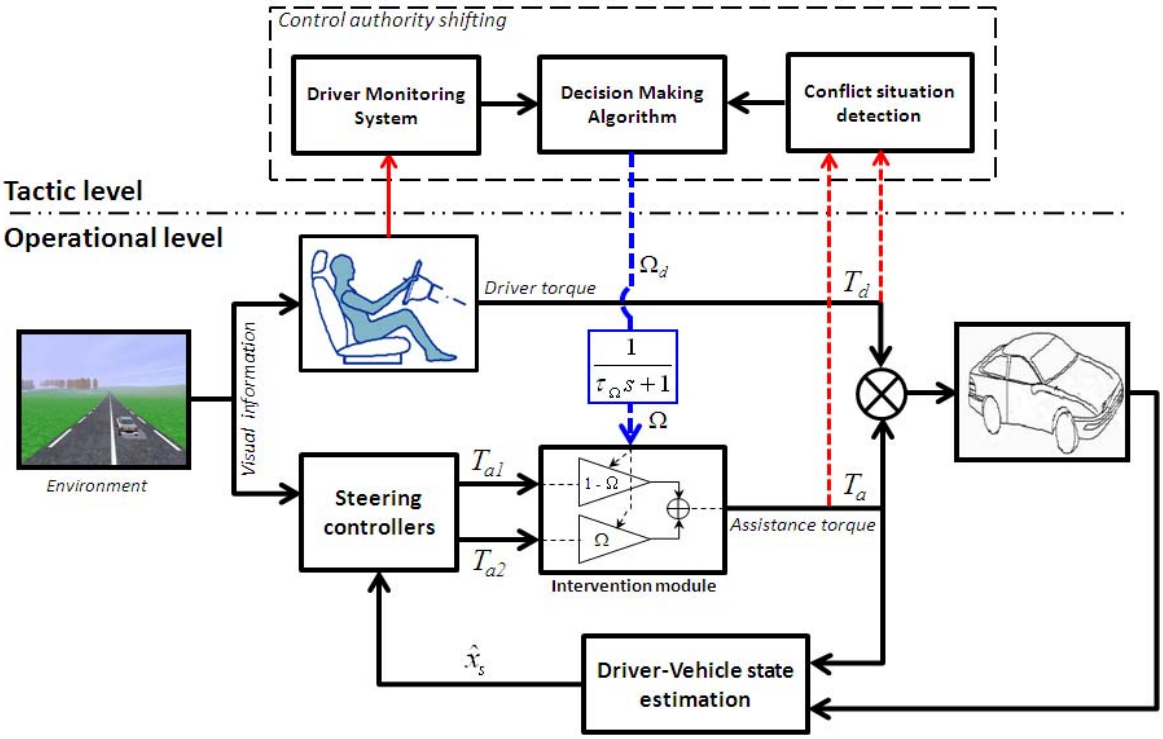

Figure 1.4 – Design of haptic guidance system proposed in [18] © 2013 IEEE.

assist controller is especially considered to reduce potential conflicts. Two steering assist controllers were defined with different strategies: one giving a best compromise between lane tracking performance and the interference level of the controller, and another for promoting the action of the driver to the controller when the driver changes his or her steering

action. The control law, T_{a1} and T_{a2}, are calculated by integrating a driver model to have a minimum of understanding on how the driver operates. In addition, a tactic level representing the control authority shifting component is introduced to select the corresponding control strategy. Experiments on a driving simulator showed that conflicts during a lane change maneuver could be detected and control strategy then changed accordingly.

Flad et al. proposed the shared control structure shown in Figure 1.5[19]. This structure describes the cooperation of human driver and assistance system on the steering wheel as a differential game. Their torque output, T_D and T_A, are obtained by minimizing their individual objective function J_D and J_A respectively. To solve this optimization problem approximately, a prediction of driver torque and vehicle states is necessary. Therefore, a proper driver model is introduced. The model consists of two parts: a set of driver-specific movement primitives (called *movemes*) and a controller model which determines a suitable *moveme* sequence to steer the vehicle. Experiments on a driver simulator proved that the designed structure can improve the objective performance of the drivers and receive a better subjective rating than a non-cooperative ADAS (i.e. without driver model considered).

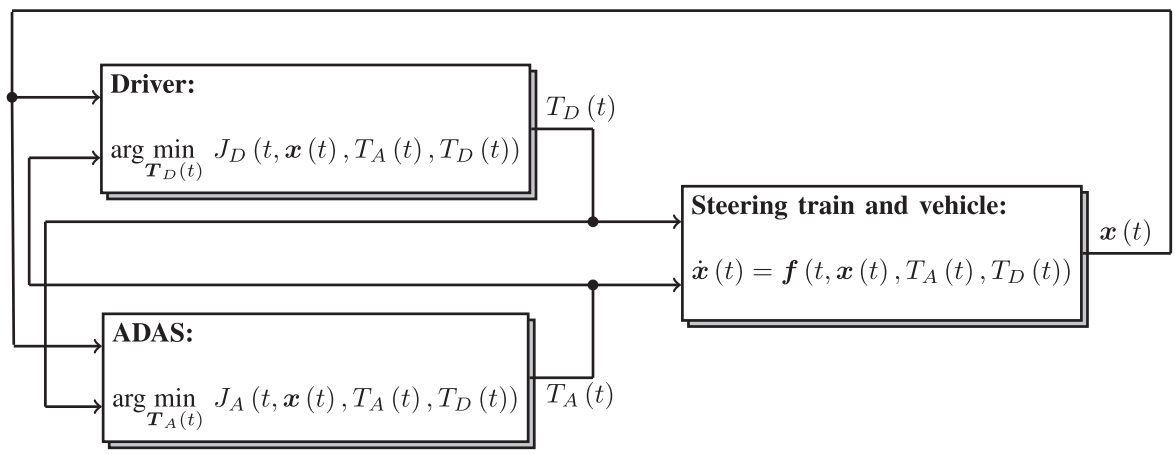

Figure 1.5 – Design of haptic guidance system proposed in [19] © 2017 IEEE.

Besides, Abbink and Mulder proposed that the haptic feedback can be designed not only to depend on a calculated error (i.e., force feedback) but also on the control device position (i.e., stiffness feedback)[20]. Powell and O'Mallay showed that the shared control haptic guidance paradigms must be matched to a task's dynamic characteristics to elicit effective training and low workload[21]. Flemisch et al. investigated four cornerstone

concepts for the design of shared control: ability, authority, control and responsibility[22]. Flad et al. stated the necessary and sufficient conditions for the design of cooperative shared control based on game theoretic modeling[23], [24]. The study of Ludwig et al. indicated that the optimal shared control is dependent on the level and homogeneity of the cooperating partners[25]. Mugge et al. pointed out that the haptic guidance needs to be intuitive not just informative to improve human motor accuracy[26]. Van Passen analyzed four design choices for haptic shared control: human-compatible reference, level of haptic support, strength of haptic feedback and level of haptic authority[27]. Hiraoka proposed a classification of the haptic shared control into two types: a direct haptic shared control and an indirect haptic shared control[28].

In summary, researches have demonstrated that the understanding and representation of driver's role are important and beneficial for haptic guidance systems. This thesis was carried out along with the AutoConduct research program, which focuses on improving the realization of haptic guidance system and studying transition of authority. It is believed that with further knowledge on human behavior during driving, the safety and comfort of haptic guidance systems must be ameliorated.

1.4 Lay-out of Thesis

This thesis consists of four main parts: an introduction of the research context; a presentation of the methodology adopted in this study, the results of experiments conducted and a conclusion. Each part consists of several chapters, which are detailed as follows.

Chapter 1 - Haptic Shared Control gives a brief introduction of haptic shared control. It explains firstly why the shared control framework was proposed. The definition of the shared control in general human-machine interaction is then presented. The realization of haptic shared control in vehicle lateral control is introduced briefly in the end as the background of this study.

Chapter 2 - Driver Model and Adaptation firstly introduces the state-of-the-art of driver steering models from compensation and preview to neuromusuclar system, and finally new trends of involving learning and adaptation in the model. Secondly, the importance of driver model in the design of haptic guidance system is discussed, while the lack of knowledge about the adaptation is also presented. This research gap leads to the objective of this study: understanding driver's adaptation to haptic guidance systems during interaction via both behavioral and model-based analysis. The main contributions of

this study are summarized.

Chapter 3 - Experiment Platform presents the experiment platform employed in this study, including a fixed-base driving simulator and a haptic guidance system which was developed in a previous study.

Chapter 4 - Parameter Identification I: Prediction Error Minimization firstly discusses the general steps of parameter estimation in system identification. Based on the hypothesis that the system to be identified is linear time-invariant, the prediction error minimization (PEM) method is then briefly introduced. The practical use of PEM in model-based analysis is particularly considered.

Chapter 5 - Parameter Identification II: Unscented Kalman Filter presents an identification method using Kalman filter when the system to be identified is assumed to be time-variant. A tuning strategy for the configuration of filter is emphasized.

Chapter 6 - Experimental studies introduces the basis of model-based analysis method, which was the guideline behind the three studies carried out in Chapter 7, 8 and 9. The experiments and results of these studies are summarized.

Chapter 7 - Driving with a Haptic Guidance System in Degraded Visibility Conditions: Behavioral Analysis and Identification of a Two-Point Steering Control Model shows the first step of this thesis. The objective of this study is to verify to what extent the two-point visual model is likely to "explain" through its parameters, the behavior of the driver-assistance system as a function of the characteristics of the haptic guidance or the type of visibility.

Chapter 8 - Towards a Driver Model to Clarify Cooperation Between Drivers and Haptic Guidance Systems reveals that the adaptation of human driver to haptic guidance system may not only affect the parameter values of driver model, but also the structure, especially the neuromuscular system. To deal with this problem and continue using driver model to study the adaptation, a new driver model which clarifies the cooperation between drivers and haptic guidance system is proposed and validated.

Chapter 9 - Driver Model Validation through Interaction with Varying Levels of Haptic Guidance studies the adaptation of human driver to haptic guidance system through usage. The new driver model proposed in this thesis is employed and proves its capacity in predicting driver's behavior.

Chapter 10 - General Conclusion and Perspectives reviews the results and methodology of this study. Hypothesis are made for possible research directions in future.

1.5 List of Publications

Below is a list of publications accepted or submitted during this thesis.

- International Journal Articles
  - Y. Zhao, P. Chevrel, F. Claveau, and F. Mars, “Driving with a Haptic Guidance System in Degraded Visibility Conditions: Behavioral Analysis and Identification of a Two-Point Steering Control Model,” submitted to IEEE Transactions on Human-Machine Systems (THMS), revised on February 2021.
- Conference Papers with Reviewer
  - Y. Zhao, B. Pano, P. Chevrel, F. Claveau and F. Mars, "Driver Model Validation through Interaction with Varying Levels of Haptic Guidance," 2020 IEEE International Conference on Systems, Man, and Cybernetics (SMC), Toronto, ON, 2020, pp. 2284-2290, doi: 10.1109/SMC42975.2020.9283382.
  - Y. Zhao, P. Chevrel, F. Claveau and F. Mars, "Towards a Driver Model to Clarify Cooperation Between Drivers and Haptic Guidance Systems," 2020 IEEE International Conference on Systems, Man, and Cybernetics (SMC), Toronto, ON, 2020, pp. 1731-1737, doi: 10.1109/SMC42975.2020.9283101.
  - Y. Zhao, P. Chevrel, F. Claveau, and F. Mars, “Continuous identification of driver model parameters via the unscented kalman filter,” IFAC-PapersOnLine, vol. 52, no. 28, pp. 126–133, 2019.
  - B. Pano, Y. Zhao, P. Chevrel, F. Claveau, and F. Mars, “Shared Control Based on an Ecological Feedforward and a Driver Model Based Feedback,” IFAC-PapersOnLine, vol. 52, no. 5, pp. 385–392, 2019.
- Conference Papers without Reviewer
  - Y. Zhao, P. Chevrel, F. Claveau and F. Mars, “Driver model parameter identification to estimate driver adaptation over time,” 3rd Jourée de l’Automatique of GdR MACS, 2018.

1.6 References

[1] J. R. Treat, N. Tumbas, S. McDonald, D. Shinar, R. D. Hume, R. Mayer, R. Stansifer, and N. Castellan, "Tri-level study of the causes of traffic accidents: final report. Executive summary.", Indiana University, Bloomington, Institute for Research in Public Safety, Tech. Rep., 1979.

[2] J. Anderson, N. Kalra, K. Stanley, P. Sorensen, C. Samaras, and O. Oluwatola, *Autonomous Vehicle Technology: A Guide for Policymakers*. RAND Corporation, Mar. 2016, p. 214, ISBN: 9780833083982.

[3] D. J. Fagnant and K. Kockelman, "Preparing a nation for autonomous vehicles: Opportunities, barriers and policy recommendations", *Transportation Research Part A: Policy and Practice*, vol. 77, pp. 167–181, 2015, ISSN: 09658564.

[4] SAE International, "Taxonomy and Definitions for Terms Related to Driving Automation Systems for On-Road Motor Vehicles (No. J3016)", SAE International, Tech. Rep., 2018.

[5] K. Bengler, K. Dietmayer, B. Farber, M. Maurer, C. Stiller, and H. Winner, "Three Decades of Driver Assistance Systems: Review and Future Perspectives", *IEEE Intelligent Transportation Systems Magazine*, vol. 6, *4*, pp. 6–22, 2014, ISSN: 1941-1197.

[6] J. J. Leonard, D. A. Mindell, and E. L. Stayton, "Autonomous Vehicles, Mobility, and Employment Policy: The Roads Ahead", Massachusetts Institute of Technology, Tech. Rep., 2020, pp. 1–34.

[7] J. Gogoll and J. F. Müller, "Autonomous Cars: In Favor of a Mandatory Ethics Setting", *Science and Engineering Ethics*, vol. 23, *3*, pp. 681–700, 2017, ISSN: 14715546.

[8] J.-M. Hoc, "From human – machine interaction to human – machine cooperation", *Ergonomics*, vol. 43, *7*, pp. 833–843, 2000.

[9] C. D. Mole, O. Lappi, O. Giles, G. Markkula, F. Mars, and R. M. Wilkie, "Getting Back Into the Loop: The Perceptual-Motor Determinants of Successful Transitions out of Automated Driving", *Human Factors*, vol. 61, *7*, pp. 1037–1065, 2019.

[10] N. Merat and A. Jamson, *Is Drivers' Situation Awareness Influenced by a Fully Automated Driving Scenario?*, © 2009, Shaker Publishing. This is an author produced version of a paper published in Human Factors, Security and Safety. Uploaded with permission from the publisher., 2009.

[11] S. S. Banerjee, S. Jha, J. Cyriac, Z. T. Kalbarczyk, and R. K. Iyer, "Hands Off the Wheel in Autonomous Vehicles?: A Systems Perspective on over a Million Miles of Field Data", *in 2018 48th Annual IEEE/IFIP International Conference on Dependable Systems and Networks (DSN)*, 2018, pp. 586–597.

[12] M. Steele and R. B. Gillespie, "Shared Control between Human and Machine: Using a Haptic Steering Wheel to Aid in Land Vehicle Guidance", *Proceedings of the Human Factors and Ergonomics Society Annual Meeting*, vol. 45, *23*, pp. 1671–1675, 2001.

[13] F. O. Flemisch, C. A. Adams, S. R. Conway, K. H. Goodrich, M. T. Palmer, and P. C. Schutte, "The H-Metaphor as a Guideline for Vehicle Automation and Interaction", Tech. Rep. December, 2003, pp. 1–30.

[14] D. A. Abbink, T. Carlson, M. Mulder, J. C. De Winter, F. Aminravan, T. L. Gibo, and E. R. Boer, "A topology of shared control systems-finding common ground in diversity", *IEEE Transactions on Human-Machine Systems*, vol. 48, *5*, pp. 509–525, Oct. 2018, ISSN: 21682291.

[15] M. Marcano, S. Diaz, J. Perez, and E. Irigoyen, "A Review of Shared Control for Automated Vehicles: Theory and Applications", *IEEE Transactions on Human-Machine Systems*, *September*, pp. 1–17, 2020, ISSN: 2168-2291.

[16] D. A. Abbink and M. Mulder, "Neuromuscular Analysis as a Guideline in designing Shared Control", *in Advances in Haptics*, M. H. Zadeh, Ed., Rijeka: IntechOpen, 2010, ch. 27.

[17] P. Griffiths and R. B. Gillespie, "Shared control between human and machine: haptic display of automation during manual control of vehicle heading", *in 12th International Symposium on Haptic Interfaces for Virtual Environment and Teleoperator Systems, 2004. HAPTICS '04. Proceedings*, Mar. 2004, pp. 358–366.

[18] C. Sentouh, B. Soualmi, J. C. Popieul, and S. Debernard, "Cooperative steering assist control system", *in Proceedings - 2013 IEEE International Conference on Systems, Man, and Cybernetics, SMC 2013*, 2013, pp. 941–946, ISBN: 9780769551548.

[19] M. Flad, L. Fröhlich, and S. Hohmann, "Cooperative Shared Control Driver Assistance Systems Based on Motion Primitives and Differential Games", *IEEE Transactions on Human-Machine Systems*, vol. 47, *5*, pp. 711–722, 2017.

[20] D. A. Abbink and M. Mulder, "Exploring the dimensions of haptic feedback support in manual control", *Journal of Computing and Information Science in Engineering*, vol. 9, *1*, pp. 1–9, 2009.

[21] D. Powell and M. K. O'Malley, "The task-dependent efficacy of shared-control haptic guidance paradigms", *IEEE Transactions on Haptics*, vol. 5, *3*, pp. 208–219, 2012, ISSN: 19391412.

[22] F. Flemisch, M. Heesen, T. Hesse, J. Kelsch, A. Schieben, and J. Beller, "Towards a dynamic balance between humans and automation: Authority, ability, responsibility and control in shared and cooperative control situations", *Cognition, Technology and Work*, vol. 14, *1*, pp. 3–18, Mar. 2012, ISSN: 14355558.

[23] M. Flad, J. Otten, S. Schwab, and S. Hohmann, "Necessary and sufficient conditions for the design of cooperative shared control", *Conference Proceedings - IEEE International Conference on Systems, Man and Cybernetics*, pp. 1253–1259, 2014, ISSN: 1062922X.

[24] ——, "Steering driver assistance system: A systematic cooperative shared control design approach", *Conference Proceedings - IEEE International Conference on Systems, Man and Cybernetics*, pp. 3585–3592, 2014, ISSN: 1062922X.

[25] J. Ludwig, G. Diehm, M. Flad, and S. Hohmann, "Optimal interaction structure of human drivers cooperation: A pilot study", *Conference Proceedings - IEEE International Conference on Systems, Man and Cybernetics*, pp. 3593–3598, 2014, ISSN: 1062922X.

[26] W. Mugge, I. A. Kuling, E. Brenner, and J. B. Smeets, "Haptic guidance needs to be intuitive not just informative to improve human motor accuracy", *PLoS ONE*, vol. 11, *3*, e0150912, Mar. 2016, ISSN: 19326203.

[27] R. van Paassen, R. Boink, D. Abbink, M. Mulder, and M. Mulder, "Four design choices for haptic shared control", English, *in Advances in Aviation Psychology*, M. Vidulich, P. Tsang, and J. Flach, Eds. 2017, vol. 2, pp. 237–256, ISBN: 978-472-48141-2.

[28] T. Hiraoka, "How do we share the "control" when using the haptic shared control for an advanced driver-assistance system? -Direct HSC and Indirect HSC-", *IFAC-PapersOnLine*, vol. 52, *19*, pp. 61–66, 2019, ISSN: 24058963.

Chapter 2

Driver Model and Adaptation

2.1 State-of-the-art of Driver Steering Model

The Oxford dictionary defines a *model* as *a copy of something*. A driver model can be defined as a copy of human behavior in one or several driving tasks. In this thesis the lateral control task is particularly concerned. Various types of driver model could be established from different perspectives. For example, one may focus on a neural model if the transmission of neural signals during steering is the interest. In control theory, the *mathematical model* is usually considered, which provides the relationship between input and output signal(s) in the form of mathematical equations. A "good" model must be a representation of the plant that will enhance the ability to *understand*, *explain*, *predict*, *change* and *control* the behavior of the system[1]. The understanding and prediction of driver's steering behavior is an important property of driver model which is demanded in the design of haptic guidance systems. However, a driver model does not fully equal to a human driver. The accuracy depends on the "goodness" of the model, which should be defined *a priori* according to the purpose of the user.

For our adaptation study and model-based analysis, a "good" model should be able to predict driver's adaptive behavior. In addition, the cybernetic approach is considered in the modeling. This approach aims to represent the underlying psychological and physiological processes in accordance with current knowledge on sensorimotor control and cognition in humans[2]. In other words, the cybernetic driver model not only represents the mathematical relation between input and output signals, but also integrates psychological and physiological knowledge into the structure and parameters of the model. As such, these models can not only be used for the development of haptic guidance system, but also for the estimation of driver's internal states, which are seldom measurable by any means.

2.1.1 Driver Models Based on Compensation and Preview

The exploration of driver modeling has started since 1960s. A short review of models that received a great deal of research attention between 1962 and 1977 was published in [3]. It presented three features needed to describe the total properties of the driver as a controller: compensation, pursuit and precognition (see Figure 2.1). In the compensatory behavior, the driver's steering-wheel motions are function primarily of errors or vehicle output motions such as the lateral position error or the vehicle heading. This closed-loop feedback control ensures the precision of path following. In the pursuit behavior, driver's control is generated from the perception of the roadway and the vehicle output motions. This open-loop feedforward control permits the driver to anticipate the desired path. When the driver is completely familiar with the vehicle dynamics and the perceptual field through continuous repetitions, he or she can expertly generate steering motions for many maneuvers as desired. This behavior is precognition and it is pure open-loop control. It is always in combination with the compensation to form a dual-mode behavior. In summary, the driver's control behavior is either compensatory, pursuit or dual mode.

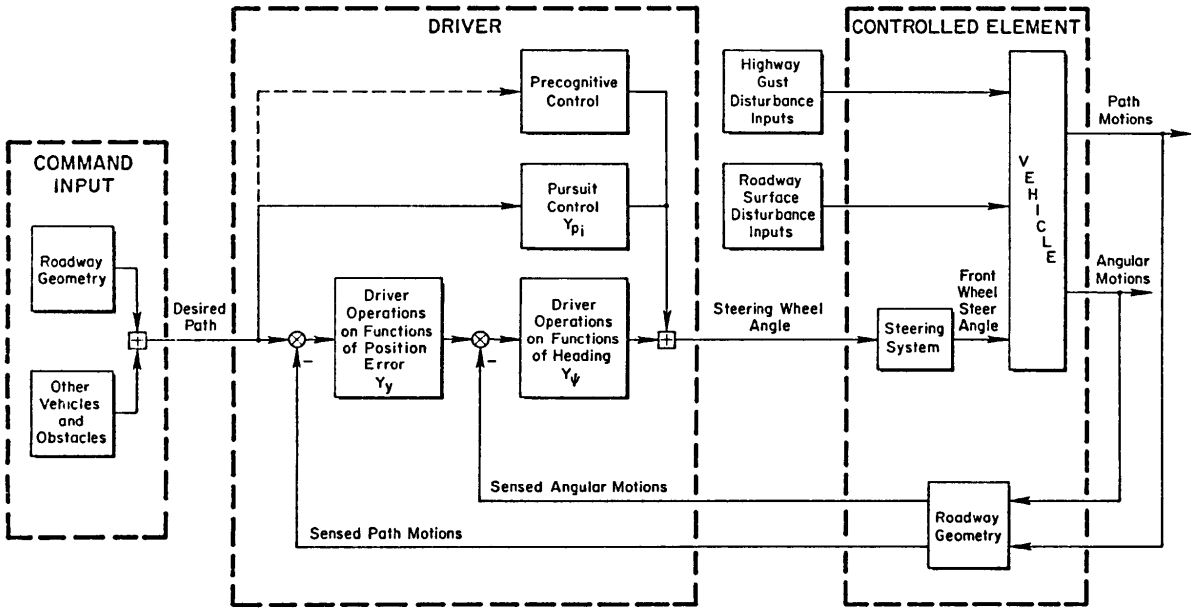

Figure 2.1 – Topology of the driver/vehicle system combining open- and closed-loop precognitive, pursuit, and compensatory control structures[3] © 1977 Sage Publications.

Following this idea of organizing the steering task hierarchically, a two-level model of driver steering behavior was proposed in [4]. As shown in Figure 2.2, the steering task is

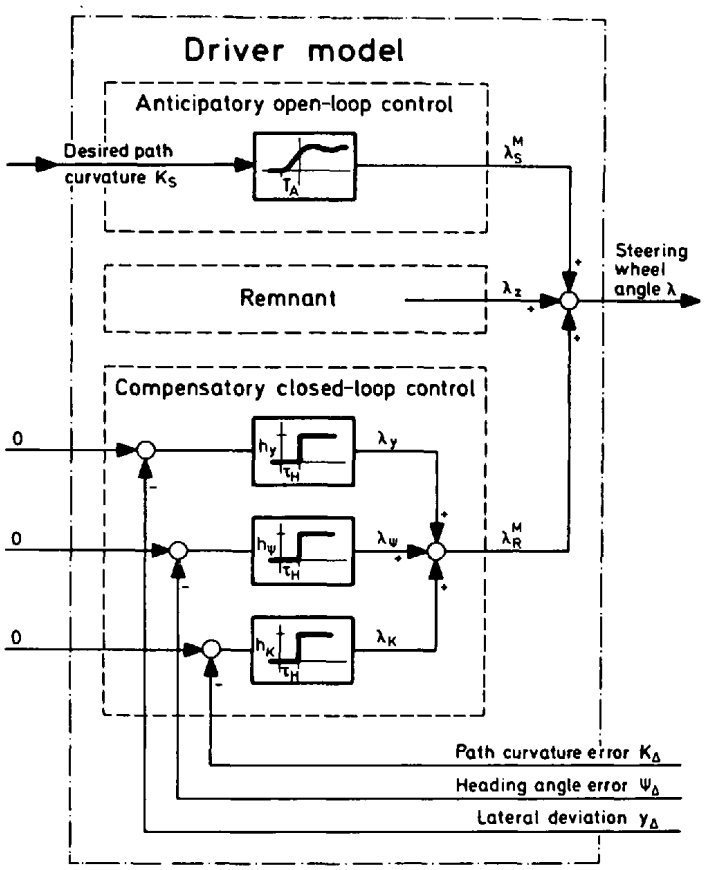

Figure 2.2 – Block diagram of the two-level model of driver steering behavior[4] © 1978 Sage Publications.

divided into two levels: a guidance level involving the perception of the instantaneous and future course of the forcing function provided by the forward view of the road, and the response to it in an anticipatory open-loop control mode; a stabilization level whereby any occurring deviations from the forcing function are compensated for in a closed-loop control mode. Compared with [3], the information that perceived by driver at these two levels were considered more precisely in this model. The curvature of the road (i.e., the reciprocal of the radius of turn) was chosen as the representation of the guidance information in the forward view of the road, which is the input of the guidance level; the stabilization information consisted of three different quantities: the lateral deviation, the vehicle heading error and the path curvature error, which are the inputs of the stabilization level. The output of the model is a steering-wheel angle. Result of parameter identification carried out sequentially on these two sub-models showed that this model is suitable for describing

human steering behavior and theoretically evaluating the dynamic interaction within the driver-vehicle-road guidance and control system.

However, from the point of view of R.A. Hess and A. Modjtahedzadeh, the before-mentioned models are mostly descriptive tools for researches instead of predictive tools for practicing engineers due to their complexity in application[5]. Therefore, they chose to model driver steering behavior as a pure compensator, which was further divided into a high and a low-frequency compensation element (see Figure 2.3). The high frequency refers to frequencies within an approximate one decade range around the crossover frequency of the overall driver/vehicle open-loop return ratio, which came from the human pilots modeling in flight control task. Besides, they mentioned a neuromuscular system of the driver's arm and "proprioceptive" feedback elements, while the output of model was still the steering-wheel angle. The input of the model was simplified to only the y-coordinates of road.

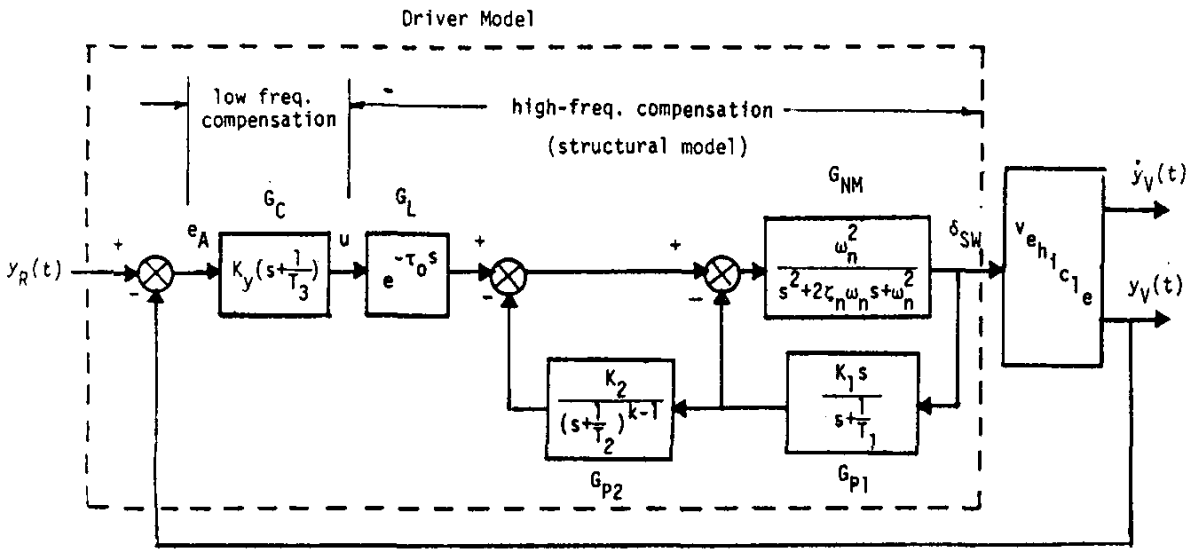

Figure 2.3 – The driver/vehicle model[5] © 1990 IEEE.

Questions arose afterward around the "real" input(s) of driver steering model, namely the information that driver effectively refers to during steering. Results from driving simulator study indicated that the answer might be two regions of the road: a distant and a near region[6]. The former is used to estimate road curvature and the latter to provide position-in-lane feedback. Yet no perceptually plausible sources of "near" and "far" visual information that is used by the driver were well defined. Thus, a two-level model of steering

control that uses the perceived visual direction of two salient visual points, a *near point* in the near region and a *far point* in the far region of the road was proposed by [7]. The near point represents the center of the road at some nearby distance with which the model can monitor both lateral position and stability. The far point is the vanishing point during navigation of a straight road, or the tangent point during navigation of a curved road. In addition, the angle from the visual direction to these points were utilized as the inputs of the proposed model, which could be described by the following equation.

$$\dot{\phi} = k_f\dot{\theta}_f + k_n\dot{\theta}_n + k_l\theta_n \tag{2.1}$$

where ϕ is the steering angle as output, θ_f is the far point angle and θ_n is the near point angle. Note that a proportional-integral, or PI, controller is applied on the near point angle to eliminate static error in lateral position.

In summary, the driver steering model at this early stage was usually hierarchical. The steering task was supposed to be achieved by several subsystems either in parallel or in sequence. Among those subsystems, there were usually a compensatory part for maintaining the lateral position of vehicle, and an anticipatory part for following the road ahead. These subsystems could be closed-loop externally with the vehicle-road model (i.e., open-loop internally), or closed-loop internally. The output of the model was always the steering-wheel angle. The inputs were mostly chosen from (angular) position signals of vehicle and road.

2.1.2 Driver Models Including Neuromuscular System

Although previous models seemed to be satisfactory in the sense of describing driver's steering behavior, there was no evidence demonstrating that human driver outputs directly steering-wheel angle to control vehicle. In reality, drivers need to interact with steering wheel via arm muscles to reach a desired angle. This fact was not explicitly included in most of the previous models. In addition, the role of steering torque feedback (i.e., the torque felt by driver on steering wheel, which is usually the self-aligning torque in completely manual control) in the dynamics of the vehicle-driver system was poorly understood. Furthermore, with increased applications of haptic shared control in the lane-keeping assistance system in recent years, neuromuscular model became even more important than before. It was emphasized in [8] that the neuromuscular analysis should be regarded as a guideline in designing shared control. Experiments showed that

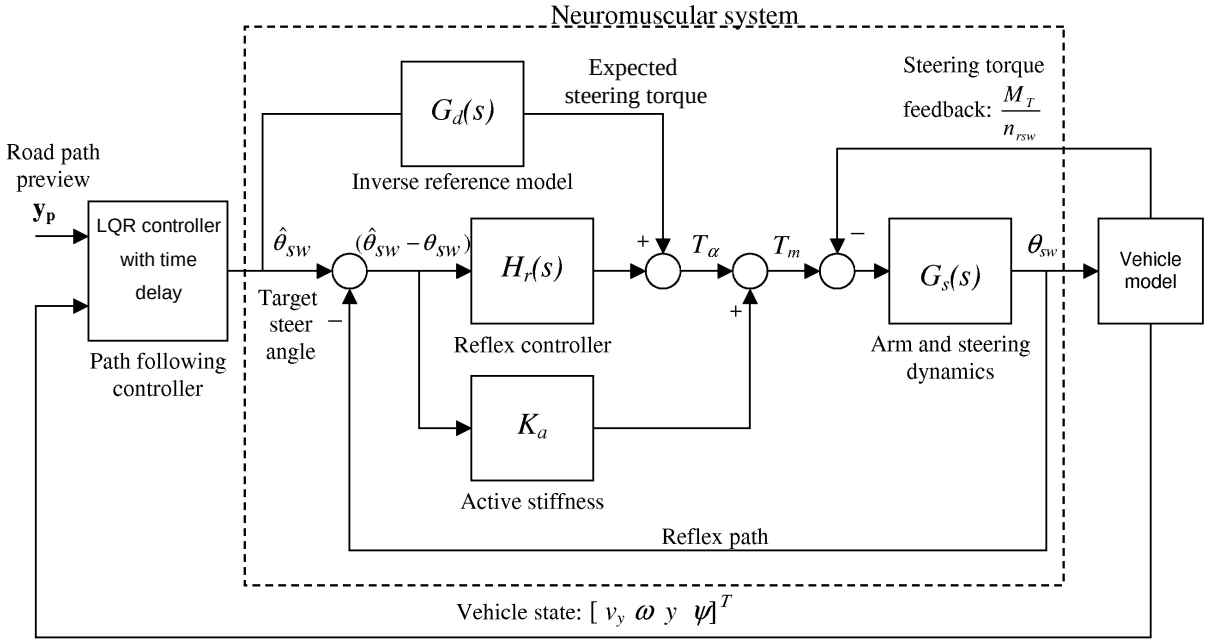

Figure 2.4 – Structure for driver path-following model with neuromuscular dynamics incorporated[10].

the measurements of the neuromuscular impedance would improve the understanding of human response to forces, and thereby, the design of haptic shared control. Another experiments in [9] showed the importance of tuning guidance torques with the correct expectation about neuromuscular response. It was demonstrated that the lateral control performance would be reduced if there was mismatch between the tuning of guidance torque and the real neuromuscular behavior.

In [10], a research was carried out aiming at investigating the neuromuscular dynamics in the vehicle steering task. A new driver model with neuromuscular system (NMS) was proposed, as shown in Figure 2.4. This model connected a path-following controller, which is a linear quadratic regulator (LQR), and a NMS. The LQR is responsible for generating an optimal targeted steer angle. The NMS is responsible for applying the steer angle through regulation of the steering system. The NMS could be further divided into three subsystems: inverse reference model, reflex controller and active stiffness. The inverse reference model represents the inverse of the steering dynamics; the reflex controller represents the reflex action via the spinal cord and muscle spindles; the active stiffness represents the increased muscle stiffness induced by muscle co-contraction. The output of all three subsystems are summed up to generate the total active muscle torque T_m

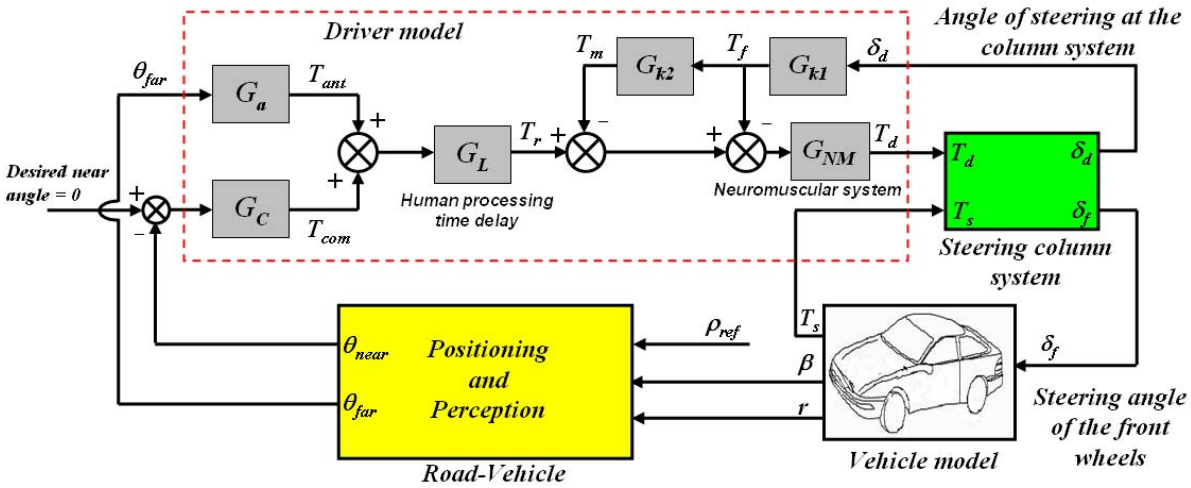

Figure 2.5 – The structure of the driver model[12] © 2009 IEEE.

applied on an arm and steering system (because they are coupled) in the presence of steering torque feedback from vehicle.

Another study revealed the role of steering torque feedback in the driving task. Results from experiments with human drivers indicated that they could actually adapt to a wide range of steering characteristics, but accurate steering was impossible in extreme situations, e.g. with an inversed or a total absence of force feedback. A modification in steering wheel force feedback is not likely to be interpreted by drivers as a change of the vehicle dynamics, and is likely to be compensated for by an adaptation of their internal model of the steering wheel compliance[11]. This important conclusion implied that the steering torque feedback should be considered as an input in the driver steering model. In accordance with this idea, a sensorimotor driver model with an emphasis on the role of visual information and kinaesthetic feedback was proposed in[12] (see Figure 2.5). This multi-input mono-output model structure combines a visual strategy similar as the two-point model in[7] and a strategy inspired from [5] in order to take into account the sensation of the steering torque feedback. It should be noted that in this model, the steering torque feedback was not directly used as an input. Instead, the torque perceived by driver from the steering system through arm muscular and joint proprioception, which is derived from steering-wheel angle, was considered. This process is represented by the transfer function G_{k1} in the figure.

Later, the estimation of steering torque feedback by drivers were extended to sensation

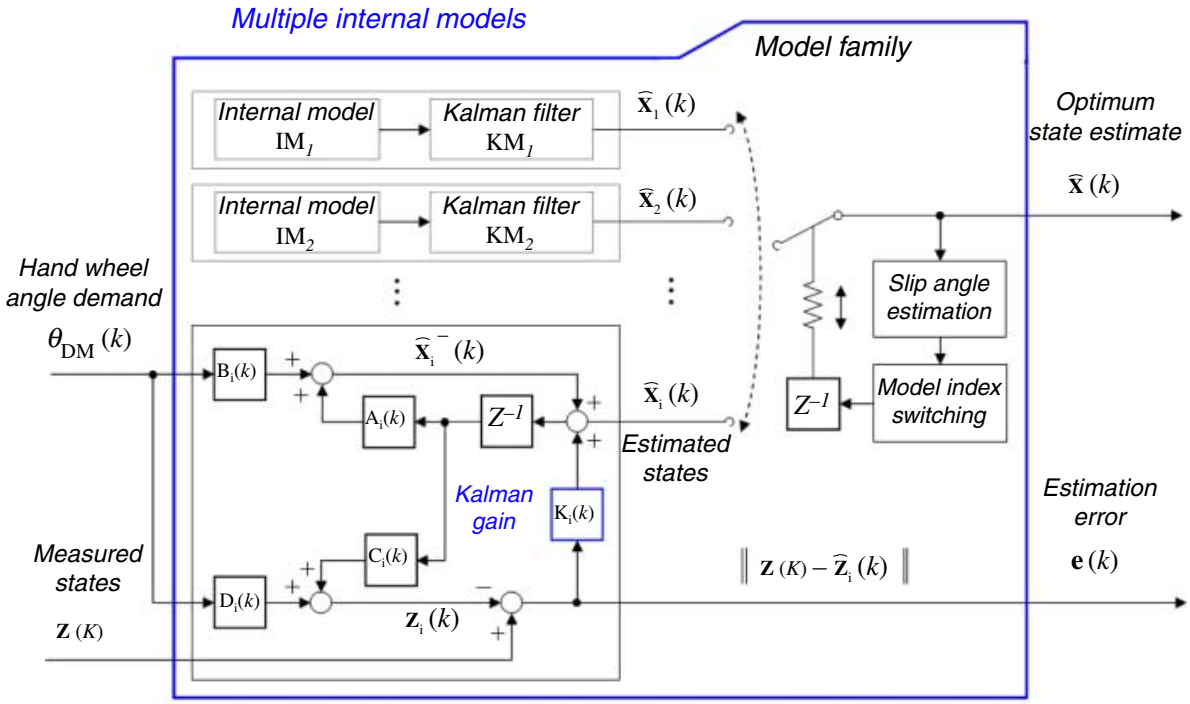

Figure 2.6 – State estimation using multiple models and Kalman filters[13].

and perception of vehicle states in [13] and [14] as well. The Kalman filter was used to represent the driver's ability to generate estimates of the vehicle-road system states from noisy sensory measurements. In [13], it was also proposed that a driver learns and stores knowledge of nonlinear vehicle dynamics in the form of a family of local linearised models and selects the one which is the nearest to the current states of vehicle, thus a series of Kalman filter corresponding to each local linear model was included in the driver model (see Figure 2.6). Experiments on a driving simulator validated the model and showed that the steering toque feedback significantly improved the path following performance.

Despite the estimation of steering torque feedback (and vehicle states) by drivers corresponds to the reality, there were different opinions whether this process should be implemented explicitly in the driver steering model or not. The driver model proposed in [15] took directly the self-aligning torque as input (see Figure 2.7). It is based on the hypothesis that the driver uses visual information to identify the upcoming road curvature, as well as the states of the vehicle. The driver then formulates an intention signal considered as the desired steering-wheel angle $\hat{\delta}_{SW}$ and applies it on the steering system through the NMS. A similar driver model in shared control that focuses on driver

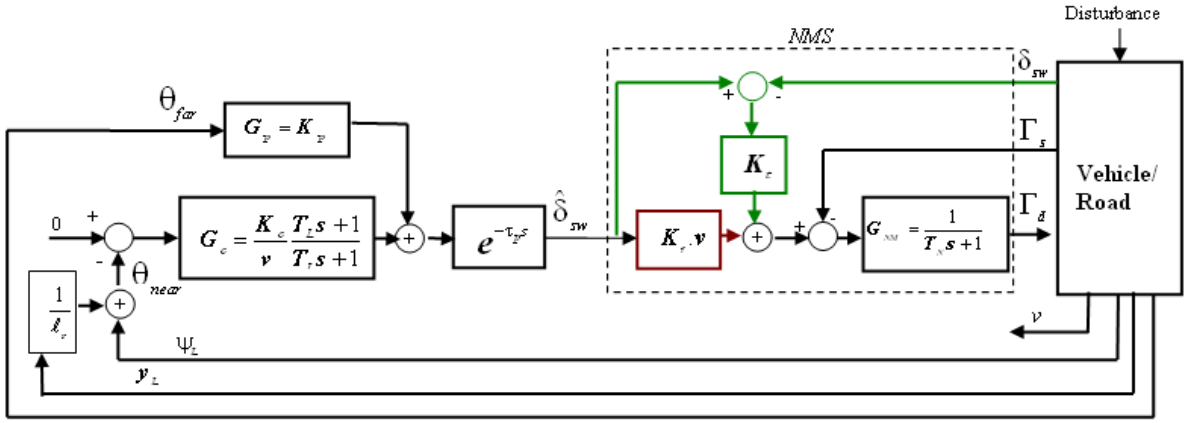

Figure 2.7 – Cybernetic driver model for lane keeping maneuver[15].

interaction with haptic guidance steering for a lane-following task was proposed in[16], while the self-aligning torque was replaced by haptic guidance torque.

2.1.3 Challenges and New Trends

Back to 1948, N. Wiener defined *cybernetics* as *the scientific study of control and communication in the animal and the machine*[17]. The cybernetic theories and approaches have guided the modeling of driver steering behavior since then, resulting a large variety of mathematical models. These models are certainly not only limited to those mentioned above, but also developed with other techniques such as fuzzy logic control, neural networks, stochastic methods, hybrid approaches etc., as summarized in [18]. However, limitations of current cybernetics theory emerged in recent years. In [19], the fundamental issues in manual control cybernetics were discussed. According to the authors, current cybernetics theory is often limited in capturing the full breadth of human cognition and control. Only the exceptions not the rule in manual control is modeled. Human drivers are always assumed to be time-invariant, which makes it difficult to model a defining attribute of human controllers, namely their ability to *adapt* to changing situations.

To advance the cybernetics theory and its applications, a new roadmap was proposed in [20]. Five fundamental research questions on human manual control were brought forward:

1. How do humans use preview of future task constraints ?
2. What are the factors and mechanisms that driver adaptation, and which invariants in adaptation exist ?

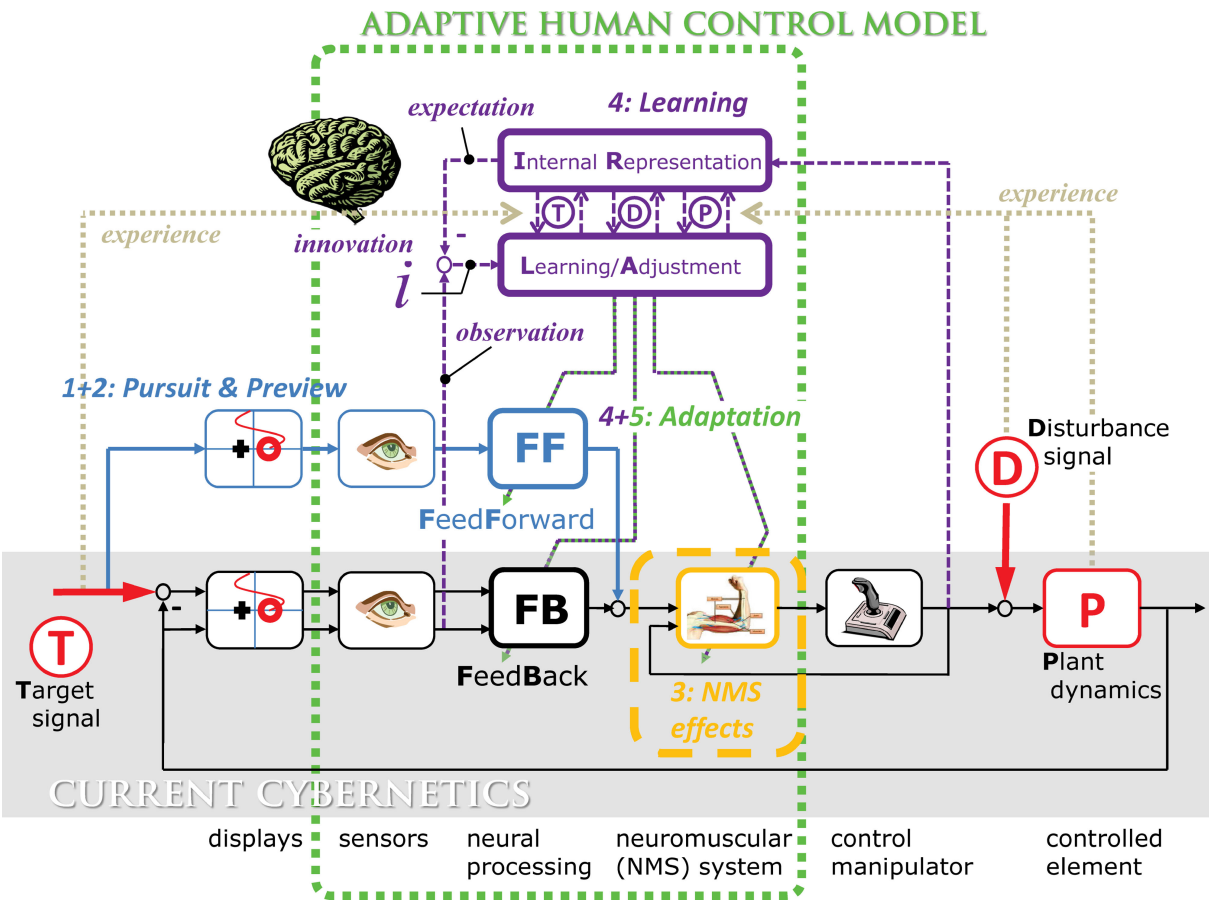

Figure 2.8 – Proposed framework for understanding the learning and adaptive human controller[20] © 2018 IEEE.

3. To what extent are measured human adaptations caused by physiological (e.g., neuromusuclar) rather than cognitive adaptations ?
4. What are the temporal scales of human adaptation and learning in changing situations ?
5. What novel control theories and system identification techniques exist that could allow us to study time-varying and possibly nonlinear manual control ?

A novel five-step framework to increase the understanding of the *learning and adaptive* human control was also introduced (see Figure 2.8). In addition to the pursuit (Step 1), preview (Step 2) and NMS effects (Step 3) levels which have been intensively studied in past years, the understanding of learning (Step 4) and adaptation (Step 5) were emphasized in this framework. Learning refers to the mastery of a certain set of tasks

which is usually a comparatively slow process. Adaptation refers to the switch between two different control strategies when the task conditions change, which is often rapid for human driver. With the additional knowledge of learning and adaptation, it is believed that human adaptive control capabilities can be interpreted and predicted. This however could not be achieved without dedicated experimentation and advanced methodologies, such as intrinsically time-varying modeling and parameter identification methods[20].

2.2 Adaptation of Human-Machine System

As summarized in Chapter 1, the analysis and understanding of human driver's behavior is important and beneficial in the design of haptic guidance system. Indeed, there are two fundamental design guidelines for human-automation interaction systems: the human operator should be able to understand the automation system, and the automation system should include knowledge of the human operator[21]. In another word, human driver and haptic guidance system should be able to fully understand the intention of each other and reach a balance of control authority that can shift towards either actor, depending on the situation[22]. This balance is not a static but a dynamic equilibrium: during driving, the human driver will continuously adjust his or her control to adapt to the system, while the system will also continuously adjust its control output to adapt to the human driver. A possible approach to realize this adaptive haptic guidance system is to include a driver model in the design, so that the driver's behavior can be predicted. However, as mentioned above, current (cybernetic) steering models are not "good" enough to predict human driver's behavior, especially the adaptation process. Although researches have reached a consensus that human are capable of adapting their control strategy or individual characteristics to changes in driving conditions, questions such as when, how and to what extent this adaptation takes place are still largely unknown[20]. As a result, increased steering torques were found in experiments due to small conflicts between the driver and the haptic guidance system[23]. In short, the understanding of the human adaptation is essential in the driver steering model, and this model can further contribute to the realization of adaptive haptic guidance system.

Several experiments aiming at investigating the driver adaptation in real-word relevant scenarios have been carried out in recent years, either with or without haptic guidance systems. It is worth noting that all these experiments were evaluated statistically by calculating and comparing lateral control metrics, such as the steering-wheel reversal rate

(SWRR)[24], standard deviation of lateral position (SDLP), etc. For example, the effect of haptic guidance system was shown in [25]. Result suggested that the drivers quickly updated their internal model of the steering system dynamics at the sensorimotor level without further behavioral adaptation afterwards. Another study focused on the influence of different degrees of haptic shared control (i.e., different levels of steering assistance) was performed in [26]. The conclusion was that the best cooperation was achieved with systems of relatively low-level haptic authority, although more intervention may be preferable in poor visibility conditions. The effect of visual degradation on anticipatory and compensatory steering control was proposed in [27]. Results showed that the compensatory process was more robust to visual degradation than the anticipatory process. The adaptation of the neuromuscular admittance was described in [28], where experiments demonstrated that increased speed and reduced road width both decrease neuromuscular admittance of the driver.

2.3 Objective of Thesis

The haptic shared control is a promising human-automation interaction framework for the development of ADAS and automated vehicles. However, its implementation in steering control, namely the haptic guidance system, has not completely met the commonly formulated design guidelines. The main problem is that the system is not enough adaptive to human driver's behavior. This imperfection is the consequence of our insufficient knowledge on the nature of human adaptation to changes in driving conditions. On the one hand, most of the current driver model does not take the adaptation into consideration. On the other hand, most of the adaptation researches are only based on behavioral analysis. The gap in between is that the current driver models are not capable of reproducing the results of adaptation studies, and these results have no corresponding projection in the driver models. In other words, the driver models and the adaptation are investigated independently and there is no connection established between them. Therefore, those designs of haptic guidance system including such driver models will have conflicts with human driver in practical application, which may cause critical situations.

The objective of this thesis consists of understanding the reciprocal adaptation between driver and the haptic guidance system through usage. The analysis of the adaptation in this thesis is performed through two different perspectives: behavioral analysis and model-based analysis. The behavioral analysis is similar to previous researches, which consists

of calculating certain types of lateral control metrics and analyzing statistical differences via analysis of variance (ANOVA). The model-based analysis method refers to analysis performed through current driver models. As stated above, the human adaptation has never been considered in these models. This method assumes firstly that these models will not be valid any more if the adaption takes place during the studied scenarios. It is further assumed that, either the structure, or the parameter values of these models need to be changed in order to account for the driver adaptive behavior. That is to say, the adaptation of human driver to changed conditions could be observed through these models in the form of either parametric or structural variation. In this case, the adaptation process could be captured via these models. For parametric variation, model parameter identification algorithm can be applied, including time-invariant and time-variant methods. For structural variation, the problem could be transformed to parametric variation by reconsidering the model structure and explicitly accounting for the potential adaptation process with parameters. Finally, the behavioral discrepancy under different driving conditions could be explained by the parametric variation in the adjusted driver models, and a connection between the behavior and the model is established.

Apparently, there is no perfect haptic guidance system at current stage for this study of adaptation. Yet to put forward the development of haptic guidance system, the knowledge of the adaptation is indispensable. This is not a “deadlock” but an iterative situation. With current haptic guidance system including basic driver model, a primary knowledge of driver adaptation can be acquired. With this primary knowledge, better driver model could be constructed and integrated in the design of more advanced and adaptive haptic guidance systems, and so on. This methodology is adopted in our study. An haptic guidance system including the driver model in [15] (see Figure 2.7) is chosen as a starting point. The analysis of the first experiment through the two-point model[7] investigated the effect of degraded visibility conditions and the haptic guidance system. It also revealed the necessity of adjustment on the model structure to take into account the neuromuscular adaptation, which was proposed afterwards. By using this new driver model, a second experiment was carried out to study the adaptation of NMS to the haptic guidance system at different levels. With the help of a proposed time-varying parameter identification algorithm, the adaptation process was successfully captured in the form of parametric variations.

2.4 Main Contributions

The principal contributions of this thesis are as follows.

1. Proposition of the model-based analysis method in the study of adaptation. The method is further formalized and developed;

2. The effect of haptic guidance system and degraded visibility on lateral control performance was captured though two gain parameters in the two-point model as a first attempt of model-based analysis.

3. A new driver model is proposed and validated in order to study the adaptation of NMS. This model especially accounts for the haptic feedback through an indirect and direct loop. The indirect control loop refers to an internal model, which is adapted according to the haptic feedback torque. The direct control refers to an inner loop, which compensates the unpredictable part of the internal model in the haptic feedback to stabilize steering wheel.

4. With the new driver model, the driver's adaptation to haptic guidance system at varying levels is successfully captured through parametric variation of the internal model.

5. This parametric variation is estimated by a multi-UKF method consisted of two unscented Kalman filters (UKF). It is a time-varying parameter identification approach investigated in this thesis. A tuning strategy based on covariance matrices for the configuration of Kalman filter is proposed.

2.5 References

[1] K. Dutton, S. Thompson, and B. Barraclough, *The Art of CONTROL ENGINEERING*. 1997, ISBN: 978-0201175455.

[2] F. Mars and P. Chevrel, "Modelling human control of steering for the design of advanced driver assistance systems", *Annual Reviews in Control*, vol. 44, *Supplement C*, pp. 292–302, 2017, ISSN: 13675788.

[3] D. T. McRuer, R. W. Allen, D. H. Weir, and R. H. Klein, "New Results in Driver Steering Control Models", *Human Factors: The Journal of the Human Factors and Ergonomics Society*, vol. 19, *4*, pp. 381–397, Aug. 1977.

[4] E. Donges, "A Two-Level Model of Driver Steering Behavior", *Human Factors: The Journal of the Human Factors and Ergonomics Society*, vol. 20, *6*, pp. 691–707, Dec. 1978.

[5] R. A. Hess and A. Modjtahedzadeh, "A Control Theoretic Model of Driver Steering Behavior", *IEEE Control Systems Magazine*, vol. 10, *5*, pp. 3–8, 1990.

[6] M. Land and J. Horwood, "Which parts of the road guide steering?", *Nature*, vol. 377, *6547*, pp. 339–340, Sep. 1995, ISSN: 00280836.

[7] D. D. Salvucci and R. Gray, "A two-point visual control model of steering", *Perception*, vol. 33, *10*, pp. 1233–1248, 2004.

[8] D. A. Abbink and M. Mulder, "Neuromuscular Analysis as a Guideline in designing Shared Control", *in Advances in Haptics*, M. H. Zadeh, Ed., Rijeka: IntechOpen, 2010, ch. 27.

[9] D. A. Abbink, M. Mulder, and E. R. Boer, "Haptic shared control: Smoothly shifting control authority?", *Cognition, Technology and Work*, vol. 14, *1*, pp. 19–28, 2012, ISSN: 14355558.

[10] A. Pick, "Neuromuscular dynamics and the vehicle steering task", Ph.D. dissertation, University of Cambridge, 2004.

[11] D. Toffin, G. Reymond, A. Kemeny, and J. Droulez, "Role of steering wheel feedback on driver performance: driving simulator and modeling analysis", *Vehicle System Dynamics*, vol. 45, *4*, pp. 375–388, 2007.

[12] C. Sentouh, P. Chevrel, F. Mars, and F. Claveau, "A sensorimotor driver model for steering control", *Conference Proceedings - IEEE International Conference on Systems, Man and Cybernetics*, *October*, pp. 2462–2467, 2009, ISSN: 1062922X.

[13] N. Kim and D. J. Cole, "A model of driver steering control incorporating the driver's sensing of steering torque", *Vehicle System Dynamics*, vol. 49, *10*, pp. 1575–1596, 2011.

[14] C. J. Nash and D. J. Cole, "Development of a novel model of driver-vehicle steering control incorporating sensory dynamics", *The Dynamics of Vehicles on Roads and Tracks - Proceedings of the 24th Symposium of the International Association for Vehicle System Dynamics, IAVSD 2015*, pp. 57–66, 2016.

[15] L. Saleh, P. Chevrel, F. Mars, J. F. Lafay, and F. Claveau, "Human-like cybernetic driver model for lane keeping", *in Proceedings of the 18th IFAC World Congress*, 2011, pp. 4368–4373, ISBN: 9783902661937.

[16] Z. Wang, T. Kaizuka, and K. Nakano, "Effect of Haptic Guidance Steering on Lane Following Performance by Taking Account of Driver Reliance on the Assistance System", *in Proceedings - 2018 IEEE International Conference on Systems, Man, and Cybernetics, SMC 2018*, 2018, ISBN: 9781538666500.

[17] N. Wiener, D. Hill, and S. Mitter, *Cybernetics or Control and Communication in the Animal and the Machine, Reissue of the 1961 second edition*. MIT Press, 2019, ISBN: 9780262355919.

[18] M. Plöchl and J. Edelmann, *Driver models in automobile dynamics application*, 7-8. 2007, vol. 45, pp. 699–741, ISBN: 0042311070143.

[19] M. Mulder, D. Pool, D. Abbink, E. Boer, and M. van Paassen, "Fundamental Issues in Manual Control Cybernetics", 19, 13th IFAC Symposium on Analysis, Design, and Evaluation of Human-Machine Systems HMS 2016, vol. 49, 2016, pp. 1–6.

[20] M. Mulder, D. M. Pool, D. A. Abbink, E. R. Boer, P. M. Zaal, F. M. Drop, K. Van Der El, and M. M. Van Paassen, "Manual Control Cybernetics: State-of-the-Art and Current Trends", *IEEE Transactions on Human-Machine Systems*, vol. 48, *5*, pp. 468–485, 2018, ISSN: 21682291.

[21] D. A. Abbink, M. Mulder, and E. R. Boer, "Haptic shared control: Smoothly shifting control authority?", *Cognition, Technology and Work*, vol. 14, *1*, pp. 19–28, 2012, ISSN: 14355558.

[22] M. Mulder, D. A. Abbink, and E. R. Boer, "Sharing control with haptics: Seamless driver support from manual to automatic control", *Human Factors*, vol. 54, *5*, pp. 786–798, 2012.

[23] R. Boink, M. M. Van Paassen, M. Mulder, and D. A. Abbink, "Understanding and reducing conflicts between driver and haptic shared control", *Conference Proceedings - IEEE International Conference on Systems, Man and Cybernetics*, vol. 2014-January, *January*, pp. 1510–1515, 2014, ISSN: 1062922X.

[24] G. Markkula and J. Engström, "A Steering Wheel Reversal Rate Metric for Assessing Effects of Visual and Cognitive Secondary Task Load", *in Proceedings of the 13th ITS World Congress.*, 2006, ISBN: 0000000302.

[25] F. Mars, M. Deroo, and C. Charron, "Driver adaptation to haptic shared control of the steering wheel", *in 2014 IEEE International Conference on Systems, Man, and Cybernetics (SMC)*, 2014, pp. 1505–1509.

[26] F. Mars, M. Deroo, and J.-M. Hoc, "Analysis of human-machine cooperation when driving with different degrees of haptic shared control", *IEEE Transactions on Haptics*, vol. 7, *3*, pp. 324–333, 2014, ISSN: 19391412.

[27] I. Frissen and F. Mars, "The Effect of Visual Degradation on Anticipatory and Compensatory Steering Control", *Quarterly Journal of Experimental Psychology*, vol. 67, *3*, pp. 499–507, Mar. 2014, ISSN: 1747-0218.

[28] D. W. J. Van Der Wiel, M. M. van Paassen, M. Mulder, M. Mulder, and D. A. Abbink, "Driver Adaptation to Driving Speed and Road Width: Exploring Parameters for Designing Adaptive Haptic Shared Control", *in 2015 IEEE International Conference on Systems, Man, and Cybernetics*, 2015, pp. 3060–3065.

Part II

Methodology

Chapter 3

Experiment Platform

3.1 Driving Simulator SCANeR

3.1.1 Hardware

All the experiments in this thesis were performed on a fixed-base driving simulator in the Laboratoire des Sciences du Numérique de Nantes (LS2N), as shown in Figure 3.1. This cockpit consists of following parts:

Figure 3.1 – Fixed-based driving simulator.

- Three liquid crystal displays (LCD) covering a field of view of 25° high and 115° wide for reproducing visual scene;
- A dashboard with a speedometer, a tachometer, an odometer and a fuel gauge;
- A steering-wheel connected with an active steering wheel system (ASWS) supplied by TRW Conekt and Stirling Dynamics Limited;

Table 3.1 – Technical specifications of sensors

Sensor	Range	Accuracy
Steering-wheel angle	±1600°	±0.1°
Steering-wheel velocity	±5 rps	±0.001 rps
Steering-wheel torque	±8 Nm	±0.001 Nm

- A basic control panel with several buttons and switches for simulating secondary tasks during driving (radio, air-conditioning, in-car entertainment systems etc.);
- A gas pedal, a brake pedal and a clutch pedal;
- A five-speed gear stick;
- A hand brake;
- A seat with seat belt;

The ASWS is mounted with sensors for measuring the angular position, angular velocity and torque on the steering wheel. Their technical specifications are listed in Table 3.1.

3.1.2 Software

The simulator is powered by SCANeR studio, which is a comprehensive driving simulation software package developed by OKTAL company. It is used for vehicle ergonomics and advanced engineering studies as well as for road traffic research and development. It is also used for human factor studies and driver training. This software package provides several applications or modules, which communicates with each other through a common communication protocol via network. The different modules are illustrated in the Figure 3.2.

- Scenario module defines the driving session such as terrain, vehicle type, weather and illumination condition etc. It also allows to manage events in order to create situations or accidents. These configurations are later used when the session is launched and simulated by the simulation module.
- Acquisition module allows the communication between the hardware and the software. Operations in the cockpit, such as turning the steering wheel or pressing the

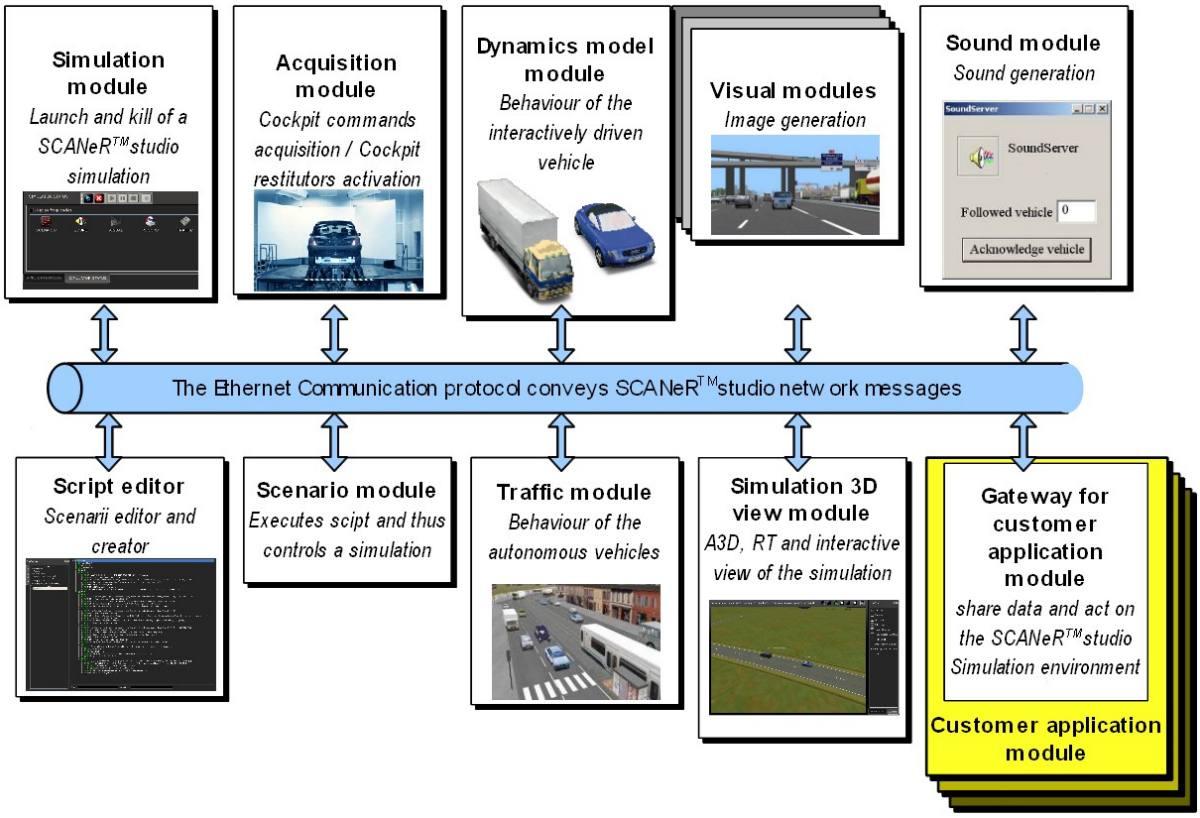

Figure 3.2 – SCANeR studio modules concept[1].

pedals, are acquired as the inputs of vehicle model in the simulation. This module also allows initialization and configuration of the steering-wheel in order to simulate the feeling of real steering systems.

- Dynamics model module is in charge of the definition and simulation of vehicle models used in each scenario. These models are established by considering detailed components including chassis, engine, steering etc. By selecting the model it is possible to simulate different kinds of vehicles with the same cockpit.

- Script editor module executes user-defined scripts during simulation. The script is usually dedicated to manage events, recording and exporting signals related to vehicle.

- Custom application module is where a custom program could be defined and executed during simulation. The module provides a set of different application programming interface (API) as a software development kit (SDK) to interface with

relevant third party software or system, such as C/C++, Simulink, Labview etc.

In this thesis, the haptic guidance system is designed in Matlab / Simulink and implemented as a custom application module. It takes signals exported from a pre-defined script as inputs. These signals are calculated by dynamics model module during simulation. The output of the system is directly applied on the steering-wheel through the acquisition module. Both the input and the output signals are recorded for analysis afterwards.

3.1.3 Vehicle Model

A common family car, the Citroën C5, was selected as the vehicle model for all the experiments. For the sake of describing the technical specifications of the vehicle in simulation and synthesizing the control law of the haptic guidance system, a simplified vehicle dynamic model is needed. The bicycle model proposed by [2] is thus adopted (see Figure 3.3). The model could be written as Equation (3.1). The description of symbols are listed in Table 3.2. The value of parameters in the table are obtained either by the vehicle static analysis report from SCANeR or system identification (see Chapter 4).

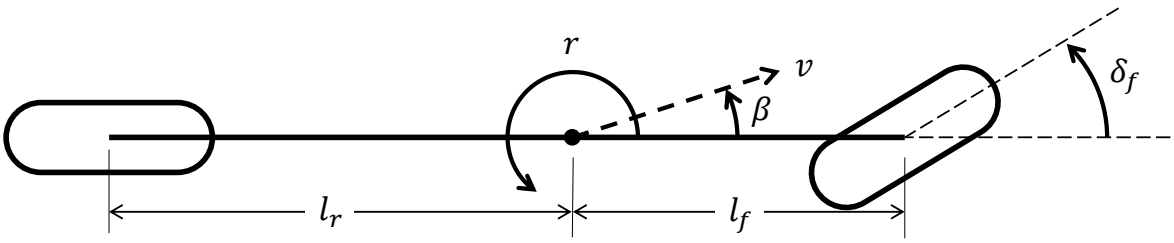

Figure 3.3 – Variables in bicycle model.

$$\begin{bmatrix} \dot{\beta} \\ \dot{r} \end{bmatrix} = \begin{bmatrix} -\dfrac{2(C_f + C_r)}{mv_x} & \dfrac{2(C_r l_r - C_f l_f)}{mv_x^2} - 1 \\ \dfrac{2(C_r l_r - C_f l_f)}{J} & -\dfrac{2(C_f l_f^2 + C_r l_r^2)}{Jv_x} \end{bmatrix} \begin{bmatrix} \beta \\ r \end{bmatrix} + \begin{bmatrix} \dfrac{2C_f}{mv_x} \\ \dfrac{2C_f l_f}{J} \end{bmatrix} \delta_f + \begin{bmatrix} \dfrac{1}{mv_x} \\ \dfrac{l_w}{J} \end{bmatrix} F_w \qquad (3.1)$$

Table 3.2 – Description of symbols in the bicycle model.

Symbol	Description (Unit)	Value
β	Slip angle (rad)	signal
r	Yaw rate (rad/s)	signal
C_f	Front tire stiffness (N/rad)	51845
C_r	Rear tire stiffness (N/rad)	54610
m	Vehicle total mass (kg)	1834.9
J	Vehicle moment of inertia ($\mathrm{kg\,m^2}$)	2800
l_f	Distance between CoG*and front axle (m)	1.289
l_r	Distance between CoG and rear axle (m)	1.611
v_x	Vehicle longitudinal speed (m/s)	signal
F_w	Wind force (N)	0
l_w	Distance between CoG and wind hit point on vehicle (m)	-

* CoG: Center of gravity.

3.2 Haptic Guidance System

The haptic guidance system employed in this thesis was chosen from the publication [3]. The proposed methodology facilitates the design and numerical implantation of lateral assistance, ensuring stability and guaranteed performance. The global architecture is shown in Figure 3.4. The vehicle-road block represents the real dynamics and movement of vehicle on road and the driver block represents the lateral control behavior of human in reality. The haptic guidance system assists the human driver by applying a guidance torque, Γ_a on steering wheel. This torque is the sum of torques generated by an anticipatory part and a compensatory part, $\Gamma_{a_{FF}}$ and $\Gamma_{a_{FB}}$, each has been scheduled by a factor called *sharing level* (the α_{ant} and α_{comp}), respectively.

The anticipatory part is a trajectory generator based on the simulation of a virtual autonomous vehicle. The virtual vehicle is represented by a vehicle-road (VR) model, which incorporates the bicycle model in Equation (3.1), a steering system and the movement of vehicle on road. The autonomous driving of the virtual vehicle is realized through a H_2-Preview feedback controller [4] taking previewed road curvature, $\rho_{previewed}$, as input. With this simulation, a reference trajectory for vehicle-road system states, x_{ref}, and steering-wheel torque, Γ_{ref}, are generated . In summary, the whole block could be written

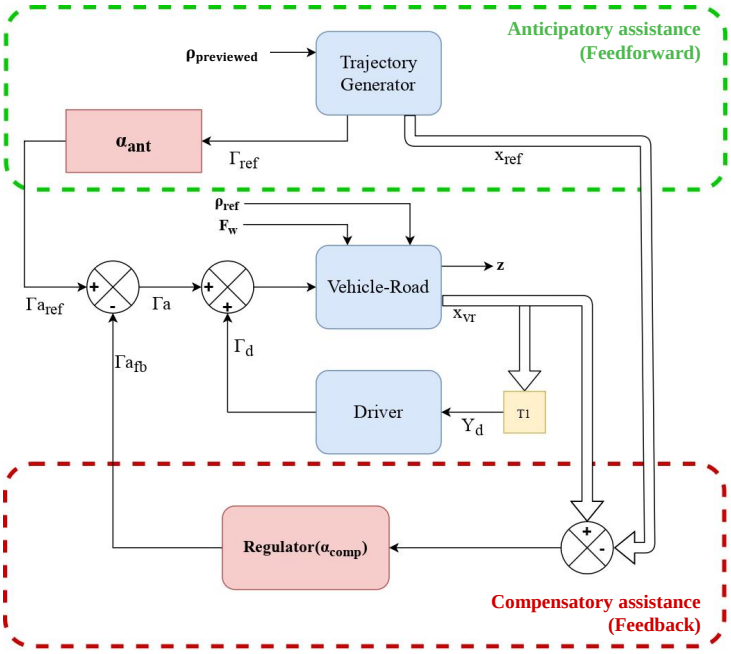

Figure 3.4 – Haptic shard control strategy [3] © 2019 IEEE.

as follows:

$$\begin{bmatrix} x_{ref} \\ \Gamma_{ref} \end{bmatrix} = K_{FF}(s)\rho_{previewed}, \Gamma_{a_{FF}} = \alpha_{ant}\Gamma_{ref} \tag{3.2}$$

where $K_{FF}(s)$ is the closed-loop transfer function matrix of the H_2-Preview controller and VR model.

The compensatory part is based on a static output feedback synthesis. A mixed H_2/H_∞ control law is applied to the difference between the real and the virtual vehicle's states from the trajectory generator . The H_2 criterion defines the lateral control performance by weighing up signals including heading error angle, lateral error, lateral acceleration and guidance torque with the matrix Q_z. The H_∞ norm is used to ensure some unstructured robustness by bounding input sensitivity function of the whole closed-loop system, $S_{input}(s)$, so that a minimum input gain-phase (or module) margin is guaranteed. The multi-criteria optimization is realized on the basis of a driver-vehicle-road (DVR) model, which is the combination of the driver model in [4] and the before-mentioned VR model. Due to the non-convexity of this problem, the optimal solution of feedback gain K_{FB} is finally obtained with the Systune tools provided by Matlab. The torque output from the

feedback block could be written as follows:

$$\Gamma_{a_{FB}} = K_{FB}(\alpha_{comp})(x_{vr} - x_{ref}) \tag{3.3}$$

where $K_{FB}(\alpha_{comp})$ depends on α_{comp} and satisfies

- the internal stability of the DVR model;
- the solution of $\min\|T_{zw}(s)\|_2$ under the constraint $\|S_{input}(s)\|_\infty < S_{max}$;

3.3 References

[1] OKTAL, "SCANeR studio version 1.7 user manual", Tech. Rep., 2017, p. 138.

[2] R. Rajamani, *Vehicle Dynamics and Control*, ser. Mechanical Engineering Series. Springer US, 2006, ISBN: 9780387288239.

[3] B. Pano, P. Chevrel, and F. Claveau, "Anticipatory and compensatory e-assistance for haptic shared control of the steering wheel", *2019 18th European Control Conference, ECC 2019*, pp. 724–731, 2019.

[4] L. Saleh, P. Chevrel, F. Mars, J. F. Lafay, and F. Claveau, "Human-like cybernetic driver model for lane keeping", *in Proceedings of the 18th IFAC World Congress*, 2011, pp. 4368–4373, ISBN: 9783902661937.

Chapter 4

Parameter Identification I: Prediction Error Minimization

4.1 Introduction

Essentially, there are two approaches to constructing a model [1]. In the first, the system is divided into several blocks. A mathematical description is then established for each block by working from the existing physical laws which describe the behavior of system. In the second, it is assumed that an experiment can be carried out on the system and that a mathematical model of the system can be found from the results. However, either single approach is not sufficient for modeling driver's behavior. For the first, the difficulty is to obtain the value of parameters in the model, as they are not directly measurable physical quantities. For the second, a pure mathematical model describing the relationship between input and output signals provides only limited information about the property of the system. An ideal method is the combination of both approaches: a model structure based on physiological or psychological laws is established firstly with meaningful parameters; the value of parameters is then estimated with experiments. The latter is usually referred to as system identification, or more specifically grey-box system identification (as the model structure is preset) which is adopted in this thesis.

4.2 General Procedure of Model Identification

In general, the construction of a driver model via the system identification is performed in several steps.

Step 1: Selection of model structure. Various types of driver model have been discussed in Chapter 2. They are obtained after careful modeling with *a prior* knowledge and researches on human behavior in steering task. In this study, models with

meaningful parameters are more interesting than an input-output abstract representation of signals. The parametric difference may give an interpretation of how the model property changes.

Step 2: Data acquisition. Experiments need to be carried out to record input-output data. These experiments should be specifically designed so that the data is maximally informative. For example, straight roads are less informative than curves; curves with constant radius of curvature are less informative than those with varying radius of curvature. In both cases there is less lateral control behavior, which makes it difficult to identify the model.

Step 3: Computation of optimal model. This is the algorithm for determining or estimating the parameter vector. A cost function, or a criterion, is usually chosen to assess the model quality of reproducing the measured data. By minimizing this criterion, an (local) optimal model with estimated parameters could be obtained. In this thesis, two methods are considered, one for linear time-invariant systems and another for linear time-variant systems. They are the main methods employed for estimating the parameters of the driver model in Chapter 7 to 9.

Step 4: The optimal solution may not be the best model which reproduces driver's behavior during the experiment. To verify the generality of the model, there are several validation methods. A simple and intuitive way is by comparing the predicted and measured data. The model and parameter uncertainties are also important when models with the same structure but different parameter values are obtained. These topics are also considered in this chapter.

Finally, this procedure is not one-way but iterative. If the model validation fails, it is necessary to go back to the first step and refine the model structure.

4.3 Prediction Error Minimization Method

Under the hypothesis that the driver model is a linear time-invariant system, the prediction error minimization (PEM) approach proposed by [2] could be applied. It is a general parameter estimation framework which integrates several well-known algorithms such as the least-squares (LS) method or the maximum-likelihood (ML) method.

Supposing that in the first step of identification, a certain driver model structure, $\mathcal{M}$, has been selected as the candidate model and each particular model $\mathcal{M}(\Theta)$ is parametrized with a d-dimension parameter vector Θ. The range of possible parameter values forms a subset of $\mathbb{R}^d$ space: $\Theta \in \mathbb{D}_{\mathcal{M}} \subseteq \mathbb{R}^d$. The set of models then can be defined as

$$\mathcal{M}^* = \{\mathcal{M}(\Theta) \mid \Theta \in \mathbb{D}_{\mathcal{M}}\} \tag{4.1}$$

A model structure also defines its input and output signals. The input vector of p-dimension is denoted as $u(t) \in \mathbb{R}^p$, while $y(t|\Theta) \in \mathbb{R}^q$ represents the output vector of q-dimension and depends on the parameter sequence.

With the second step of identification, a batch of experimental data, $\mathcal{Z}^N$, could be sampled:

$$\mathcal{Z}^N = [(y[1], u[1]), (y[2], u[2]), \ldots, (y[N], u[N])] \tag{4.2}$$

where N is the number of samples. The brackets ($y[\cdot]$ and $u[\cdot]$) represent the fact that the sampled signals are discrete. The parameter estimation method thus consists of determining a mapping from the data $\mathcal{Z}^N$ to the parameter value set $\mathbb{D}_{\mathcal{M}}$:

$$\mathcal{Z}^N \rightarrow \hat{\Theta}_N \in \mathbb{D}_{\mathcal{M}} \tag{4.3}$$

In general, the prediction ability of a model is the main aspect for evaluating such a mapping obtained. For a certain model $\mathcal{M}(\Theta)$ with a parameter vector Θ, the prediction error of the model could be calculated for all data points in $\mathcal{Z}^N$:

$$e[k|\Theta] = y[k] - \hat{y}[k|\Theta], k = 1, 2, ..., N \tag{4.4}$$

where $\hat{y}[k|\Theta_*]$ is the predicted output from the model $\mathcal{M}(\Theta)$. The principle of parameter estimation using prediction error is therefore defined as follows, according to [2]:

> *Based on $\mathcal{Z}^N$ we can compute the prediction error $e[k|\Theta]$ as (4.4). At time $k = N$, select $\hat{\Theta}_N$ so that the prediction errors $e[k|\hat{\Theta}_N]$ becomes as small as possible for $k = 1, 2, \ldots, N$.*

The prediction error is a vector with q-dimension as the output signal y. If each prediction error vector at time step k is concatenated after the previous one, a matrix of prediction errors in $q \times N$ dimension can then be formed. To measure the "size" of the

matrix, any norm in $\mathbb{R}^{q\times N}$ could be applied. In the PEM method, the following norm is chosen:

$$J_N(\Theta, \mathcal{Z}^N) = \frac{1}{N}\sum_{k=1}^{N} \ell(e[k|\Theta])) \tag{4.5}$$

where $\ell(\cdot)$ is a scalar-valued function. The estimate $\hat{\Theta}_N$ is then defined by minimizing this criterion:

$$\hat{\Theta}_N = \underset{\Theta\in\mathbb{D}_{\mathcal{M}}}{\arg\min}\, J_N(\Theta, \mathcal{Z}^N) \tag{4.6}$$

A common choice of $\ell(\cdot)$ would be an Euclidean norm:

$$\ell(e[k|\Theta]) = \|e[k|\Theta]\|_2^2 = e^T[k|\Theta]e[k|\Theta] \tag{4.7}$$

Therefore, the criterion becomes:

$$J_N(\Theta, \mathcal{Z}^N) = \frac{1}{N}\sum_{k=1}^{N} e^T[k|\Theta]e[k|\Theta] \tag{4.8}$$

In case of mono-output system, the prediction error $e[k|\Theta]$ is scalar, and the criterion (4.8) becomes:

$$J_N(\Theta, \mathcal{Z}^N) = \frac{1}{N}\sum_{k=1}^{N} e^2[k|\Theta] \tag{4.9}$$

4.4 Practical Use of PEM

4.4.1 Identifiability

The identifiability concept deals with a fundamental question in the application of system identification[2]: will the identification procedure yield a unique solution for the parameter Θ, and/or is the resulting model enough general to represent the true system? These questions involve two aspects: the selected model structure and the collected experimental data. On the one hand, if different parameter values determine different models, the identifiability of the selected model structure could be guaranteed. A usual counterexample of this situation is when several gain parameters are connected serially, each has an interpretation and the intermediate signal in-between is not measurable. In that case all the gain parameters are not identifiable because only their product is unique. On the

other hand, the data set needs to be informative enough to excite the system in order to distinguish between different models. In driver steering model identification, this issue always happens when driving on a straight road or even a curve with constant radius, because there are less steering behavior and the input signals are less informative. It is thus proposed to carry out experiments on curve roads with changing curvature, and try to identify the model sequentially (part-by-part) if there is an identifiability issue in the model structure.

4.4.2 Model Validation

Once the optimal estimates of parameters are given by calculation, a crucial question at this stage is whether the model with this set of parameters is "good" enough. To answer this question, the model validation could be performed by verifying whether the model agree sufficiently well with the observed data. A model quality metric, the FIT value, is commonly used to assess the quality of identified model. One possible calculation using normalized root mean squared error is as follows:

$$FIT = \left(1 - \frac{\left\| y[k] - \hat{y}[k|\hat{\Theta}_N] \right\|_2}{\left\| y[k] - mean(\hat{y}[k|\hat{\Theta}_N]) \right\|_2}\right) \times 100\% \tag{4.10}$$

where $y[k]$ is the measured output and $\hat{y}[k|\hat{\Theta}_N]$ is the predicted output from the model with estimated parameters $\hat{\Theta}_N$. This metric varies between $-\infty$ (worst) to 100% (best). If it equals to 0, the model is then no better than a straight line equal to the mean of the data. In practice, the experimental data is always separated into to two parts: one part for identification and another for validation. If the FIT values calculated with both parts are acceptable, it suggests that the model agrees well with the observed data and has a good capacity of prediction.

4.4.3 Distribution of Parameter Estimates

Another crucial question is the reliability of the estimated parameter values. One may view a data set collected from an experiment with human driver as a sample due to the randomness of noise signals. If the experiment is repeated, all the estimated values of each parameter should be distributed around the "true" parameter value, if it exists. This distribution indicates the distance between the identified and the "true" value. To

assess this distribution, an analysis of parameter uncertainty could be performed. It has been demonstrated in [2] that the parameters estimated by PEM method follow the Theorem 4.1.

Theorem 4.1 *Consider the estimate* $\hat{\Theta}_N$ *determined by* (4.6) *and* (4.8)*. Assume that the model structure is linear and uniformly stable and that the data set* $\mathcal{Z}^N$ *is informative. Assume also that for a unique value* $\Theta^* \in \mathbb{D}_{\mathcal{M}}$ *we have*

$$\hat{\Theta}_N \to \Theta^*, \textit{with probability 1 as } N \to \infty \tag{4.11}$$

and

$$\sqrt{N}(\hat{\Theta}_N - \Theta^*) \sim As\mathcal{N}(0, Q_\Theta) \tag{4.12}$$

The $\sim As\mathcal{N}(0, Q_\Theta)$ means that the difference asymptotically follows a d-dimensional normal distribution with 0 mean and covariance Q_Θ ($d = dim(\Theta)$) when the number of data samples N tends to infinity. For a quadratic norm as (4.7), the analytic solution of Q_Θ is given in [2]:

$$\begin{aligned} Q_\Theta = &\left(\overline{E}\psi[k|\Theta^*]\psi^T[k|\Theta^*]\right)^{-1} \\ &\times \left(\overline{E}\psi[k|\Theta^*]\Lambda^*\psi^T[k|\Theta^*]\right)\left(\overline{E}\psi[k|\Theta^*]\psi^T[k|\Theta^*]\right)^{-1} \end{aligned} \tag{4.13}$$

where

$$\psi[k|\Theta^*] = \left.\frac{\partial \hat{y}[k|\Theta]}{\partial \Theta}\right|_{\Theta=\Theta^*} \tag{4.14}$$

is a $d \times p$ matrix and

$$\Lambda^* = \overline{E}e[k|\Theta^*]e^T[k|\Theta^*] \tag{4.15}$$

is a $p \times p$ matrix. The symbol $\overline{E}$ denotes the following calculation:

$$\overline{E}f[k] = \lim_{N\to\infty} \frac{1}{N}\sum_{k=1}^{N} Ef[k] \tag{4.16}$$

with E as the expectation and an implied assumption that the limit exists.

In reality, the number of data samples N is finite and the limit Θ^* cannot be reached. It is possible to use $\hat{\Theta}_N$ as an estimate of Θ^* and replace the symbol $\overline{E}$ with $\frac{1}{N}\sum_{k=1}^{N}$. In

this case an estimate of Q_Θ from data set $\mathcal{Z}^N$ could be written as follows:

$$\hat{Q}_N = \left(\frac{1}{N}\sum_{k=1}^{N}\psi[k|\hat{\Theta}_N]\psi^T[k|\hat{\Theta}_N]\right)^{-1} \times \left(\frac{1}{N}\sum_{k=1}^{N}\psi[k|\hat{\Theta}_N]\hat{\Lambda}_N\psi^T[k|\hat{\Theta}_N]\right)\left(\frac{1}{N}\sum_{k=1}^{N}\psi[k|\hat{\Theta}_N]\psi^T[k|\hat{\Theta}_N]\right)^{-1} \tag{4.17}$$

with

$$\psi[k|\hat{\Theta}_N] = \left.\frac{\partial\hat{y}[k|\Theta]}{\partial\Theta}\right|_{\Theta=\hat{\Theta}_N} \tag{4.18}$$

$$\hat{\Lambda}_N = \frac{1}{N}\sum_{k=1}^{N} e[k|\hat{\Theta}_N]e^T[k|\hat{\Theta}_N] \tag{4.19}$$

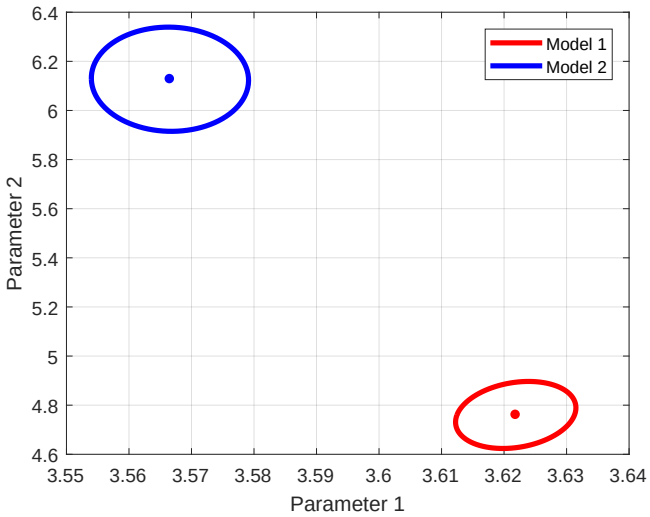

Figure 4.1 – Example of two confidence regions. As there are only two identified parameters, the ellipsoid becomes ellipse. Each ellipse is one confidence region. The center is the estimated parameter vector $\hat{\Theta}_N$.

Furthermore, from (4.12) there is

$$\eta_N = (\hat{\Theta}_N - \Theta_*)^T Q_\Theta^{-1}(\hat{\Theta}_N - \Theta_*) \sim As\chi^2(d) \tag{4.20}$$

which implies that η_N converges in distribution to the $\chi^2(d)$ distribution as N tends to infinity. A confidence level α (e.g., 90%) could be chosen in this case to obtain a confidence

region given by the following equation:

$$P\Big((\hat{\Theta}_N - \Theta^*)^T \hat{Q}_N^{-1} (\hat{\Theta}_N - \Theta^*) \leq \chi_\alpha^2(d)\Big) = \alpha \tag{4.21}$$

with $\chi_\alpha^2(d)$ as the α-level of the $\chi^2(d)$-distribution and Q_Θ approximated by $\hat{Q}_N$. This equation indicates that, with α probability, the "true" parameter vector Θ^* lies inside an ellipsoid defined in the R^d space, of which the center is $\hat{\Theta}_N$ and the axes are determined by the eigenvalues and eigenvectors of $\chi_\alpha^2(d)\hat{Q}_N$ (see Figure 4.1 for an example).

The analysis of parameter uncertainties is important for studying the parameter variation in driver model under different driving conditions. It decides whether the difference between two parameter sets is the consequence of randomness in experiment, or the different experimental conditions. If the confidence region of two parameter sets do not intersect with each other, it can be concluded that these two models are statistically different, and the difference is probably caused by the variables manipulated during experiments.

4.5 References

[1] K. Dutton, S. Thompson, and B. Barraclough, *The Art of CONTROL ENGINEERING*. 1997, ISBN: 978-0201175455.

[2] L. Ljung, *System Identification: Theory for the User*, 2nd ed., ser. Prentice Hall information and system sciences series. Prentice Hall PTR, 1999, ISBN: 9780136566953.

Chapter 5

Parameter Identification II: Unscented Kalman Filter

5.1 Introduction

As proposed by the new cybernetics theory in Chapter 2, drivers should be considered as time-variant system to be able to account for learning and adaptation process. In addition, a time-variant system identification method is needed to study the parametric evolution during these process. The method based on the unscented Kalman filter (UKF) proposed in [1] was adopted and further developed in this thesis. The basic idea is to consider varying parameters as augmented system states and estimate them together with original system states using Kalman filter. A tuning methodology was also proposed on the basis of a compromise between the rapidity and noise sensitivity of estimations.

5.2 Full article

This article was accepted and presented at the 3rd IFAC Workshop on Linear Parameter Varying Systems (LPVS) 2019. It is available at: `https://doi.org/10.1016/j.ifacol.2019.12.359`. Note that some symbols and the chapter numbering were modified to be coherent with those used in thesis.

5.2.1 Abstract

Advanced Driver-Assistance Systems (ADAS) have become an essential part of modern cars. Among the solutions proposed, haptic shared control of the steering wheel is increasingly being studied. A fundamental question is how drivers adapt their behavior to these systems. This article proposes to use the unscented Kalman filter (UKF) to identify the variation over time in the psychological and neuromuscular parameters of a driver struc-

tured model. The goal here is to understand how the driver adapts to changes, whether regarding the behavior of the steering system, the visibility or the road conditions. The LPV system considered for identification is known as the cybernetic driver model. Two experiments carried out respectively with Simulink and on a driving simulator provide the data. The methodology proposed for tuning the UKF is studied from the results obtained with those data. A multi-UKF strategy is also considered. The methodology reveals useful when a compromise between rapidity and precision has to be achieved for parameters estimation. It opens the way to a detailed analysis of the driver's parameter variations within the multi-UKF framework.

5.2.2 Introduction

Modern cars are more and more equipped with Advanced Driver-Assistance Systems (ADAS). For example, the Lane Departure Avoidance (LDA) systems warn the driver when the vehicle begins to move out of its lane unless a turn signal is on in that direction. The Lane Keeping Support (LKS) or lane centering systems help driver stay in the lane relieving driver of the steering task. Such systems either warn the driver in a critical situation, like the LDA, or take over full control of a subtask like the LKS. When steering is fully automated, the human driver will act like a supervisor of the system and monitors unexpected changes. As a consequence, the driver is out of the perceptual-motor loop, without any direct feedback from the steering wheel [2].

An alternative approach, haptic "shared control" has been proposed [3], [4]. In shared control, both human driver and automation interact through the steering wheel, which continuously provides feedback of the system actions. In addition, the human can override the system or give way to it, if it is safe and necessary to do so [5]. Haptic shared control driver-assistance systems have shown their advantages in improvement of driver's objective performance [6] and become an increasingly popular approach to facilitate control and communication between human and intelligent machines.

One of the fundamental questions in the development and implementation of haptic shared control systems concerns how the action of driver-assistance systems can smoothly take part in the driver's sensorimotor loop. Incorporating a cybernetic driver model in the controller design has been proposed as a solution [7]–[10]. This approach allows to take into account the predictions of the driver model to improve human-machine cooperation.

Another open question related to the design of haptic shared control systems is how to consider the driver potential adaption to the system. Adaptation may be due to the

prolonged use of the system [11] or to variations in the environment [12], for instance. This may be achieved by adaptation of the driver model parameters as a function of time or conditions. The present paper aims to evaluate a method to achieve this goal.

Previous interdisciplinary researches focusing on the estimation of driver's distraction [1] showed that one possible methodology is identifying in real-time the variation of perceptual and neuromuscular parameters in a driver cybernetic model. Since the parameters in the driver model are varying, this approach is actually dealing with a Linear Parameter-Varying (LPV) system identification problem.

To deal with the driver's adaptation process to different changes in his or her driving environment, this article adopts the idea of using the unscented Kalman filter (UKF) to identify an embedded driver model. The tuning methodology will be emphasized and a multi-UKF approach will be proposed. The method is validated through experiments. In section 5.2.3, the parametrized cybernetic driver model is presented. Section 5.2.4 implements the identification method based on UKF, section 5.2.5 discusses its tuning methodology and proposes a practical approach. Section 5.2.6 shows results of two experiments to validate the method, one with simulation data and another with experimental data from a driving simulator. Section 5.2.7 summarizes general conclusions.

5.2.3 Cybernetic Driver Model

The principle of a cybernetic driver model is based on a "perception-action" cycle which represents perceptual and motor processes [13]. The development of such models originates from human operator model in aeronautics [14] during the 1950s. [15] proposed a seminal two-level model for vehicle control with anticipatory open loop control and compensatory closed loop control. During the 1980s and 1990s, human physical attributes and neuromuscular system were taken into consideration [16]. A visual control model of steering has been proposed later [17]. In an effort to integrate all those models, a new model has been proposed [7], [8], [10]. It represents the driver's visual behavior as the processing of two points on the road, a far point and a near point. The near point is used to compensate for lateral position errors while the far point is used to anticipate the road ahead. The visual information is then processed with a neural delay before feeding to the neuromuscular model. The neuromuscular action is modeled based on neurophysiology [18]. The block diagram of the cybernetic driver model is shown in Figure 5.1. Signals and parameters are described in Table 5.1 and Table 5.2.

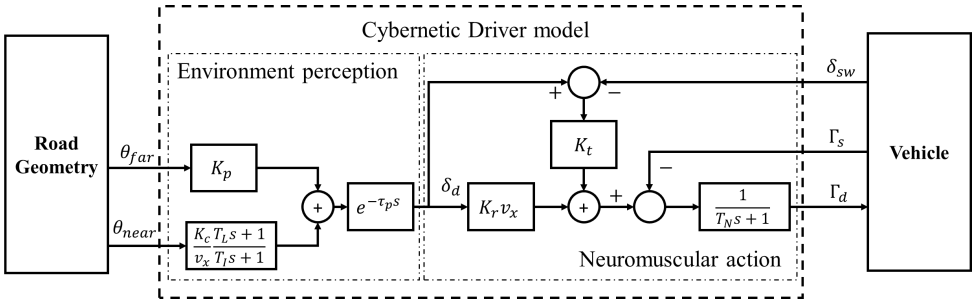

Figure 5.1 – Cybernetic driver model.

Table 5.1 – Description of signals in driver model.

Signal	Description
θ_{far}	Visual anticipation angle
θ_{near}	Visual compensation angle
δ_{SW}	Steering wheel angle
Γ_s	Self-aligning torque
Γ_d	Driver steering wheel torque
δ_d	Driver intention of steering wheel angle

Table 5.2 – Description of parameters in driver model.

Parameter	Description	Nominal Value
K_p	Visual anticipatory gain	3.4
K_c	Visual compensatory gain	15
T_I, T_L	Compensation time constant	1, 3
τ_p	Processing delay	0.04
K_r	Internal gain of steering column stiffness	1
K_t	Gain of stretch reflex	12
T_N	Neuromuscular time constant	0.1
v_x	Vehicle longitudinal velocity	18

The delay can be approximated by using 1st order Padé model:

$$e^{-\tau_p s} \approx \frac{1 - 0.5\tau_p s}{1 + 0.5\tau_p s} \tag{5.1}$$

The minimal realization of the cybernetic driver model depicted in Figure 5.1 could be written as follows:

$$\begin{cases} \dot{x}(t) = A(\Theta)x(t) + B(\Theta)u(t) + w(t) \\ y(t) = C(\Theta)x(t) + D(\Theta)u(t) + v(t) \end{cases} \tag{5.2}$$

with

Input $$u(t) = \begin{bmatrix} \theta_{far} & \theta_{near} & \delta_{SW} & \Gamma_s \end{bmatrix}^T \tag{5.3}$$

Output $$y(t) = \begin{bmatrix} \Gamma_d & \delta_d \end{bmatrix}^T \tag{5.4}$$

Parameters $$\Theta(t) = \begin{bmatrix} K_p & K_c & T_I & T_L & \tau_p & K_r & K_t & T_N \end{bmatrix}^T \tag{5.5}$$

$$A(\Theta) = \begin{bmatrix} -\frac{1}{T_I} & 0 & 0 \\ \frac{K_c}{v_x}\frac{2}{\tau_p}\left(1 - \frac{T_L}{T_I}\right) & -\frac{2}{\tau_p} & 0 \\ -\frac{K_r v_x + K_t}{T_N}\frac{K_c}{v_x}\left(1 - \frac{T_L}{T_I}\right) & 2\frac{K_r v_x + K_t}{T_N} & -\frac{1}{T_N} \end{bmatrix} \tag{5.6}$$

$$B(\Theta) = \begin{bmatrix} 0 & \frac{1}{T_I} & 0 & 0 \\ K_p\frac{2}{\tau_p} & \frac{K_c}{v_x}\frac{2}{\tau_p}\frac{T_L}{T_I} & 0 & 0 \\ -K_p\frac{K_r v_x + K_t}{T_N} & -\frac{K_r v_x + K_t}{T_N}\frac{K_c}{v_x}\frac{T_L}{T_I} & -\frac{K_t}{T_N} & -\frac{1}{T_N} \end{bmatrix} \tag{5.7}$$

$$C(\Theta) = \begin{bmatrix} 0 & 0 & 1 \\ -\frac{K_c}{v_x}\left(1 - \frac{T_L}{T_I}\right) & 2 & 0 \end{bmatrix} \tag{5.8}$$

$$D(\Theta) = \begin{bmatrix} 0 & 0 & 0 & 0 \\ -K_p & -\frac{K_c}{v_x}\frac{T_L}{T_I} & 0 & 0 \end{bmatrix} \tag{5.9}$$

where $w(t)$ and $v(t)$ are process noise and measurement noise, with respective covariance matrix Q_x and R.

5.2.4 Parameter Identification

Identification methods for LPV system have been intensively studied recently. For example, Tóth proposed an extension of the Refined Instrumental Variable (RIV) approach for closed loop LPV systems [19]; Zhang discussed about the local approach by interpolating individually estimated local linear time invariant (LTI) models [20]; Darwish introduced a nonparametric Gaussian regression approach based on prediction-error [21]; Rizvi presented another nonparametric method for state-space LPV model using kernelized machine learning [22]. In this section a parametric method based on unscented Kalman filter is proposed. It is demonstrated that under certain hypothesis, the driver LPV model (5.2) can be rewritten as a non-linear system (5.10) (see below) by augmenting system states in (5.2) with parameter dynamics. It therefore turns the parameter identification problem of the LPV system (5.2) to a non-linear state estimation problem associated to system (5.10). Compared to methods previously pointed out, the one chosen has the possibility of 1) balancing the rapidity and sensitivity of identification via tuning the dynamics of the state observer and 2) defining the dynamic of parameters according to a prior knowledge on the nature of parameter variations such as continuity, derivability, time constant etc.

5.2.4.1 Augmented Model and State Estimation

Before rewriting the driver model as an augmented system, working hypothesis must be made to guarantee the conditions of utilizing unscented Kalman filter (UKF) for parameter identification.

Hypothesis 5.1 *The driver model parameters are considered as time varying and are modeled as Wiener processes, i.e.* $\dot{\Theta}(t) = w_\Theta(t)$ *where* $w_\Theta(t) \sim N(0, \sigma_\Theta^2)$*, namely the* $\Theta(t)$ *is a Wiener process (scaling limit of a random walk), or a random walk itself in discrete time.*

Actually, different kinds of stochastic process could be chosen for $w_\Theta(t)$ based on *a priori* knowledge of parameter dynamics. For example, if $w_\Theta(t)$ is a sum of several Dirac functions with random amplitude at random time, the $\Theta(t)$ is thus a piece-wise constant signal.

Hypothesis 5.2 *The variations of all parameters are slower than those of system states.*

This hypothesis distinguishes, within the augmented system states defined below (see (5.10)), the variables predefined as "parameters" from the state variables as defined

in (5.2). If the parameters evolved more rapidly than the system states, the linearization performed implicitly to design the Kalman filter would be unjustified.

Under Hypothesis 5.1 & 5.2, the augmented system is defined as:

$$\begin{cases} \dot{x_a}(t) = f\Big(x_a(t), u(t)\Big) + w_a(t) \\ y(t) = g\Big(x_a(t), u(t)\Big) + v(t) \end{cases} \tag{5.10}$$

with

$$\text{Augmented system states } x_a(t) = \begin{bmatrix} x(t) & \Theta(t) \end{bmatrix}^T \tag{5.11}$$

$$\text{Augmented process noise } w_a(t) = \begin{bmatrix} w(t) & w_\Theta(t) \end{bmatrix}^T \tag{5.12}$$

$$\text{Paramter process noise covariance } Q_\Theta \tag{5.13}$$

$$\text{Augemented process noise covariance } Q_a \tag{5.14}$$

$$\text{State-transition function } f\Big(x_a(t), u(t)\Big) = \begin{bmatrix} A(\Theta)x(t) + B(\Theta)u(t) \\ 0 \end{bmatrix} \tag{5.15}$$

$$\text{Measurement function } g\Big(x_a(t), u(t)\Big) = C(\Theta)x(t) + D(\Theta)u(t) \tag{5.16}$$

A commonly used state estimator is the Luenberger observer. For the augmented system (3), such observer can be written as

$$\dot{\hat{x}}_a(t) = f\Big(\hat{x}_a(t), u(t)\Big) + L(t)\Big[y(t) - g\Big(\hat{x}_a(t), u(t)\Big)\Big] \tag{5.17}$$

where $L(t)$ is the observer gain. If the augmented system (5.10) is considered as a deterministic system without noise $w_a(t)$ and $v(t)$, an optimal observer gain for state estimation, which is also the Kalman gain, can be obtained by minimizing the cost function (5.18).

$$\begin{aligned} J(\hat{x}_{a,0}, \hat{x}_a) = {} & \hat{x}_{a,0}^T P_{a,0}^{-1} \hat{x}_{a,0} \\ & + \int_0^{t_f} \Big[\dot{\hat{x}}_a(t) - f\Big(x_a(t), u(t)\Big)\Big]^T Q_a^{-1} \Big[\dot{\hat{x}}_a(t) - f\Big(x_a(t), u(t)\Big)\Big] dt \\ & + \int_0^{t_f} \Big[y(t) - g\Big(x_a(t), u(t)\Big)\Big]^T R^{-1} \Big[y(t) - g\Big(x_a(t), u(t)\Big)\Big] dt \end{aligned} \tag{5.18}$$

where $P_{a,0}$, Q_a and R are respectively weighting matrices for initial states, state transitions and measurements in this case instead of covariance matrices. From this point of view, the dynamic of observer can thus be configured via tuning these weighting matrices.

In following sections, the LPV system states in (5.2) are still called as "system states" or just "states", except if it is explicitly pointed out to be "augmented system states". Same for "process noise" and "augmented process noise".

5.2.4.2 Discretization

For numerical calculation and implementation of UKF, the augmented system (5.2) needs to be discretized. With Euler's approximation the augmented system in discrete time becomes

$$\begin{cases} \dot{x}(t) = A(\Theta)x(t) + B(\Theta)u(t) + w(t) \\ y(t) = C(\Theta)x(t) + D(\Theta)u(t) + v(t) \end{cases} \tag{5.19}$$

with

Discretized noise $w_{a,d}[k] = T_s w_a(kT_s), v[k] = v(kT_s)$ (5.20)

Noise covariance $Q_{a,d} = T_s Q_a, R_d = R/T_s$ (5.21)

State-transition function $f_d\Big(x_a[k], u[k]\Big) = \begin{bmatrix} \Big(T_s A(\Theta) + I\Big)x[k] + T_s B(\Theta)u[k] \\ \Theta[k] \end{bmatrix}$ (5.22)

Measurement function $g_d\Big(x_a[k], u[k]\Big) = C(\Theta)x[k] + D(\Theta)u[k]$ (5.23)

where T_s is sample time, I is identity matrix.

The observer (5.17) is now considered in discrete time according to the discrete augmented system (5.19).

$$\hat{x}_a[k+1] = f_d\Big(\dot{\hat{x}}_a[k], u[k]\Big) + L[k]\Big(y[k] - g_d\Big(\hat{x}_a[k], u[k]\Big)\Big) \tag{5.24}$$

5.2.4.3 Unscented Transformation

In order to calculate the optimal Kalman gain $L[k]$ in (5.24), the extended Kalman filter (EKF) uses Jacobian matrices of functions f and g. This is actually an approximation using a first-order Taylor series expansion to locally linearize the non-linear system. However, when high non-linearity appears, the computational complexity increases and result may be inaccurate [23]. The unscented Kalman filter (UKF) utilizes the "unscented transformation" (UT) to calculate the statistical properties of a random variable that has undergone a nonlinear transformation [24]. Given a vector of random variables x of dimension N propagating through a non-linear function $z = h(x)$ with mean $\bar{x}$ and covariance

C_{xx}, the statistics of z is calculated by Algorithm 5.1.

Algorithm 5.1 Unscented transformation.

Step 1: Sigma points.
Form a matrix X of $2N+1$ vectors. Each vector, called sigma point (in N dimension space), is calculated by

$$X_i = \begin{cases} \bar{x}, & i = 0 \\ \bar{x} + \left(\sqrt{NC_{xx}}\right)_i, & i = 1, 2, ..., N \\ \bar{x} - \left(\sqrt{NC_{xx}}\right)_{i-N}, & i = N+1, N+2, ..., 2N \end{cases} \tag{5.25}$$

where $\sqrt{NC_{xx}}$ is the square root matrix of NC_{xx} such that $\sqrt{NC_{xx}}\left(\sqrt{NC_{xx}}\right)^T = NC_{xx}$ and $\left(\sqrt{NC_{xx}}\right)_i$ is the i-th column of $\sqrt{NC_{xx}}$.
Step 2: Propagated sigma points.
The sigma points are propagated through the non-linear function h.

$$Z_i = h(X_i), i = 0, 1, 2, ..., 2N \tag{5.26}$$

Step 3: Mean and covariance of propagated sigma points.

$$\bar{z} = \sum_{i=0}^{2N} W_i Z_i \tag{5.27}$$

$$C_{zz} = \sum_{i=0}^{2N} W_i (Z_i - \bar{z})(Z_i - \bar{z})^T \tag{5.28}$$

where W_i is a weighting factor.
Step 4: Cross-covariance between x and z.

$$C_{xz} = \sum_{i=0}^{2N} W_i (X_i - \bar{x})(Z_i - \bar{z})^T \tag{5.29}$$

Adjustment of weighting factor W_i can improve the quality of approximation when the function h is highly non-linear. This is not the case here of the augmented system (5.10) that will be considered. So it is chosen hereafter

$$W_i = \begin{cases} 0, & i = 0 \\ 1/2N, & i = 1, 2, ..., 2N \end{cases} \tag{5.30}$$

5.2.4.4 Unscented Kalman Filter Algorithm

The following Algorithm 5.2 details the calculation steps of UKF for estimating the augmented system states in system (5.19).

Algorithm 5.2 Estimation of $x_a[k]$ with the unscented Kalman filter.

Step 1: Initialization.
At time step $k = 0$, initialize augmented system states value $\hat{x}_a[0]$, augmented system states covariance matrix $P_a[0]$, augmented process noise covariance matrix $Q_{a,d}$ and measurement noise covariance matrix R_d.
Step 2: Calculation of the output prediction.
At time step $k > 0$, estimate the output prediction using the unscented transformation (UT).

$$(\hat{y}[k|k-1], C'_{yy}[k], C_{xy}[k]) = UT(g_d, \hat{x}_a[k|k-1], P_a[k|k-1]) \tag{5.31}$$

$$C_{yy}[k] = C'_{yy}[k] + R_d \tag{5.32}$$

Step 3: Correction with measurements.
At time step k, correct the values and the covariance of the augmented states with the measurements:

$$L[k] = C_{xy}[k]C_{yy}^{-1}[k] \tag{5.33}$$

$$\hat{x}_a[k|k] = \hat{x}_a[k|k-1] + L[k]\Big(y[k] - \hat{y}[k|k-1]\Big) \tag{5.34}$$

$$P_a[k|k] = P_a[k|k-1] - L[k]C_{xy}^T[k] \tag{5.35}$$

Step 4: Prediction of next step states' value.
At time step k, predict system states (and the associated covariance) at next time step $k+1$ using UT:

$$(\hat{x}_a[k+1|k], P'_a[k+1|k]) = UT(f_d, \hat{x}_a[k|k], P_a[k|k]) \tag{5.36}$$

$$P_a[k+1|k] = P'_a[k+1|k] + Q_{a,d} \tag{5.37}$$

Step 5: Increase one time step and repeat step 2 to 4 until the last time step.

5.2.5 Practical Use of UKF

5.2.5.1 UKF Tuning Methodology

Tuning, or initialization is one of the common issues in using Kalman filter. Some empirical conclusions in linear KF can be referred in UKF. As stated above, from a deterministic

point of view, the dynamic of an optimal observer can be tuned via the weighting matrices $P_a[0]$, $Q_{a,d}$ and R_d. From a stochastic point of view, the UKF will give an accurate result when ideally the augmented process noise covariance $Q_{a,d}$ equals to the real augmented process noise covariance, and the same for the measurement noise covariance R_d. Whether from the deterministic or the stochastic point of view, reducing the magnitude of the elements in $Q_{a,d}$, or increasing the magnitude of the elements in R_d informs the UKF so that it is adapted to the situation for which the measurement noise is important compared to the augmented process noise. As a result, the UKF will give more confidence or weight to the augmented state transition model than to measurements. The Kalman gain matrix will have reduced value components focusing more on the augmented state predictions and less on measurement corrections [25]. Under this condition, the augmented state reconstruction dynamics will be slow (low correction level from the measurements) but will be more weakly impacted by a worse measurement quality. On the contrary, i.e. by assuming *a priori* that the measurement noise is lower compared to augmented process noise, the augmented system states reconstruction will be faster but also more sensitive to the quality of the measurements.

To study the parameter evolution in driver's adaptation process, the initial augmented states value $\hat{x}_a[0]$ and states covariance $P_a[0]$ are not quite important. We focus mainly on the tuning of matrix $Q_{a,d}$ and R_d. A simple and intuitive choice is that $Q_{a,d}$ is block-diagonal, i.e.

$$Q_{a,d} = \begin{bmatrix} Q_{x,d} & 0 \\ 0 & Q_{\Theta,d} \end{bmatrix} \tag{5.38}$$

where $Q_{x,d}$ and $Q_{\Theta,d}$ are respectively the covariance matrices of the discretized states and parameters process noise. (5.38) means the following hypothesis is admitted:

Hypothesis 5.3 *There is no correlation within the process noise between system states and parameters.*

In addition, for measurement noise:

Hypothesis 5.4 *There is no correlation in measurements noise between system outputs, i.e. R_d is diagonal.*

One of the difficulties in applying the aforementioned tuning rules (confidence on measurements versus states evolution) to define the magnitude of the elements of the matrix $Q_{a,d}$ and R_d comes from its qualitative nature. Normalization is required because

the signals can be very diverse, concerning their range of amplitude values, but also their impact on states and output signals. On one side, for output signals with scattered ranges of variation, it is important to *a priori* normalize measurement noise properly accordingly, by adequate choice in R_d (see (5.39)). On the other side, the process noise may be normalized through its effects on the system outputs. These effects may be evaluated through using the observability Gramian for $Q_{x,d}$ tuning, as proposed in [26] for setting a Kalman filter with a homogenized observer dynamics. It is more easily derived for $Q_{\Theta,d}$ tuning from the parametric sensitivity of the output. In this case, normalization from the nominal value of the parameters is possible and will be considered to simplify presentation. Algorithm 5.3 details the UKF tuning process.

Algorithm 5.3 Tuning unscented Kalman filter.

Step 1: Choose R_d.
Given outputs data $y[k]$ on $k \in [0, N]$ with dimension M, supposing each output has an error ratio of σ_i (inverse of the confidence level as stated above), R_d is

$$R_d = diag(\sigma_i^2 y_{i,max}^2), i = 1, 2, ..., M \tag{5.39}$$

where $y_{i,max} = \max_{k\in[0,N]} |y_i[k]|$.
Step 2: Normalize $Q_{x,d}$.
Given (5.2) with parameters fixed at normal values in Table 5.2 as a normal LTI system, calculate the observability Gramian of the discretized normal LTI system

$$G_o = \sum_{k=0}^{\infty} (A_d^T)^k C_d^T C_d A_d^k \tag{5.40}$$

Step 3: Choose $Q_{x,d}$.
Choose a time scaling factor T_x so that $Q_{x,d} = [T_x G_o]^{-1}$ lead the LTI observer inherited from (5.2) (with nominal parameters) having its poles with real part less than $-1/T_x$. Verification is possible by solving the adequate algebraic Riccati equation.
Step 4: Choose $Q_{\Theta,d}$.
Choose an error ratio of α_i for each parameter and a time scaling factor T_Θ according to the Hypothesis 2:

$$Q_{\Theta,d} = \frac{1}{T_\Theta^2} diag(\alpha_i^2 \Theta_{i,nom}^2), i = 1.2, ..., N_\Theta \tag{5.41}$$

where $\Theta_{i,nom}$ is the nominal value of i-th parameter and N_Θ is the number of parameters to be identified.

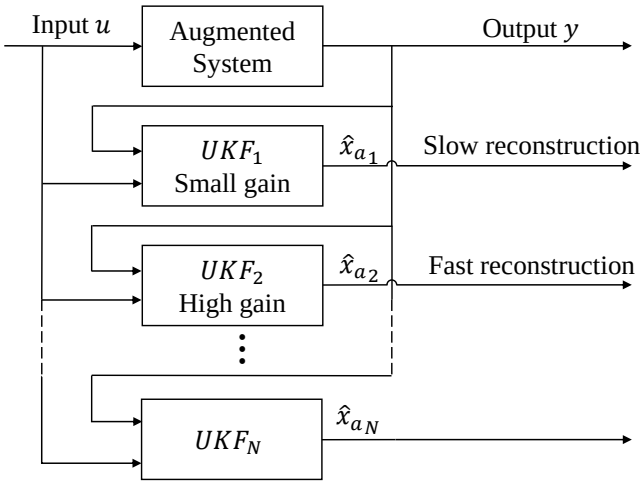

Figure 5.2 – Multi-UKF schema.

5.2.5.2 Multi-UKF Approach

As the result of such a tuning is always a compromise between rapidity and precision (noise sensitivity) in the process of parameter estimation, a multi-model UKF based approach is considered. At least two UKF will be used (see Figure 5.2). One is configured to get a precise steady-state value of the parameters considered. The other is configured to detect possible fast variations.

5.2.6 Experiments

The identification method as well as the tuning methodology are validated by two experiments: one in Simulink and one on the driving simulator SCANeR. In these experiments, the cybernetic driver model (5.2) is utilized as a virtual driver. Some of its parameters are *a priori* increased gradually at different times. In this case study, the increase of both visual gains (K_p and K_c) may depict increasing stress in driver's mind, or weak visibility conditions (like foggy or dark). The experiment steps are the following: the virtual driver steers a vehicle on a predefined road; the parameters change during driving; inputs and outputs data are collected; the data is used to identify the augmented system states including the searched parameters. The main differences between the two experimental platforms are: on the driving simulator 1) the vehicle is more realistic and precise, 2) the vehicle is controlled by a real steering column instead of a mathematical model and 3)

some inputs and outputs data are collected by sensors. Besides, the multi-UKF approach is used in the second experiment so as to evaluate the tuning methodology.

5.2.6.1 Experiment in Simulink

The first experiment is realized by simulating a Driver-Vehicle-Road (DVR) model [9] in Matlab / Simulink. The simulation environment (see Figure. 5.3a) was established in previous researches. The vehicle-road (VR) model is a bicycle model of which parameters were identified from experimental data. The cybernetic driver model "steers" the VR model with a fixed speed 64 km/h on a predefined road (see Figure. 5.3b).

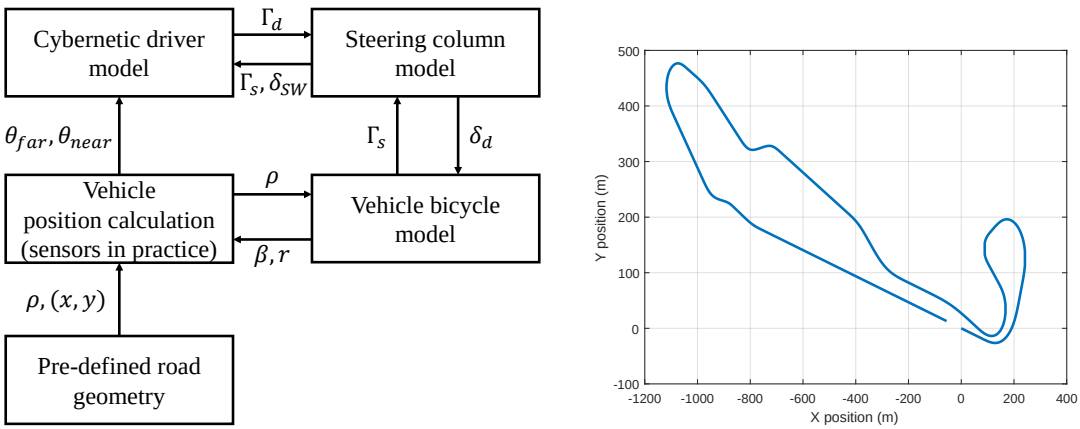

(a) Models in Simulink. (b) Road in Matlab.

Figure 5.3 – First experiment in Simulink.

Three different situations are simulated in this experiment: 1) only K_p increases; 2) only K_c increases; and 3) both K_p and K_c increase. A small gain UKF is implemented in all situations, of which the configuration could be found in (5.42), (5.43), (5.45) and (5.46). The identification results are shown respectively in Figure 5.4a, 5.4b, 5.4c and 5.4d. The red solid line is the actual variation of parameters during simulation, the blue dashed line is the estimated variation of parameters and the yellow dotted line represents for the related input signals (θ_{far} for K_p, θ_{near} for K_c, see Figure 5.1).

Several observations could be obtained from these figures. Firstly, the results prove the feasibility of the identification method in tracing variation of parameters. Secondly, as long as the related input signal becomes "weak", i.e. the input excitation is low, the corresponding parameter keeps constant due to "weak" identifiability. For example, in Figure 5.4a from 80 s to 90 s, the input signal θ_{far} is almost 0, in the meantime the

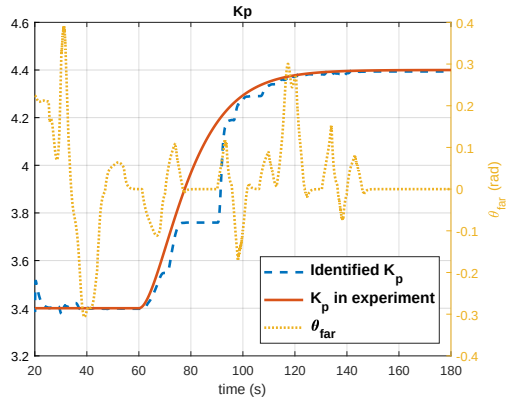

(a) Only K_p increased in the experiment.

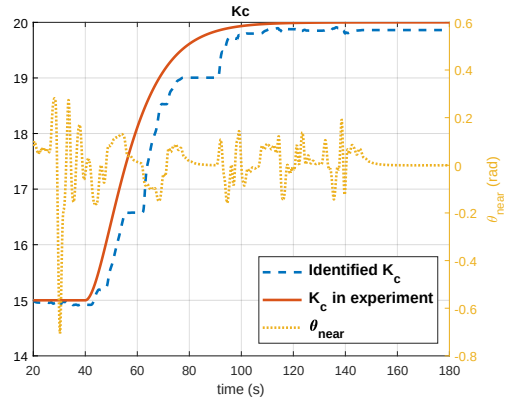

(b) Only K_c increased in the experiment.

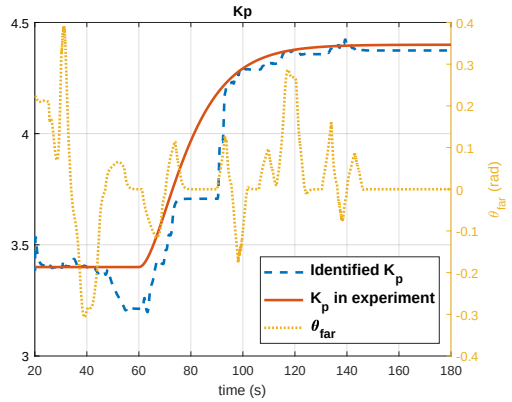

(c) Both K_p and K_c increased in the experiment, the variation of identified K_p.

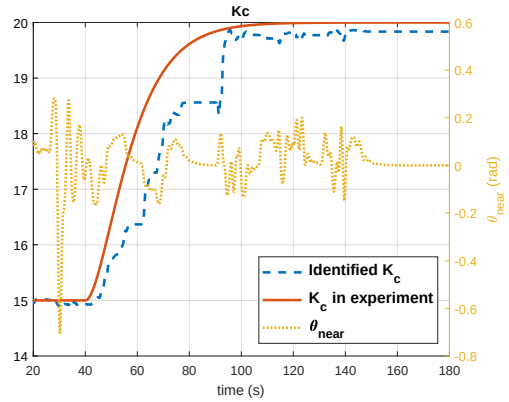

(d) Both K_p and K_c increased in the experiment, the variation of identified K_c.

Figure 5.4 – First experiment results.

identified K_p is constant. Same in the Figure 5.4b for θ_{near} and the identified K_c during 80 s and 90 s. The reason of "weak" input signals here is trivial: the "driver" is driving on a straight road. Thirdly, in Figure 5.4c the variation of the identified K_p is different from that in Figure 5.4a during 40 s to 60 s, this is caused by the correlation between two parameters, since K_c starts changing at 40 s.

5.2.6.2 Experiment in SCANeR

The second experiment is realized on the driving simulator SCANeR (see Figure 5.5a), where researches on human driver's adaptation will take place afterwards. It is equipped with a complete dashboard, a common five-speed gear stick, pedals of gas, brake and clutch, and a TRW direction system with steering wheel. The visual scene is displayed

on 3 LCD screens, a central one in front of driver and two others oriented to the center one with 45°. They cover a field of view of 25° on height and 115° on width. The visual scene transmits the road characteristics as perceived by driver via the windshield. A small family car of type Peugeot 307 is chosen as vehicle model in this experiment. The driver model also "steers" the vehicle with a fixed speed 64 km/h on a predefined road (see Figure 5.5b). Both parameters, K_p and K_c, are supposed to change.

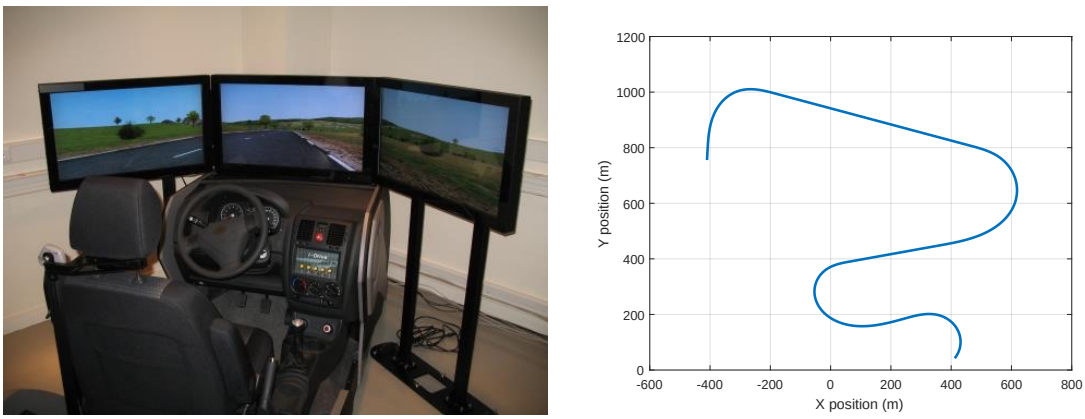

(a) Driving simulator SCANeR. (b) Experiment road.

Figure 5.5 – Second experiment in SCANeR.

The multi-UKF approach with two different configurations of UKF is used to identify the parameter evolution. In both UKFs, the value for initial system states are simply 0, while the estimated parameters are initialized without error to the initial values (see Table 5.2) used for the simulation.

$$\hat{x}_a[0] = \begin{bmatrix} 0 & 0 & 0 & 3.4 & 15 \end{bmatrix}^T \tag{5.42}$$

The initial augmented system state covariance $P_a[0]$ is chosen arbitrarily as stated in Section 5.2.5.1.The UKFs are now tuned according to Algorithm 5.3:

$$R_d = diag(9 \times 10^{-4}, 25 \times 10^{-4}) \tag{5.43}$$

$$Q_{x,d} = 10^{-7} \times G_o^{-1} \tag{5.44}$$

This tuning leads to poles at: -1, -10 and -50 meaning that the slowest dynamics of observer will have a time constant of 1 s, which seems sufficient. In fact, the state observer in open-loop is fast enough. Finally, different tuning are made for $Q_{\Theta,d}$ to get the two UKF. For

UKF1:

$$Q_{\Theta,d} = 10^{-8} \times diag(3.4^2, 15^2) \tag{5.45}$$

The scaling factor in $Q_{\Theta,d}$ is modified for UKF2:

$$Q_{\Theta,d} = 10^{-6} \times diag(3.4^2, 15^2) \tag{5.46}$$

The results are shown respectively in Figure 5.6. Same as in the first experiment, identified parameters are constant when "weak" identifiability happens. In addition, compared with Figure 5.6a and 5.6b, the constant values are greater in Figure 5.6c and 5.6d. For example K_c is almost constant from 40 s to 60 s, while its value is about 15.5 in Figure 5.6a and 16 in Figure 5.6c. This proves the rapidity of the UKF2. Besides, the results of UKF2 are more sensible to noise, this is obvious on the figures during 120 s to 160 s. It should be noted that K_c has an undesired variation from 80 s to 110 s in UKF1. Although the estimations eventually converge, there is also some slowness for UKF2 between 120 s and 180 s for K_p.

5.2.7 Conclusion

This article shows the interest and the feasibility of tracking the variations of parameters related in particular to the visual part of a driver model, so called cybernetic driver model. This problem is essential to study the adaptation of the driver's behavior to different changes in his driving environment, e.g. adaptation to active steering control systems, road features or meteorology. The driver model chosen is based on knowledge concerning neurophysiology and psychology of human driver, useful to study the driver's adaptation. The LPV identification problem was solved by first augmenting LPV system states with the state-space differential equations characterizing parameters' evolution dynamics. Then the unscented Kalman filter was applied by considering the identification problem as a state estimation problem. Referring to methodological experiences concerning classical Kalman filter, the tuning of UKF was mainly accomplished by setting the parameters' process and measurement noise covariance matrices. The compromise between rapidity and precision of parameter estimation was discussed through considering a multi-UKF approach. One UKF estimates the mean value of parameters while another one makes it possible to detect fast parametric variations. Two experiments considering a sequential change of parameters showed good identification results, compatible with the aim (driver

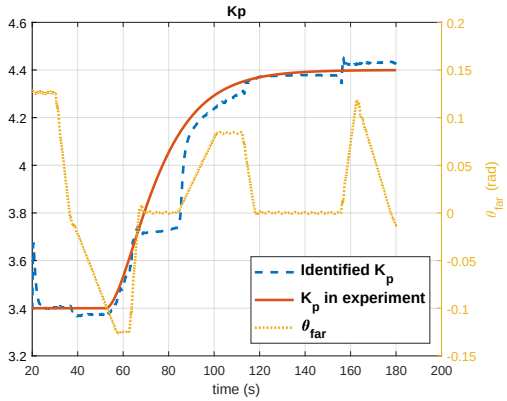

(a) K_p identified by UKF1 with slow reconstruction.

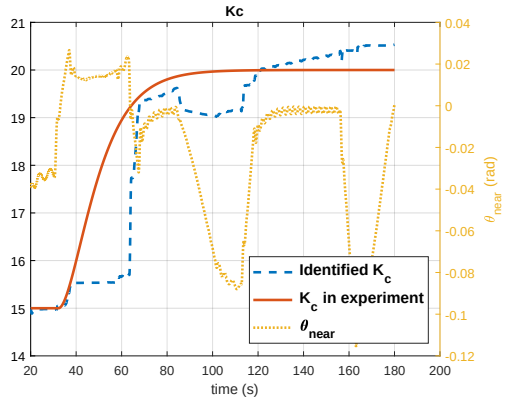

(b) K_c identified by UKF1 with slow reconstruction.

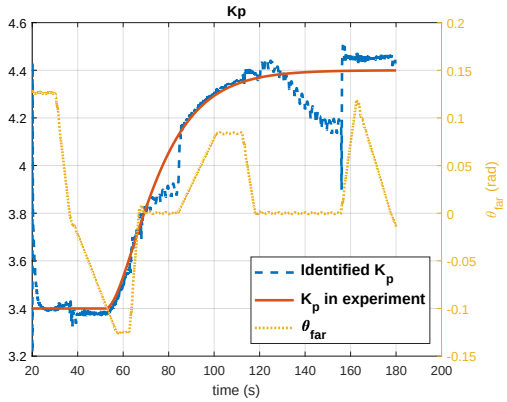

(c) K_p identified by UKF2 with fast reconstruction.

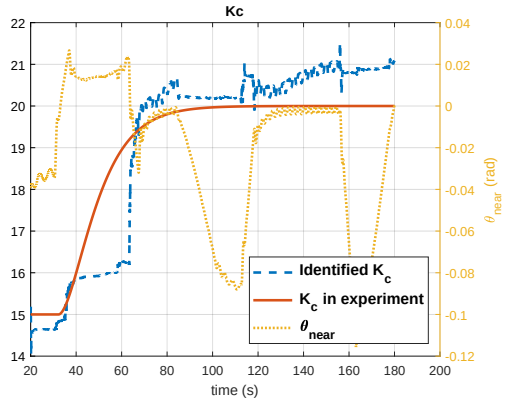

(d) K_c identified by UKF2 with fast reconstruction.

Figure 5.6 – Second experiment results.

adaptation analysis). However, a coupling effect may appear especially if the UKF is configured for high dynamic performance. Nevertheless, although this effect still needs to be understood more in depth from a theoretical point of view, the identification method considered (multi-UKF approach) proved to be useful in the future, for investigating especially the adaptation of human driver to the driver-assistance systems.

Extensive tests will now be performed on the LS2N driving simulator, with a significant number of human drivers. We believe that the proposed methodology will allow us to better understand driver's adaptive dynamics over time.

5.3 References

[1] A. Ameyoe, P. Chevrel, E. Le-Carpentier, F. Mars, and H. Illy, "Identification of a Linear Parameter Varying Driver Model for the Detection of Distraction", *1st IFAC Workshop on Linear Parameter Varying Systems LPVS 2015*, vol. 48, *26*, pp. 37–42, 2015, ISSN: 2405-8963.

[2] C. D. Mole, O. Lappi, O. Giles, G. Markkula, F. Mars, and R. M. Wilkie, "Getting Back Into the Loop: The Perceptual-Motor Determinants of Successful Transitions out of Automated Driving", *Human Factors*, vol. 61, *7*, pp. 1037–1065, 2019.

[3] D. A. Abbink, M. Mulder, and E. R. Boer, "Haptic shared control: Smoothly shifting control authority?", *Cognition, Technology and Work*, vol. 14, *1*, pp. 19–28, 2012, ISSN: 14355558.

[4] M. Mulder, D. A. Abbink, and E. R. Boer, "Sharing control with haptics: Seamless driver support from manual to automatic control", *Human Factors*, vol. 54, *5*, pp. 786–798, 2012.

[5] M. Steele and R. B. Gillespie, "Shared Control between Human and Machine: Using a Haptic Steering Wheel to Aid in Land Vehicle Guidance", *Proceedings of the Human Factors and Ergonomics Society Annual Meeting*, vol. 45, *23*, pp. 1671–1675, 2001.

[6] M. Flad, L. Fröhlich, and S. Hohmann, "Cooperative Shared Control Driver Assistance Systems Based on Motion Primitives and Differential Games", *IEEE Transactions on Human-Machine Systems*, vol. 47, *5*, pp. 711–722, 2017.

[7] F. Mars and P. Chevrel, "Modelling human control of steering for the design of advanced driver assistance systems", *Annual Reviews in Control*, vol. 44, *Supplement C*, pp. 292–302, 2017, ISSN: 13675788.

[8] F. Mars, L. Saleh, P. Chevrel, F. Claveau, and J.-F. Lafay, "Modeling the visual and motor control of steering with an eye to shared-control automation", *in Human Factors and Ergonomics Society 55th Annual Meeting*, vol. 55, 2011, pp. 1422–1426.

[9] L. Saleh, P. Chevrel, F. Claveau, J. F. Lafay, and F. Mars, "Shared steering control between a driver and an automation: Stability in the presence of driver behavior uncertainty", *IEEE Transactions on Intelligent Transportation Systems*, vol. 14, pp. 974–983, 2013.

[10] L. Saleh, P. Chevrel, F. Mars, J. F. Lafay, and F. Claveau, "Human-like cybernetic driver model for lane keeping", *in Proceedings of the 18th IFAC World Congress*, 2011, pp. 4368–4373, ISBN: 9783902661937.

[11] F. Mars, M. Deroo, and C. Charron, "Driver adaptation to haptic shared control of the steering wheel", *in 2014 IEEE International Conference on Systems, Man, and Cybernetics (SMC)*, 2014, pp. 1505–1509.

[12] F. Mars, M. Deroo, and J.-M. Hoc, "Analysis of human-machine cooperation when driving with different degrees of haptic shared control", *IEEE Transactions on Haptics*, vol. 7, *3*, pp. 324–333, 2014, ISSN: 19391412.

[13] M. Mulder, M. M. Van Paassen, and E. R. Boer, "Exploring the roles of information in the manual control of vehicular locomotion: From kinematics and dynamics to cybernetics", *Presence: Teleoperators and Virtual Environments*, vol. 13, *5*, pp. 535–548, 2004.

[14] D. T. McRuer, R. W. Allen, D. H. Weir, and R. H. Klein, "New Results in Driver Steering Control Models", *Human Factors: The Journal of the Human Factors and Ergonomics Society*, vol. 19, *4*, pp. 381–397, Aug. 1977.

[15] E. Donges, "A Two-Level Model of Driver Steering Behavior", *Human Factors: The Journal of the Human Factors and Ergonomics Society*, vol. 20, *6*, pp. 691–707, Dec. 1978.

[16] R. A. Hess and A. Modjtahedzadeh, "A Control Theoretic Model of Driver Steering Behavior", *IEEE Control Systems Magazine*, vol. 10, *5*, pp. 3–8, 1990.

[17] D. D. Salvucci and R. Gray, "A two-point visual control model of steering", *Perception*, vol. 33, *10*, pp. 1233–1248, 2004.

[18] W. Hoult and D. J. Cole, "A neuromuscular model featuring co-activation for use in driver simulation", *Vehicle System Dynamics*, vol. 46, *sup1*, pp. 175–189, 2008.

[19] R. Tóth, V. Laurain, M. Gilson, and H. Garnier, "On the closed loop identification of LPV models using instrumental variables", *in 18th IFAC World Congress*, vol. 44, 2011, pp. 7773–7778.

[20] Q. Zhang and L. Ljung, "From structurally independent local LTI models to LPV model", *Automatica*, vol. 84, pp. 232–235, 2017.

[21] M. A. H. Darwish, P. B. Cox, I. Proimadis, G. Pillonetto, and R. Tóth, "Prediction-error identification of LPV systems: A nonparametric Gaussian regression approach", *Automatica*, vol. 97, pp. 92–103, 2018.

[22] S. Z. Rizvi, J. M. Velni, F. Abbasi, R. Tóth, and N. Meskin, "State-space LPV model identification using kernelized machine learning", *Automatica*, vol. 88, pp. 38–47, 2018.

[23] E. A. Wan, R. van der Merwe, and A. T. Nelson, "Dual estimation and the unscented transformation", *Advances in neural information processing systems*, pp. 666–672, 2000, ISSN: 10495258.

[24] S. J. Julier and J. K. Uhlmann, "New extension of the Kalman filter to nonlinear systems", *in Proc. SPIE 3068,Signal Processing, Sensor Fusion, and Target Recognition VI*, 1997.

[25] K. Dutton, S. Thompson, and B. Barraclough, *The Art of CONTROL ENGINEERING*. 1997, ISBN: 978-0201175455.

[26] P. de Larminat, *Automatique Appliquée*, 2nd ed. Paris: LAVOISIER, 2009, p. 390.

Part III

Experiments and Results

Chapter 6

Experimental studies

Haptic guidance systems continuously provide human driver with assistance torques. When human beings are repeatedly confronted with an external force that modifies the relationship between the motor command and the resulting movement, motor adaptation occurs [1]. This thesis focuses on understanding how drivers adapt to the haptic guidance system through usage. The final objective is not only to understand the human adaptation process, but also to be able to "reproduce" it, so that this knowledge could contribute to the design and development of haptic guidance systems.

Behavioral analysis and model-based analysis are two methods adopted in this study. The behavioral analysis is a statistic method commonly used in existing researches. It consists of calculating metrics to evaluate signals recorded during driving experiments. This analysis can be comprehensive by choosing direct and indirect metrics. The direct metrics refer to evaluations based on physiological signals of human driver, such as eye direction, heart rate, electromyography (EMG) etc. The indirect metrics refer to evaluations based on lateral control performance of vehicle, such as steering-wheel reversal rate (SWRR), standard deviation of lateral position (SDLP), time to lane-crossing (TLC) etc. The behavioral analysis usually ends up with the analysis of variance (ANOVA), which analyzes the differences among group means in a sample. The behavioral analysis helps the understanding of adaptation process. However, it can only analyze based on data and is not able to "reproduce" driver's behavior.

The model-based analysis is the key research interest in this thesis. The principle of this method is to try to *capture* the adaptation using driver steering models. As models have the ability to "reproduce", or predict driver behavior, the results can be directly integrated into model-based controller design. To be clear, a "model" here refers to a model structure with an estimated parameter vector, $\mathcal{M}(\hat{\Theta}_N)$, which may be obtained from system identification with empirical data. The fundamental hypothesis of model-based analysis is Hypothesis 6.1:

Hypothesis 6.1 *Driver model is able to capture human driver's adaptation process, and in particular, the model captures this process in the form of parametric variation.*

As stated in [2], there is good reason to believe that human driver can be modeled as a parameter-varying system during adaptation. This hypothesis expects that the variation of certain parameters in the model would reproduce a similar adaptive behavior as human does. Yet this is the ideal case. Currently, there is no perfect driver model for capturing full breadth of human driver behavior, especially the adaptation[2]. All driver models are obtained and validated in quasi steady driving situations when the adaptation is already finished. These models could be used as a starting point for the design of haptic guidance system, but might not satisfy the Hypothesis 6.1 for model-based analysis. In fact, when these models are used beyond their scope for predicting driver's adaptive behavior, its validity in terms of output prediction becomes a question. Generally, there will be three different results:

1. The model is still valid without making any change;
2. The model is not valid, but it could be valid again with varying parameters;
3. The model is not valid, and it cannot be valid by only changing parameter values.

A model resulting in the second case is possible to achieve a *successful capture* of the adaptation due to the validity of model after parameter variation. For the first case, the model appears to be irrelevant to the scenario studied, and for the third cases, the chosen model is inappropriate. A possible solution in these two cases is to reconsider the model structure, so that the driver adaptation is explicitly included and represented with parametrized system blocks. As such, the analysis based on the new model will be able to *capture* the adaptation, as in the second case. In summary, at current stage, the model-based analysis with "imperfect" driver model would help both the investigation of driver behavior and the amelioration and perfection of driver models.

This part of thesis contains three articles that present the experiments and results of our adaptation studies. These studies were carried out progressively, following the before-mentioned procedure of model-based analysis. The first article is our first attempt of model-based analysis. It tried to explain through two parameters of a two-point visual model, the effect of haptic guidance systems and degraded visibility conditions on lateral control performance. Results showed that when dealing with the influence of visual conditions on steering-wheel angle, this model satisfied the Hypothesis 6.1 and captured

successfully via parametric variations. When it came to driver's neuromuscular action and torque output, this model was not sufficient. The advanced model proposed in [3], which combines the two-point visual model with a neuromuscular system, was then selected. However, the capture through this model was failed, because the haptic guidance torque was not considered in this model and it could not be valid by only changing parameter values. Therefore, a new cybernetic driver model with reconsidered neuromuscular system is proposed in the second article. In this new model, the haptic feedback torque, which is the combination of haptic guidance torque and self-aligning torque, was particularly considered. Parameter identification showed that when driving with a haptic guidance system of 50% sharing level, the new model could be valid by changing the internal model gain. In addition, the internal model gain seemed to be related to the driver adaptation to the haptic guidance system. To validate this conjecture, two experiments were finally carried out in the third article. Results demonstrated that the new model satisfied the Hypothesis 6.1 and successfully captured driver model adaptation to varying levels of haptic guidance system by changing the internal model gain. Note that some symbols and the chapter numbering in all three articles were modified to be coherent with those used in thesis.

Driving with a Haptic Guidance System in Degraded Visibility Conditions: Behavioral Analysis and Identification of a Two-Point Steering Control Model

This article aimed to determine the ability of a two-point steering control model to account for the influence of a haptic guidance system in different visibility conditions. In fact, the interactive effect of haptic guidance system and visibility conditions had been studied through behavioral analysis in [4], [5]. By performing a similar experiment, our goal was to verify to what extent a simple and robust model, such as the one used to account for the vision-based vehicle lateral control (i.e., two-point visual model), is likely to "explain" through its parameters, the behavior of the driver-assistance system as a function of the characteristics of the haptic guidance or the type of visibility.

The literature review [6] summarized on the methods and tools for conducting behavioral analysis. In our experiment, four metrics were adopted: the steering-wheel reversal rate (SWRR)[7], the mean and standard deviation of lateral position and the L^2-norm of driver steering torque. These metrics were selected from three different aspects to evaluate

driver's lateral control behavior: the steering performance, the lane keeping performance and the driver control effort. The ANOVA was performed after calculation of metrics to compare their values between different scenarios and determine whether the manipulated variable has a significant influence on the metrics or not.

The model-based analysis in this article was performed with the two-point visual model[8]. It was based on the fact that during driving, human always refers to a far region and a near region for getting information about the direction of the road and the position of vehicle in lane. In this model, two points in these regions, a far point and a near point, are chosen as a reasonable approximation of this dual visual process. The far point is the tangent point of the inner edge of the road on curves, or the vanishing point on straight line. This point gives information about the road curvature. The near point is a point that is a few meters ahead of the vehicle. This point provides information about the deviation of vehicle from lane center. The part related to the far point was called "anticipation", and "compensation" for the near point.

Several aspects were especially noticed when performing the model-based analysis. Firstly, it was assumed that during one driving scenario, there was almost no adaptation, so that driver could be regarded as a time-invariant system. In other words, when participants switched from one scenario to another, they quickly adapted to the new driving environment at the very beginning and reached a steady state. Our goal was only to capture this final steady state instead of the whole adaptation procedure, and compare it with those of other scenarios. Secondly, the visual anticipatory and compensatory gain were chosen as potential parameters. The other parameters were fixed at their nominal values. Thirdly, the two-point visual model actually represented a combination of the dynamics of the lateral control and steering-wheel (LC-SW) system. This system covered both human driver behavior and haptic guidance system, including extreme cases of human or haptic guidance driving alone. By identifying the gain parameters, our goal was to project the input-output relationship of the LC-SW system onto the visual model to check the contribution of each input signal to the output signal. If results turn out that the anticipatory gain increases or the compensatory gain decreases, it may imply that the steering wheel angle is determined more by the anticipatory than the compensatory part. Finally, before comparing the value of parameters, the parameter uncertainties were firstly checked to ensure the difference between parameters were caused by experimental conditions rather than system identification algorithm.

Results from behavioral analysis demonstrated that the effects of haptic guidance and

fog on the different considered metrics were cumulative without any interaction. This result differed from those reported in previous research [5], which showed that drivers could benefit more from haptic shared control in reduced visibility. The difference could be explained by the diverse design of haptic guidance system in the two cases. It could also be related to a difference in the difficulty of the lane-keeping task. In our study, it appeared that drivers benefited as much from haptic guidance in good visibility conditions as in the fog.

A synthesis was made by combining the behavioral analysis and model-based analysis. The behavioral analysis showed that fog did not affect the driving trajectory with corner-cutting behavior, while the haptic guidance system induced the lateral position of vehicle to be closer to the center of lane. The model-based analysis showed that the anticipatory gain proved to be very sensitive to the road profile. Therefore, it was concluded that this parameter represented visual anticipation to the extent that this anticipation defined the followed trajectory. The compensatory gain was expected to increase as SDLP decreased, and this was the case in our study, whether due to fog, haptic guidance, or both, in which case the effect was cumulative. It was also noted that the reduction of SDLP was not of the same nature under two conditions: in the case of fog it was the consequence of increased human steering control (increased SWRR); in another case it was determined by the design strategy of haptic guidance system. In short, the compensatory gain proved to be very sensitive to the variability of the lateral position while it was not able to tell the origin (human or haptic guidance system) of this consequence.

In conclusion, the model-based analysis in this article succeeded with a simple two-point visual model. Changes in the lateral control performance of the LC-SW system were captured by the anticipatory and compensatory gains. However, it had flaws. Such model considered only the steering-wheel angle as output for the performance evaluation. It could not independently distinguish between the action of the human driver and those of the haptic guidance system on the steering-wheel. The next step would be using more advanced driver model with neuromuscular system, such as the one proposed in [3], [9], [10].

Towards a Driver Model to Clarify Cooperation Between Drivers and Haptic Guidance Systems

The first article concluded on the requirement of an advanced driver model for further

capturing human adaptation and separating the action of human driver and haptic guidance system on the steering wheel. A possible solution is to select a driver model with a neuromuscular system (NMS) and taking driver steering torque as output. Besides, the importance of including NMS knowledge has been mentioned in several researches [11], [12]. At first, the cybernetic driver model proposed in [3], [9], [10] was chosen as our candidate model. Later, several difficulties were encountered. The most important problem was that the model became non-valid when haptic guidance torque intervened in the steering-wheel control, and it could not be valid again by simply adjusting parameter values. Finally, a new cybernetic driver model with reconsidered NMS was proposed and validated in this second article.

Three points were clarified before the reconsideration of model structure. Firstly, instead of using only the self-aligning torque, a haptic feedback torque should be included in the model as an input. This torque represents the torques perceived by drivers on the steering wheel. In our case, it refers to the self-aligning torque and the haptic guidance torque. In most cases it is difficult for drivers to distinguish between them because they act together on the steering wheel and are perceived through the same channel. Therefore, it was their combination that was defined as the haptic feedback torque. Secondly, despite the invalidity, the basic hypothesis in previous model could be maintained. The hypothesis was that driver's lateral control behavior could be divided into two steps: environment perception and neuromuscular action. In the step of environment perception, drivers consult visual information and generate a target steering-wheel angle as intention. In the step of neuromuscular action, they convert this angle to force (torque) control and apply it on the steering wheel though muscles. This hypothesis allowed us to keep the visual part of the previous model and focus on the NMS. Finally, the NMS modeling should cover two fundamental mechanisms: how muscles convert the target steering-wheel angle into steering torque and how haptic feedback was involved in driver's control.

To represent the first mechanism in NMS modeling, a notion called *internal model*, inspired from neural science, was introduced. An internal model is an internal representation of external world used by organisms. The central nervous system uses internal models to control and predict. Control turns desired sensory consequences into motor commands, while prediction turns motor commands into expected sensory consequences. Similarly, drivers should have an internal representation of the limb-steering system (i.e., an internal model). This model is actually the representation of human feeling about the steering system. It should be approximate and correspond to a low-order system. A simple gain

was thus used as the internal model.

For the second mechanism of NMS modeling, an implicit and an explicit involvement of haptic feedback were proposed. The implicit involvement referred to adaptation of the internal model gain. This is also related to the learning property of the internal model, because human can easily adapt to a different steering system by adapting their internal models. The explicit involvement referred to a closed-loop control formed with the haptic feedback torque for compensating the inaccurate internal model and stabilizing steering wheel.

A simple experiment was carried out in the first place to verify if this model could be valid when human driver and haptic guidance system control the steering wheel simultaneously. A haptic guidance system at 50% sharing level was used in this experiment. Results showed that the output prediction of the proposed model was very close to the measured data, either in the case with haptic guidance system or without it. In particular, the internal model gain was found being sensitive to this specific haptic guidance system. The proposed driver model structure became valid in both manual driving and assisted driving by especially varying this parameter. At this point, it was concluded that this model could be a good choice for our model-based analysis. However, additional tests involving more drivers and haptic guidance systems set at different sharing levels were necessary for completing the validation and confirming the role of the internal model gain as potential parameter for capturing human adaptation.

Driver Model Validation through Interaction with Varying Levels of Haptic Guidance

This article aimed to validate the proposed model and use it to conduct model-based analysis when human driver interacts with different sharing levels of haptic guidance. The sharing level is a coefficient used in the design of haptic guidance systems. The torque output of controllers is adjusted by this coefficient so that the system can provide drivers with more or less haptic feedback. In practice, the sharing level may change according to driver's demand or state in order to minimize potential conflicts between human driver and haptic guidance systems. Therefore, it is important to understand how drivers may adapt to the variation of this coefficient.

Two experiments were carried out in this paper. The objective of the first experiment was to verify whether the driver model can cooperate effectively with a haptic guidance

system as soon as the gain of the internal model corresponds to the chosen sharing level. The experiment was performed by simulating the driver model as a "virtual driver" in cooperation with the haptic guidance system. As the second article implied the potential relationship between with the internal model gain and sharing level, they were chosen as two independent variables manipulated in this experiment. Each variable had four levels, resulting in 16 pairs in total as scenarios. The lateral control performance of the "virtual driver" was evaluated through behavioral analysis. The standard deviation of lateral position from lane center was selected as the indicator. Results showed that a stable cooperation between the driver model and haptic guidance system could only be achieved when the internal model gain and the sharing level matched each other. In other words, the adjustment of the internal model gain through the haptic feedback is imperative when the driver model interacts with the haptic guidance system at different sharing levels. The model would be suitable for model-based analysis of human adaptation in this situation.

The objective of the second experiment is then obvious: instead of "virtual driver", capturing the adaptation of human driver to the haptic guidance system at different sharing levels through the internal model gain parameter. The experiment was performed by asking human driver cooperating with the haptic guidance system when the sharing level was changing continuously. The sharing level firstly increased from 0% to 100%, maintained at 100% for a while and then decreased to 0%. Results showed that for all 17 participants the internal model gain varied with the same trend. When the sharing level was increasing, the internal model gain decreased and vice versa. At fully automatic driving (100%), the parameter was almost 0. In summary, the results demonstrated that the internal model gain of the driver model was directly related to the sharing level of the haptic guidance system. By adjusting this parameter, the prediction of the driver model in cooperation with the haptic guidance was always valid, even though the sharing level changed.

In conclusion, our first experiment was to verify if the internal model gain was the most sensible parameter to changes in haptic feedback torque, as found in the second article. The results revealed that the model identified for a given sharing level was no longer able to drive alongside the haptic guidance system with a different sharing level. The first experiment further demonstrated that by varying only the internal model gain parameter, the model could be valid again. This corresponded to the meaning attributed to this model: the internal model should be a representation of the steering system compliance. When

the haptic feedback changed, from the viewpoint of human drivers, the steering system dynamics was changed, and thus they adjusted their internal model accordingly to stay in cooperation with the new steering system. The first experiment indicated that the adjustment of this parameter was imperative when the sharing level of haptic guidance system changed. The second experiment with human drivers was then conducted. The adaptation to varying levels of haptic guidance system was successfully captured through the variation of the internal model gain parameter. The results suggested that driver adaptation to the haptic guidance system was mostly achieved by updating the internal representation of the steering system. At this point, the model-based analysis of driver adaptation to haptic guidance system was accomplished.

6.1 References

[1] F. Mars, M. Deroo, and C. Charron, "Driver adaptation to haptic shared control of the steering wheel", *in 2014 IEEE International Conference on Systems, Man, and Cybernetics (SMC)*, 2014, pp. 1505–1509.

[2] M. Mulder, D. M. Pool, D. A. Abbink, E. R. Boer, P. M. Zaal, F. M. Drop, K. Van Der El, and M. M. Van Paassen, "Manual Control Cybernetics: State-of-the-Art and Current Trends", *IEEE Transactions on Human-Machine Systems*, vol. 48, *5*, pp. 468–485, 2018, ISSN: 21682291.

[3] L. Saleh, P. Chevrel, F. Mars, J. F. Lafay, and F. Claveau, "Human-like cybernetic driver model for lane keeping", *in Proceedings of the 18th IFAC World Congress*, 2011, pp. 4368–4373, ISBN: 9783902661937.

[4] S. Y. De Nijs, M. Mulder, and D. A. Abbink, "The value of haptic feedback in lane keeping", *in Conference Proceedings - IEEE International Conference on Systems, Man and Cybernetics*, vol. 2014-Janua, Institute of Electrical and Electronics Engineers Inc., 2014, pp. 3599–3604.

[5] F. Mars, M. Deroo, and J.-M. Hoc, "Analysis of human-machine cooperation when driving with different degrees of haptic shared control", *IEEE Transactions on Haptics*, vol. 7, *3*, pp. 324–333, 2014, ISSN: 19391412.

[6] E. Johansson, J. Engström, C. Cherri, E. Nodari, A. Toffetti, R. Schindhelm, and C. Gelau, "Review of existing techniques and metrics for IVIS and ADAS assessment", Tech. Rep. March, 2004, pp. 1–93.

[7] G. Markkula and J. Engström, "A Steering Wheel Reversal Rate Metric for Assessing Effects of Visual and Cognitive Secondary Task Load", *in Proceedings of the 13th ITS World Congress.*, 2006, ISBN: 0000000302.

[8] D. D. Salvucci and R. Gray, "A two-point visual control model of steering", *Perception*, vol. 33, *10*, pp. 1233–1248, 2004.

[9] F. Mars and P. Chevrel, "Modelling human control of steering for the design of advanced driver assistance systems", *Annual Reviews in Control*, vol. 44, *Supplement C*, pp. 292–302, 2017, ISSN: 13675788.

[10] F. Mars, L. Saleh, P. Chevrel, F. Claveau, and J.-F. Lafay, "Modeling the visual and motor control of steering with an eye to shared-control automation", *in Human Factors and Ergonomics Society 55th Annual Meeting*, vol. 55, 2011, pp. 1422–1426.

[11] D. A. Abbink and M. Mulder, "Neuromuscular Analysis as a Guideline in designing Shared Control", *in Advances in Haptics*, M. H. Zadeh, Ed., Rijeka: IntechOpen, 2010, ch. 27.

[12] D. A. Abbink, M. Mulder, and E. R. Boer, "Haptic shared control: Smoothly shifting control authority?", *Cognition, Technology and Work*, vol. 14, *1*, pp. 19–28, 2012, ISSN: 14355558.

Chapter 7

Driving with a Haptic Guidance System in Degraded Visibility Conditions: Behavioral Analysis and Identification of a Two-Point Steering Control Model

Abstract

The objective of this study is to determine the ability of a two-point steering control model to account for the influence of a haptic guidance system in different visibility conditions. For this purpose, the lateral control of the vehicle was characterized in terms of driving performance but also through the identification of anticipation and compensation parameters of the driver model. The hypothesis is that if the structure of the model is still valid in the considered conditions, the value of the parameters will change in coherence with the observed behavior. The results of an experiment conducted on a driving simulator demonstrate that the identified model can account for the cumulative influence of the haptic guidance system and degraded visibility. The anticipatory gain is sensitive to changes in driving conditions that have a direct influence on the produced trajectory, and the compensatory gain is sensitive to a decrease in the variability of the lateral position. However, a model with only the steering wheel angle as output is not able to determine whether the change in lateral position variability is due to the driver's lack of anticipation or to the assistance provided by the haptic guidance system.

7.1 Introduction

Advanced driver assistance systems for road vehicles have been intensively studied in recent years due to the potential to improve driving comfort and safety. Part of this research focuses on avoiding or reducing persistent issues in human-automation interaction. These issues are usually caused by a lack of effective communication between the driver and the assistance system. A specific mode of assistance, called haptic shared control, has been proposed and meets commonly formulated design guidelines for human-automation interaction, especially in automotive applications[1]–[4]. Applied to the steering control (i.e., haptic guidance system), an automation system continuously provides human drivers with additional assisting torque through the steering wheel. Because the steering wheel is controlled simultaneously by the human driver and automation system, it acts as a communication interface between them. In this case, the driver can feel the additional force generated by the automation system and can decide whether to follow the "optimal" control operated by the system or to override it if necessary. As such, shared control is distinct from systems that binarily switch authority between humans and machines. The benefits of haptic guidance systems have been observed in lane-keeping performance[5]–[10].

The effectiveness of haptic guidance systems depends on various aspects, including the design method and its parameter[11], the level of authority of the system[12], the driver's age and driving experience[7], [8], fatigue[10], and the driver's reliance on the system[13]. In addition to system or driver-related aspects, the influence of the driving environment, especially visibility conditions, is one of the key issues because of the predominant role of visual information in driving[14]. Indeed, several studies have already studied the benefits of haptic guidance systems in degraded visibility conditions[15], [16]. The driving performance was evaluated through behavioral analysis, which consists of statistical comparison of different metrics such as steering wheel reversal rate, steering effort and mean lateral position of the vehicle. It has been shown that a haptic guidance system is more effective in compensating for a loss of near visual information than a loss of far vision[15]. Moreover, a study varying the level of haptic authority of a guidance system has shown that the optimum distribution of control between the driver and the system depends on the visibility conditions, with drivers relying more on the system in the presence of fog[16].

To better understand how haptic guidance systems modify the lateral control of the vehicle as a function of visibility conditions, this study proposes to adopt, in addition to behavioral analysis, a model-based analysis method. Our objective is to link the results

of the behavioral analysis to the parameter values of a driver steering model, in order to understand to what extent the model can account for the combined effect of haptic guidance and visibility on driving performance. Driver models are useful tools for understanding information processing in humans but also for estimating driver state. Recent work has shown, for example, that it is possible to discriminate different driver distraction modalities through the parametric analysis of a steering control model[17], [18]. In addition, these models can be used for the realization of controllers in haptic guidance systems[19]. Controllers based on driver models have many advantages such as reduction of undesired steering conflicts with the guidance system, a smooth authority transition, and the consideration of the driver's state[20]–[26].

The model chosen to meet the objective of this paper is similar to the two-point model proposed by [27]. and which is in line with [28]. Since then, it has been established that steering on a sinuous road can be summarized by the complementary action of two processes: the visual anticipation of the road curvature and the compensation of lateral positioning errors [16], [27]–[31]. The anticipation process refers to the visual exploration of the road ahead, while the compensation process represents the task of maintaining an appropriate distance from the edges of the lane. The two-point model combines anticipation and compensation by considering a simple additive process, and predicts the steering wheel angle. The model has been validated in three different contexts by[27]. First, the two-point model can account for the effect of partial occlusion of the visual scene (driving with near and/or far vision) [29]. The model can also predict human-like steering profiles for perturbation correction and lane change maneuvers.

Our assumption for the model-based analysis is that the model structure is still valid in the presence of haptic guidance and reduced visibility, but that the parameter values will change accordingly. Specifically, it is assumed that when visibility is degraded, the steering wheel angle will depend more on error compensation than on anticipation. The hypothesis of a decrease in the anticipation gain and an increase in the compensation gain can therefore be made. When driving with the haptic guidance system, the driver can rely on the system, which may facilitate lane keeping and smoothen steering control . In this case, an increase in the anticipation gain and a decrease in the compensation gain may be observed. If there is an interaction between the two factors, which could have an antagonistic action on some behavioral indicators, it will be interesting to examine how the model parameters capture this phenomenon.

In summary, the objective of this study is to verify to what extent a simple and robust

model, such as the two-point steering model, is likely to "explain" through its parameters, the behavior of the driver-assistance system as a function of haptic guidance and visibility. This paper is organized as follows: Section 7.2 presents the way the experiment was conducted with a brief description of the haptic guidance system enrolled. The methods of data analysis, including the identification of the model parameters, are described in Section 7.3. Section 7.4 presents the results obtained from behavioral analysis and model parameter identification. Section 7.5 summarizes the effect of the experimental conditions on driving performance and the model parameters. Finally, Section 7.6 concludes with the predictive capability of the selected model and the prospects for this work.

7.2 Experiment

7.2.1 Participants

A group of 15, comprising 11 male and four female participants, took part in the experiment. The participants were primarily recruited from students and staff of the Laboratory of Digital Sciences in Nantes and Institute Mines-Télécom Atlantique Nantes. All participants possessed a valid driver's license with at least three years of driving experience. The participants had no known medical issues that could affect their driving skills and had normal or corrected vision. None of them had ever experienced a haptic guidance system. The research was conducted in accordance with the standards of the CNRS ethical committee and with the 1964 Declaration of Helsinki. Informed consent was obtained from all individual participants involved in the study.

7.2.2 Independent Variables

Two independent variables were manipulated in this study according to our objectives: the visibility conditions of the driving environment (F) and the haptic guidance system (A). Visibility was manipulated by applying a thick fog in the driving scene (Figure 7.1a and 7.1b), so that it was difficult for the driver to anticipate changes in road curvature. The visibility variable therefore has two degrees: with fog ($+F$) or without fog ($-F$). The same applies to the haptic guidance system with two conditions: with guidance ($+A$) and without guidance ($-A$). The combination of these two variables provides the following four different experimental scenarios:

1. without fog, without haptic guidance ($-F$, $-A$);

2. without fog, with haptic guidance (-*F*, +*A*);
3. with fog, without haptic guidance (+*F*, -*A*);
4. with fog, with haptic guidance (+*F*, +*A*).

(a) Screenshot of scenario without fog.

(b) Screenshot of scenario with fog.

(c) Fixed base driving simulator SCANeR.

7.2.3 Haptic Guidance System

The haptic guidance system employed in this study was developed by [26]. The total guidance torque applied on the steering wheel Γ_a comes from anticipatory and compensatory assistance (Figure 7.2):

$$\Gamma_a = \Gamma_{a_{ref}} + \Gamma_{a_{fb}} \tag{7.1}$$

The anticipatory assistance, the feed-forward (FF) controller, is a trajectory generator that generates reference vehicle-road model states and the torque control on the basis of

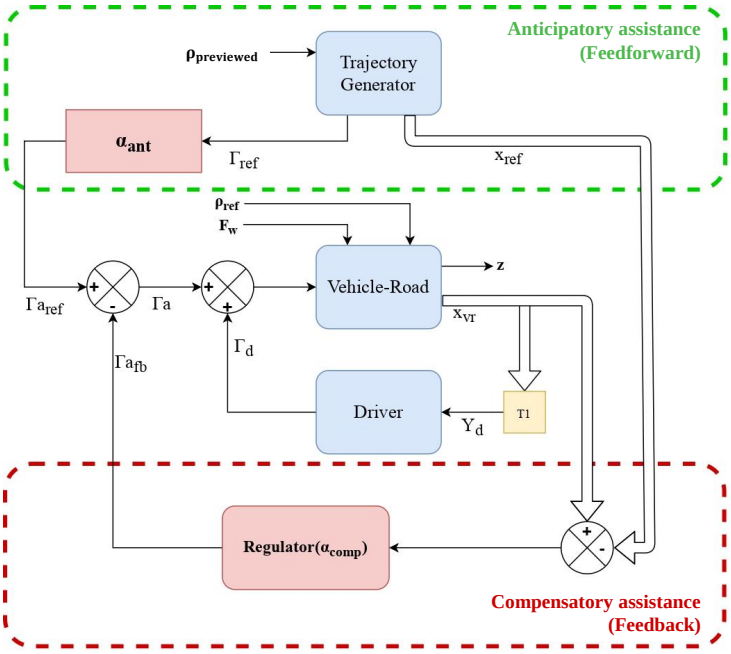

Figure 7.2 – Design strategy of haptic guidance system.

the previewed road curvature $\rho_{previewed}$:

$$\begin{pmatrix} \Gamma_{ref} \\ x_{ref} \end{pmatrix} = K_{FF}(p)\rho_{previewed} \tag{7.2}$$

where $K_{FF}(p)$ represents the transfer function of the trajectory generator. The applied FF torque is then determined by the sharing level of the anticipatory part: $\Gamma_{a_{ref}} = \alpha_{ant}\Gamma_{ref}$.

Compensatory assistance, namely the feedback controller, is static output feedback obtained by an H_2/H_∞ multi-objective control synthesis:

$$\Gamma_{fb} = K_{fb}(x_{vr} - x_{ref}) \tag{7.3}$$

Similarly, the applied feedback torque control is determined by the sharing level of the compensatory part: $\Gamma_{a_{fb}} = \alpha_{comp}\Gamma_{fb}$.

The sharing levels are used for regulating the total haptic guidance torque. When the sharing level is highly in favor to automation (close to 100%, see [26]), the haptic guidance system can drive the vehicle by itself. In this study, both sharing levels were fixed at 50%, which provides a system that delivers clear haptic guidance, although it will eventually leave the lane during navigation on a curve without driver's intervention.

7.2.4 Apparatus

The experiment in this study was conducted on a fixed-base driving simulator powered by SCANeR Studio (Figure 7.1c). It is equipped with a complete dashboard; a five-speed gear stick; gas, brake and clutch pedals; and a steering wheel connected to a TRW steering system. A torque sensor is mounted on the steering column to measure driver steering torque. The visual scene is displayed on three LCD screens: a central one in front of the driver and two others oriented at 45° relative to the center. The screens cover a field of view of 25° in height and 115° in width. A small family car, a Citroën C5, was chosen as the vehicle model in this experiment.

7.2.5 Scenarios

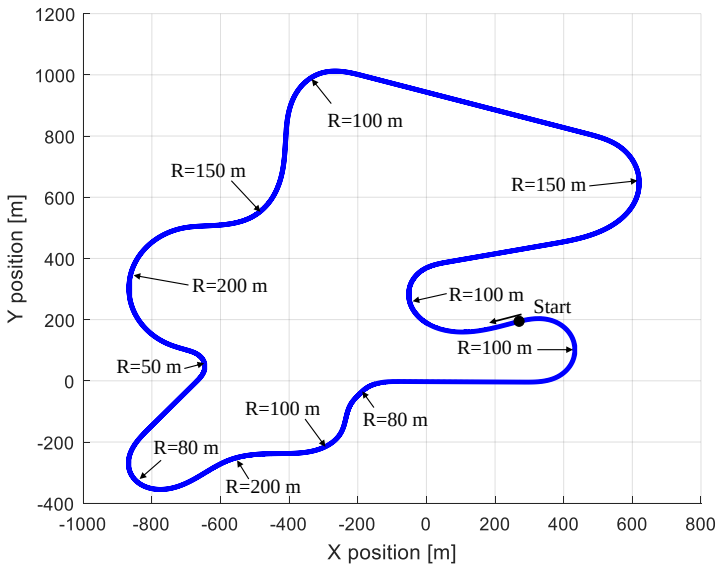

Figure 7.3 – Route used for experiment.

The track used for the four experimental scenarios is shown in the bottom right-hand corner of Figure 7.3 and is a two-lane road that each lane is 3.5 m wide. It consists of 11 bends of various length (from 150 m to 650 m) and radius of curvature (from 50 m to 200 m). All bends are Euler spirals with continuous changes in the curvature. The longitudinal speed of the vehicle was set at 64 km/h (18 m/s). A brief introduction to each scenario, including the operation of the haptic guidance system, was provided to the drivers at the beginning of the experiment. The participants were instructed to drive in the right-hand lane without making any lane changes. The order of the four scenarios was randomized

between participants. Moreover, each scenario lasted 10 minutes, which is equivalent to nearly two laps on the track, given the chosen speed. Finally, participants were allowed to take a short break between scenarios.

7.3 Data Analysis Methods

7.3.1 Driving Metrics

Steering Performance Steering performance was assessed using the steering wheel reversal rate (*SWRR*). This measure represents the frequency of changes in the direction of the steering wheel rotation by a magnitude greater than a given angle, or gap. It is one of the most commonly used measures of steering performance[32], [33]. The algorithm proposed in [33] has been adopted with a gap of 2°. *SWRR* is expected to decrease with haptic guidance and to increase with fog.

Lane-Keeping Performance Lane-keeping performance was evaluated using the deviation, y_a, of the lateral position of the vehicle's center of gravity from the lane center (in meters). The mean and the standard deviation of y_a were chosen as the metrics. In addition, y_a was considered positive if the vehicle deviated from the lane center towards the inner edge of the lane so that the mean provided information on the driver's behavior in terms of cornering independently of the direction of the curve. In contrast, y_a was negative if the deviation was towards the outside of the bend. Because the deviation of the lateral position on the simulator used the lane center as a reference, the adjustment was as follows. The calculation of the standard deviation of the lateral position (*SDLP*) is still based on the non-adjusted deviation of the lateral position $y'_a[k]$. The $\overline{y}_a$ is expected to decrease with haptic guidance. This might also happen if the driver adopts a more conservative path planning behavior, with less corner-cutting. The *SDLP* is expected to decrease with haptic guidance and fog.

For a deviation of the lateral position signal vector $y'_a[k], k = 1, 2, \ldots, N$, the adjusted mean is

$$\overline{y}_a = \frac{1}{N} \sum_{k=1}^{N} y_a[k] \tag{7.4}$$

where $y_a[k]$ is the adjusted deviation of the lateral position:

$$y_a[k] = \begin{cases} y'_a[k], & if\ \rho[k] \geq 0 \\ -y'_a[k], & if\ \rho[k] < 0 \end{cases} \tag{7.5}$$

with $\rho[k]$ denoting the sampled road curvature vector.

Driver Control Effort The driver control effort is evaluated through the torque applied by the driver on the steering wheel, Γ_d. The L^2-norm, which is equivalent to signal energy, is chosen as metric ($\|\Gamma_d\|_2$). The calculation is as follows.

$$\|\Gamma_d\|_2 = \sqrt{\sum_{k=0}^{N} \Gamma_d^2[k]} \tag{7.6}$$

where N is the number of samples. The $\|\Gamma_d\|_2$ is expected to decrease with haptic guidance.

7.3.2 Model Identification

The model chosen in this study is shown in Figure 7.4a. It is a two-point visual model inspired by [18], [27], [28], [34], [35]. In this model, the steering wheel angle δ_{SW} is a combination of anticipatory and compensatory behavior in a lateral control task. The anticipatory part represents the behavior of looking far ahead to determine the road direction, and the compensatory part corresponds to the use of near visual information to maintain the vehicle in the lane. Two points on the road, a far and near point, are chosen as a representation of the areas where the visual information is acquired. The angles between the direction of these points and the heading of the vehicle, which are defined as the far-point angle θ_{far} and near-point angle θ_{near}, respectively, are used as inputs in the model. The calculation of these inputs is shown in Figure 7.4b and in (7.7). For the far-point angle, it is assumed that the vehicle heading is aligned with the road. For the near point angle, it is assumed that the line segment y_L is perpendicular to the vehicle heading. The y_L is the lateral position error at distance l_s in front of the vehicle, which is directly available from the vehicle-road (VR) model (see [26]). The model parameters are described in Table 7.1.

$$\theta_{far} \approx D_{far} \times \rho, \theta_{near} \approx y_L/l_s \tag{7.7}$$

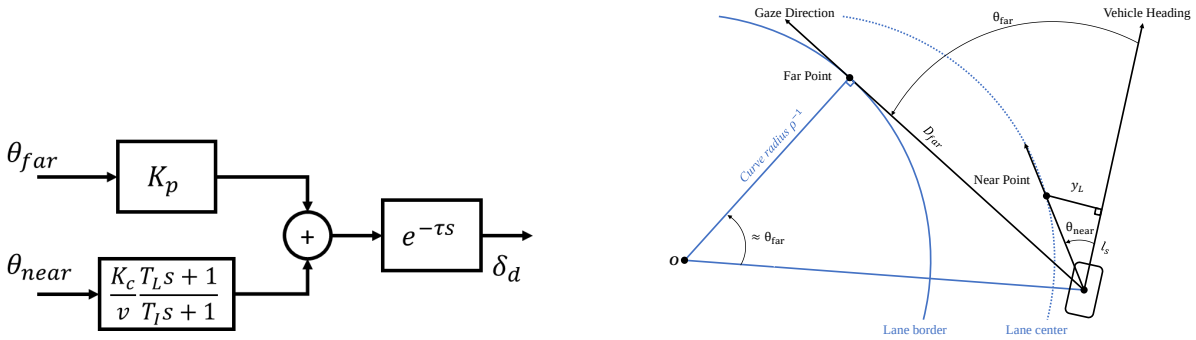

(a) Two-point visual model.

(b) Calculation of far-point angle and near-point angle

Figure 7.4 – Inputs of the two point model.

Table 7.1 – Description of parameters in the model.

Parameter	Description	Nominal values
K_p	Visual Anticipation Gain	-
K_c	Visual Compensation Gain	-
T_I, T_L	Compensation Time Constants	1, 3
τ_p	Processing Delay	0.04
v	Vehicle Longitudinal Speed	-

By approximating the delay block using a first-order Padé model, the minimal realization of the two-point visual model shown in Figure 7.4a can be written as follows.

$$\begin{cases} \dot{x}(t) = Ax(t) + Bu(t) \\ y(t) = Cx(t) + Du(t) \end{cases} \tag{7.8}$$

with

$$\text{Input} \qquad u(t) = \begin{bmatrix} \theta_{far} & \theta_{near} \end{bmatrix}^T \tag{7.9}$$

$$\text{Output} \qquad y(t) = \delta_{SW} \tag{7.10}$$

$$A = \begin{bmatrix} -\frac{1}{T_I} & 0 \\ -\frac{2}{\tau_p}\frac{K_c}{v}(\frac{T_L}{T_I} - 1) & -\frac{2}{\tau_p} \end{bmatrix} \qquad B = \begin{bmatrix} 0 & \frac{1}{T_I} \\ \frac{2}{\tau_p}K_p & \frac{2}{\tau_p}\frac{K_c}{v}\frac{T_L}{T_I} \end{bmatrix} \tag{7.11}$$

$$C = \begin{bmatrix} \frac{K_c}{v}(\frac{T_L}{T_I} - 1) & 2 \end{bmatrix} \qquad D = \begin{bmatrix} -K_p & -\frac{K_c}{v}\frac{T_L}{T_I} \end{bmatrix} \tag{7.12}$$

The model identification aims to estimate the parameter values by the prediction error minimization (PEM)[36] method using measured input and output data from the experiment. The system identification toolbox in MATLAB is used to compute the identification results. The criterion is as follows:

$$J = \frac{1}{N}\sum_{k=1}^{N} e^2[k] \tag{7.13}$$

where $e[k]$ represents the difference between the measured output and predicted output of the model (Figure 7.5):

$$e[k] = \delta_{SW}[k] - \hat{\delta}_{SW}[k] \tag{7.14}$$

In this study the visual anticipatory and compensatory gain (K_p and K_c) are chosen as the parameters to be identified, and the other parameters are fixed at their nominal value (the longitudinal speed is fixed at 18 m/s, see section 7.2.5). Although the concepts of anticipation and compensation have some commonalities with the strategy of the haptic guidance system, it is beyond the scope of this paper to evaluate the relevance of this control architecture because the sharing level of the anticipatory and compensatory controller have not been manipulated. In addition, the two-point visual model represents a combination of the dynamics of the lateral control and steering wheel (*LC-SW*) system in Figure 7.5. This *LC-SW* system covers both human driver behavior and haptic guidance behavior, including extreme cases of human or haptic guidance driving alone. By identifying the parameters, we aim to project the input-output relationship of the *LC-SW* system onto the visual model to check the contribution of each input signal to the output signal. In other words, if we obtain a decrease in the anticipatory gain or an increase in the compensatory gain, the steering wheel angle (δ_{SW}) is determined more by the anticipatory than the compensatory part. Such results offer an idea regarding how the steering-control strategy changes according to the conditions.

7.3.3 Validation of Identified Model

Before comparing the values of the identified parameters, each model obtained for every participant must be validated by verifying the model fit and the parameter uncertainties. The fit percentage is calculated as follows:

$$FIT = \left(1 - \frac{\|\delta_{SW} - \hat{\delta}_{SW}\|_2}{\|\delta_{SW} - m_{\delta_{SW}}\|_2}\right) \times 100\% \tag{7.15}$$

where $m_{\delta_{SW}} = \frac{1}{N}\sum_{k=1}^{N}\delta_{SW}[k]$ is the arithmetic mean of the measured steering wheel angle, and $\hat{\delta}_{SW}$ is the predicted steering wheel angle. The value of FIT varies between $-\infty$ (worst) and 100% (best).

The magnitude of the parameter uncertainties provides a measure of the model reliability. When model parameters are estimated from the data, these estimates are precise in a confidence region that can be assessed. The size of this region is determined by the value of the parameter uncertainties computed during the estimation. It is important to always verify this information before exploiting the value of the identified parameters. Supposing an estimated parameter vector $\hat{\theta}^{(M)} = \begin{bmatrix}\hat{K}_p & \hat{K}_c\end{bmatrix}^T$ and its limit θ^*, the "true" parameter vector, under certain conditions, the following is known[36]:

$$\sqrt{M}(\hat{\theta}^{(M)} - \theta^*) \in AsN(0, Q_\theta) \tag{7.16}$$

where M is the number of data samples and Q_θ is the asymptotic covariance matrix of θ. It demonstrates that the distribution of the random variable $\sqrt{M}(\hat{\theta}^{(M)} - \theta^*)$ converges asymptotically to the normal distribution $N(0, Q_\theta)$ if M tends to infinity. In addition, we obtain the following:

$$(\hat{\theta}^{(M)} - \theta^*)^T Q_\theta^{-1}(\hat{\theta}^{(M)} - \theta^*) \in \chi^2(d) \tag{7.17}$$

where $d = \dim\left(\hat{\theta}^{(M)}\right) = 2$ (indicating that two parameters are to be identified) and $\chi^2(d)$ is the chi-square distribution with d degrees of freedom. In this case, the confidence level α (e.g., 90%) could be chosen to obtain a confidence region given by the following:

$$P\Big((\hat{\theta}^{(N)} - \theta^*)^T Q_\theta^{-1}(\hat{\theta}^{(N)} - \theta^*) \leq \chi^2_\alpha(d)\Big) = \alpha \tag{7.18}$$

with $\chi^2_\alpha(d)$ as the α-level of the $\chi^2(d)$-distribution. This equation indicates that, with α probability, the "true" parameter vector lies inside an ellipsoid (an ellipse in our case) defined in the R^d space, of which the center is $\hat{\theta}^{(N)}$ and the axes are determined by the eigenvalues and eigenvectors of $\chi^2_\alpha(d)Q_\theta$. For each participant, to verify whether any intersection exists between the model ellipses from scenario i and j, we defined the value d_{ij}, which is the difference between the Euclidean distance of the center of two ellipses and the sum of two semi-major axes, as follows:

$$d_{ij} = \|\hat{\theta}_i - \hat{\theta}_j\|_2 - (\sqrt{\lambda_i} + \sqrt{\lambda_j}) \tag{7.19}$$

where λ_i and λ_j are the largest eigenvalues of matrices $\chi^2_\alpha(d)Q_{\theta_i}$ and $\chi^2_\alpha(d)Q_{\theta_j}$, respec-

tively. No intersection exists if $d_{ij} > 0$, which indicates that these two models are statistically different; thus, it is likely that any difference between identified parameters should be caused by the independent experimental variables rather than the parameter uncertainties.

7.3.4 Summary Diagram

Figure 7.5 illustrates how the data analysis was conducted in this study. The lateral control process is represented by white boxes. The human driver performs the task with or without the haptic guidance system through the steering column and generates the steering wheel angle as vehicle input. The vehicle interacts with the road and provides *ad hoc* information to the driver and haptic guidance system. The "Signal Generation" block represents the computational interface, allowing from the state of the vehicle-road model to format or even estimate the input signals to the driver model and to the haptic guidance system (see Figure 7.2 and [26]). The performance of the lateral control task is evaluated using the metrics in the green boxes and the identified parameters of the *LC-SW* system in the red box.

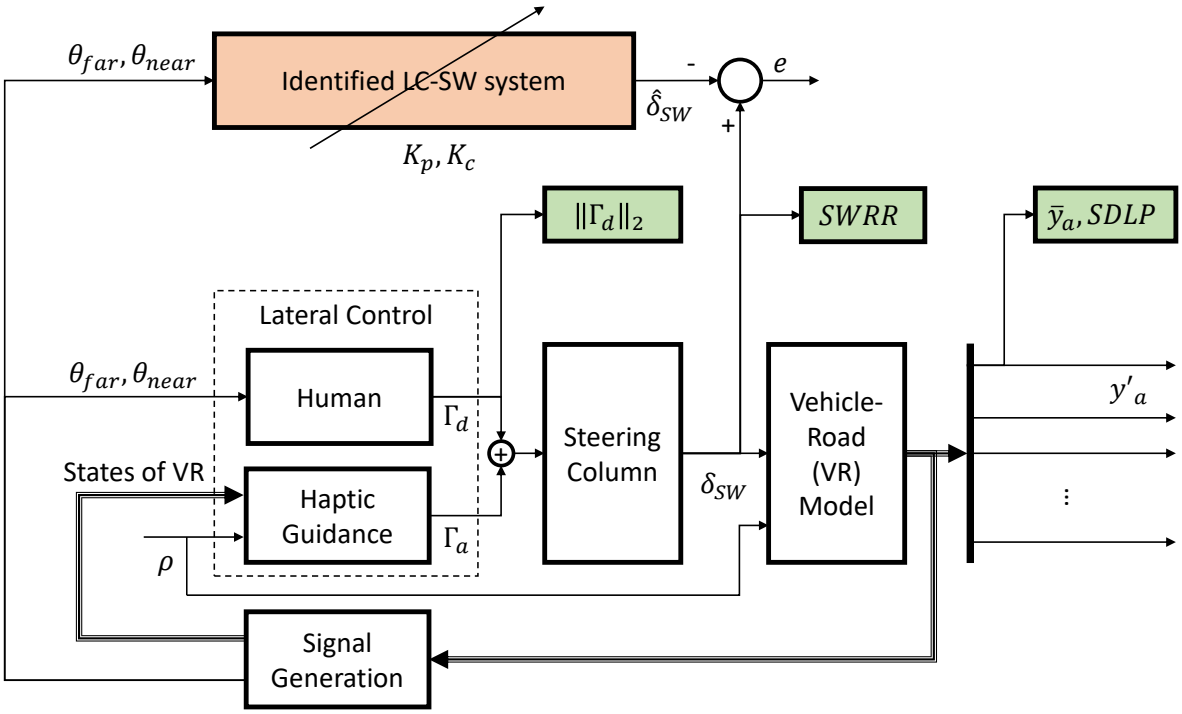

Figure 7.5 – Summary of data analysis methods.

7.4 Results

All data from each scenario were used to calculate the metrics and to identify the two model parameters. To represent the distribution of participants, the results are presented in box plots around the mean value for all participants. The red bar is the median. The blue triangles are mean values. The blue box represents the first quartile and the third quartile data points. The whiskers represent the minimum and maximum data points which are not beyond the interquartile range. The red crosses are outliers.

A repeated-measures analysis of variance ($ANOVA$) with 2 within-subject factors was used to evaluate the effects of the visibility (F) and haptic guidance (A). The differences between the degrees of the independent variables were considered statistically significant for p-values less than .05.

7.4.1 Steering Performance

The $SWRR$ per minute with a gap-size of 2° indicates a significant main effect for both F ($F(1,14) = 69.92, p < .001, \eta_p^2 = 0.833$) and A ($F(1,14) = 14.42, p < .005, \eta_p^2 = 0.507$), as shown in Figure 7.6. The $SWRR$ is significantly higher with fog ($+F$) than without fog ($-F$). With haptic guidance ($+A$), the $SWRR$ is significantly lower than it is without haptic guidance ($-A$). No significant interaction effect exists between F and A ($F(1,14) = 2.7087, p = .12, \eta_p^2 = 0.162$).

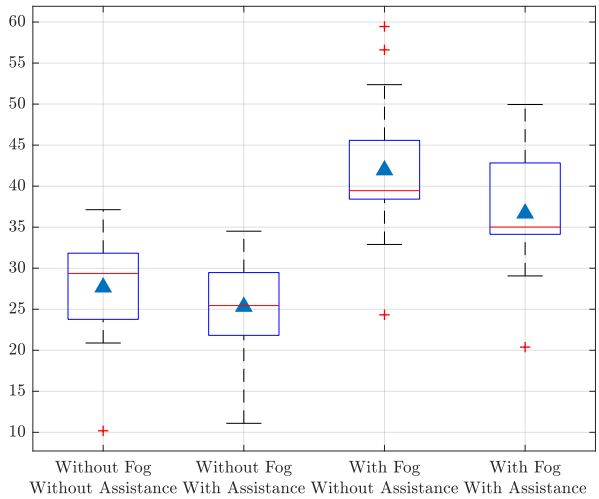

Figure 7.6 – $SWRR$ per minute with gap-size 2°.

7.4.2 Lane Keeping Performance

The mean of adjusted deviation of the lateral position ($\overline{y}_a$) shows a significant main effect for A ($F(1,14) = 10.73, p < .01, \eta_p^2 = 0.434$) but not for F ($F(1,14) = 3.30, p = .091, \eta_p^2 = 0.191$), Figure 7.7). With the haptic guidance ($+A$), $\overline{y}_a$ is significantly lower than without haptic guidance (-A), which indicates that the curve-cutting behavior was reduced. No significant interaction effect exists between F and A ($F(1,14) = 0.49, p = .49, \eta_p^2 = 0.034$), which reflects that $\overline{y}_a$ is lower with the haptic guidance in the two visibility conditions.

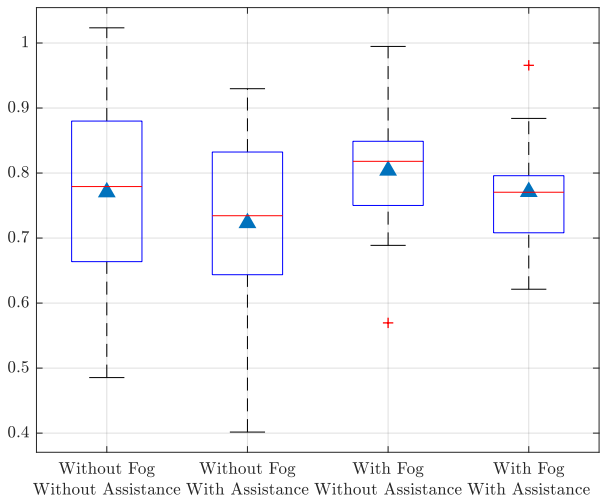

Figure 7.7 – Mean of adjusted deviation of the lateral position.

The *SDLP* shows a significant main effect for both F ($F(1,14) = 6.06, p < .05, \eta_p^2 = 0.301$) and A ($F(1,14) = 10.23, p < .01, \eta_p^2 = 0.422$), Figure 7.8. Either with fog ($+F$) or with haptic guidance ($+A$), the *SDLP* is significantly lower than the scenarios without fog (-F) or without haptic guidance (-A). No significant interaction effect exists between F and A ($F(1,14) = 0.0005, p = .98, \eta_p^2 \approx 0$). Thus, the *SDLP* is significantly higher in the presence of either fog or haptic guidance.

7.4.3 Driver Control Effort

The L^2-norm of the driver steering wheel torque $\|\Gamma_d\|_2$ indicates a significant main effect for A ($F(1,14) = 562.89, p < .001, \eta_p^2 = 0.976$) but not for F ($F(1,14) = 1.34, p = .27, \eta_p^2 = 0.087$), as shown in Figure 7.9. With haptic guidance ($+A$), $\|\Gamma_d\|_2$ is significantly lower than it is without haptic guidance (-A). With haptic guidance, the mean value of

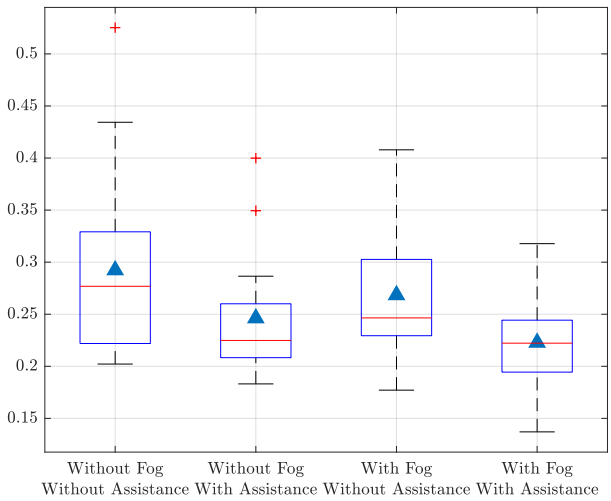

Figure 7.8 – Standard deviation of the deviation of the lateral position.

$\|\Gamma_d\|_2$ is about half of that without haptic guidance. This corresponds to the sharing levels defined in section 7.2.3. No significant interaction effect exists between F and A ($F(1, 14) = 3.37, p = .088, \eta_p^2 = 0.194$). Hence, the driver steering wheel torque energy is significantly lower with haptic guidance in all visibility conditions.

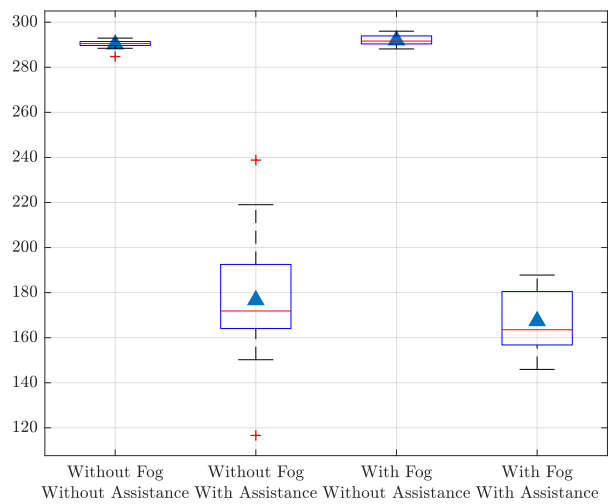

Figure 7.9 – Driver steering torque energy.

7.4.4 Identified Model Validation

The FIT value of each identified model indicates a significant main effect for F ($F(1,14) = 30.44, p < .001, \eta_p^2 = 0.685$) but not for A ($F(1,14) = 0.15, p = .70, \eta_p^2 = 0.011$), as shown in Figure 7.10. No significant interaction effect exists between F and A ($F(1,14) = 3.84, p = .07, \eta_p^2 = 0.215$). Although the FIT is significantly lower with fog (+F) than without fog (-F), almost all FIT values were above 70%, which is perfectly acceptable in terms of model validation.

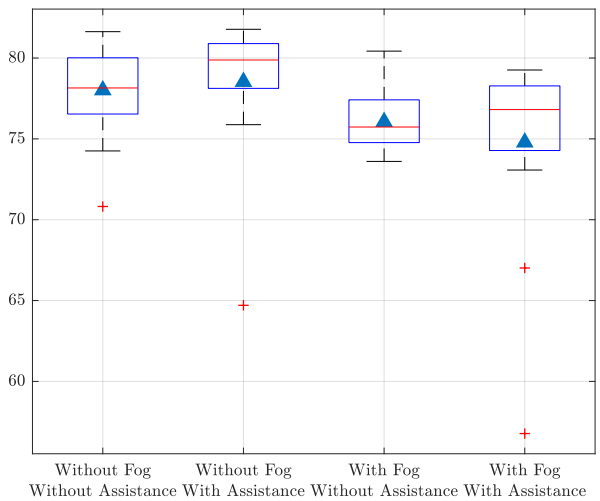

Figure 7.10 – FIT for all participants.

The d_{ij} values indicating the intersection between the model parameter confidence ellipses are shown in Table 7.2 (see section 7.2.2 for numeration of scenarios). Because four different scenarios exist, six pairs of comparisons exist in total for each participant. The table shows that most identified models differ from each other with several exceptions (negative values). The negative values are of relatively small magnitudes. In addition, having a positive d_{ij} is a sufficient but not necessary condition for not having any intersections between ellipses. As an example, Figure 7.11 shows the worst case, that of participant 3 Although d_{13} (red vs. blue ellipse) and d_{24} (green vs. black ellipse) are negative, the regions of confidence do not overlap. Consequently, the observed parameter variations are attributed to the experimental manipulations rather than the parameter uncertainties.

Table 7.2 – Comparison of model parameter uncertainties.

Participant	d_{12}	d_{13}	d_{14}	d_{23}	d_{24}	d_{34}
1	0.67	2.13	4.14	1.05	3.06	1.27
2	0.24	2.72	0.56	3.31	1.16	1.52
3	1.49	*-0.11*	0.91	1.17	*-0.3*	0.61
4	*-0.06*	0.74	2.66	0.55	2.46	1.62
5	2.86	4.62	4.01	1.46	0.85	0.14
6	0.72	1.02	1.6	*-0.12*	0.41	0.17
7	0.52	*-0.14*	0.75	0.76	*-0.24*	0.99
8	0.75	2.21	0.93	1.15	*-0.11*	0.46
9	0.37	1.51	3.44	0.72	2.64	1.6
10	0.28	2.18	1.63	2.9	2.35	*-0.1*
11	0.52	0.08	0.92	0.88	1.71	0.36
12	1.56	2.2	0.49	0.28	0.67	1.31
13	*-0.21*	*-0.27*	0.73	*-0.01*	0.99	0.59
14	1.77	*-0.02*	0.7	1.41	2.73	0.94
15	0.43	0.2	2.95	*-0.02*	2.29	2.37

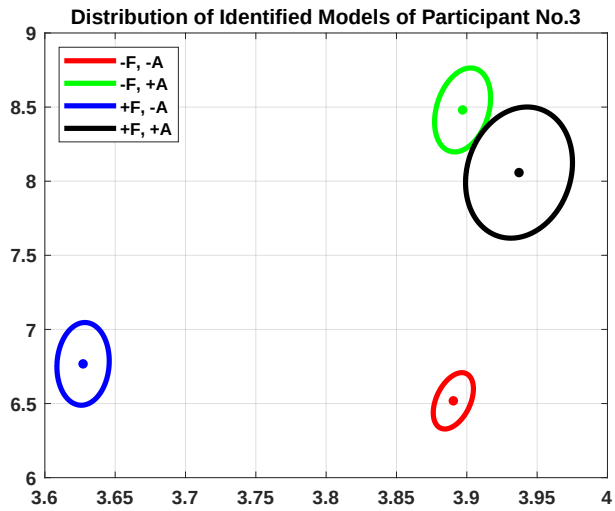

Figure 7.11 – Confidence regions of identified parameters for participant No. 3.

7.4.5 Anticipatory and Compensatory Gain

The identified anticipatory gain (K_p) shows a significant main effect for A ($F(1,14) = 29.03, p < .001, \eta_p^2 = 0.675$) but not for F ($F(1,14) = 2.23, p = .16, \eta_p^2 = 0.138$), as shown in Figure 7.12. With haptic guidance ($+A$), the anticipatory gain is significantly higher than it is without haptic guidance (-A). No significant interaction effect exists between F and A ($F(1,14) = 3.19, p = .096, \eta_p^2 = 0.186$). Thus, the anticipatory gain is significantly higher with haptic guidance in all visibility conditions.

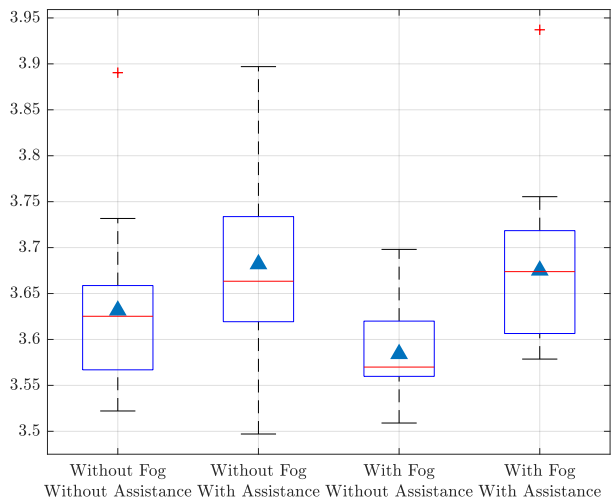

Figure 7.12 – Identified anticipatory gain (K_p).

The identified compensatory gain (K_c) shows a significant main effect for both F ($F(1,14) = 12.88, p < .01, \eta_p^2 = 0.479$) and A ($F(1,14) = 5.54, p < .05, \eta_p^2 = 0.283$), as shown in Figure 7.13. Either with fog ($+F$) or with haptic guidance ($+A$), the compensatory gain is significantly higher than without fog (-F) or without haptic guidance (-A). No significant interaction effect exists between F and A ($F(1,14) = 1.15, p = .30, \eta_p^2 = 0.076$). Thus, the compensatory gain is significantly higher in the presence of either fog or haptic guidance.

7.5 Discussion

The results demonstrate that the effects of assistance and fog on the different considered indicators were cumulative without any interaction. This result differs from those reported by [16], who showed that drivers could benefit more from haptic shared control in reduced

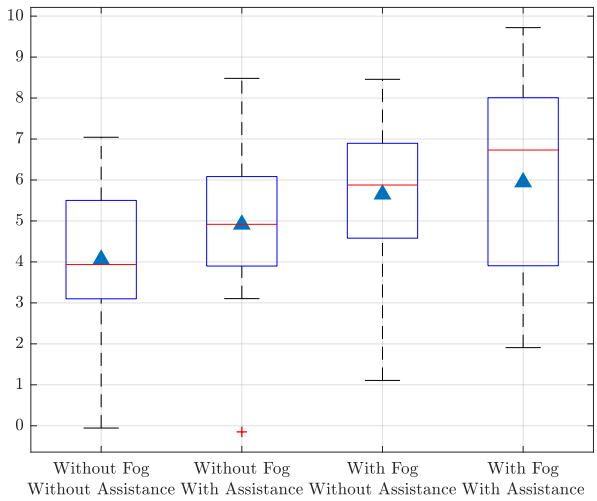

Figure 7.13 – Identified compensatory gain (K_c).

visibility. The difference between the studies can be explained by the diverse control strategies used in the two cases to achieve shared control. It could also be due to a difference in the difficulty of the lane-keeping task. The track in our study was more demanding with more variation in road curvature and some sections of higher curvature. Regardless of this, it appears that the drivers benefited as much from haptic shared control in good visibility conditions as in the fog. The following discussion first focuses on the main effect of fog, and haptic shared control is considered separately before proposing a synthesis of the results.

7.5.1 Effect of Fog

Fog reduces the driver's ability to anticipate. This can result in more short-term corrections at the steering wheel and increased safety margins. Fog can also sometimes make it more difficult to keep the vehicle on the desired trajectory [27], [29], [31]. Frissen & Mars [31] manipulated near and far vision artificially by applying to the visual scene a mask whose degree of opacity was controlled. They showed that steering control was robust up to 60% degradation of far vision and became less stable starting at 80%. It is difficult to assess the degree of opacity of the fog used in our study. In any case, its effect would also depend on vehicle speed and road profile. In practice, the density of the fog was determined empirically in such a way that it was difficult, but possible, to anticipate changes in road curvature for the selected speed. The results show that no major difficulties were

observed. The value of $\overline{y}_a$ was almost the same in both cases (i.e., with and without fog), indicating that the driving trajectory remained similar. In contrast, an increase in *SWRR* and a decrease in *SDLP* were observed. The effect of the fog was therefore limited to an increase in the frequency of small correction movements at the steering wheel, resulting in a slight decrease in the variability of the lateral position. Consistently, the parametric identification of the model captured this increase in compensatory behavior through the increase in the compensatory gain (K_c). The anticipatory gain (K_p) remained stable because no significant change exists in the path taken by the participants.

7.5.2 Effect of Haptic Guidance

The purpose of haptic shared control is to facilitate steering control by delegating some of the effort to the system while providing gesture guidance to the driver. As in previous work [2], haptic guidance has made it possible to reduce the driver control effort, which is observed through $\|\Gamma_d\|_2$. When haptic guidance was present, the control effort by the driver was half of the effort required without haptic guidance, which corresponds to the chosen system sharing level. Although the validation of the control strategy used was not the main objective of this study, the results demonstrated that it is relevant. The reduction in effort is accompanied by smoother steering wheel control, which is evidenced by a slight decrease in *SWRR*. Haptic guidance also induced the lateral position of the vehicle to be closer to the center of the lane, even if the participants continued to cut corners, especially if participants had sufficient visual information for anticipation. In other words, it appeared that the participants essentially followed the haptic guidance provided by the system, so that the produced trajectories were more consistent with the curvature of the road and were less variable. The results of the parametric identification were consistent with these observations. The new profile trajectory, which conforms more to the curvature, resulted in a net increase of anticipatory gain (K_p), and the smoother control increased the compensatory gain (K_c).

7.5.3 Synthesis

By considering both the effect of fog and haptic guidance, we can now synthesize the relationship between driving performance and the identified parameters of the *LC-SW* system. As mentioned, the anticipatory gain parameter represents the visual anticipation of changes in road curvature. One might logically expect this parameter to be particularly

sensitive to any experimental manipulation that prevents the road from being correctly anticipated (i.e., the introduction of fog into the visual scene). However, this was not the case in this study because, in the end, the fog did not change the trajectory path followed by the vehicle profile. Nevertheless, haptic guidance had a significant influence. By reducing the driver's propensity to cut corners even very slightly, trajectories became closer to the road profile, and the anticipatory gain proved to be very sensitive to this. Therefore, it is reasonable to conclude that anticipatory gain represents visual anticipation only to the extent that this anticipation defines the followed trajectory.

The parameter compensatory gain represents the online compensation of the deviations in the lateral position during driving. It was expected to increase as the *SDLP* decreased. This is the case in our study, whether due to fog, haptic guidance, or both, in which case the effect was cumulative. However, the reduction in the variability of the lateral position is not of the same nature under the two conditions. The variability is the consequence of an increase in *SWRR* in the case of fog, whereas it decreased in the case of haptic guidance. In other words, compensatory gain proved to be very sensitive to a decrease in the variability of the lateral position whether it was the result of more corrections due to a decrease in visual anticipation capability or to the smoother steering wheel control induced by haptic guidance.

7.6 Conclusion

The objective of this work was to verify to what extent a simple and robust model like the two-point model is likely to "explain" through its parameters, the behavior of the driver-assistance system as a function of the characteristics of the haptic guidance or the type of visibility. To achieve this goal, this study proposed to evaluate the performance of the human-machine system by combining two types of indicators: the usual metrics used to evaluate driving performance and the values resulting from the identification of a steering-control model. As a first approach, we chose a simple two-parameter model that accounts for visual steering control. We concluded that a two-point visual model can capture the effect of certain driving conditions very well, particularly those that influence the produced trajectory. However, such a model considers only the steering wheel angle as an output for the performance evaluation. Therefore, it does not independently distinguish between the actions of the human driver and those of the haptic guidance systems on the steering wheel. In further work, we aim to use other more comprehensive models, including

models incorporating a neuromuscular system and using torque as the output[18], [34], [35]. It would also be interesting to study the response of the model parameters if drivers can control the speed of vehicle. Moreover, other control settings, such as variant sharing levels, should be tested to help generalize the validity of the conclusions.

Acknowledgment

This work was supported by RFI Atlanstic 2020, funded by Région Pays de la Loire.

7.7 References

[1] M. Steele and R. B. Gillespie, "Shared Control between Human and Machine: Using a Haptic Steering Wheel to Aid in Land Vehicle Guidance", *Proceedings of the Human Factors and Ergonomics Society Annual Meeting*, vol. 45, *23*, pp. 1671–1675, 2001.

[2] D. A. Abbink and M. Mulder, "Exploring the dimensions of haptic feedback support in manual control", *Journal of Computing and Information Science in Engineering*, vol. 9, *1*, pp. 1–9, 2009.

[3] D. A. Abbink, M. Mulder, and E. R. Boer, "Haptic shared control: Smoothly shifting control authority?", *Cognition, Technology and Work*, vol. 14, *1*, pp. 19–28, 2012, ISSN: 14355558.

[4] D. A. Abbink, T. Carlson, M. Mulder, J. C. De Winter, F. Aminravan, T. L. Gibo, and E. R. Boer, "A topology of shared control systems-finding common ground in diversity", *IEEE Transactions on Human-Machine Systems*, vol. 48, *5*, pp. 509–525, Oct. 2018, ISSN: 21682291.

[5] P. Griffiths and R. B. Gillespie, "Shared control between human and machine: haptic display of automation during manual control of vehicle heading", *in 12th International Symposium on Haptic Interfaces for Virtual Environment and Teleoperator Systems, 2004. HAPTICS '04. Proceedings*, Mar. 2004, pp. 358–366.

[6] P. G. Griffiths and R. B. Gillespie, "Sharing Control Between Humans and Automation Using Haptic Interface: Primary and Secondary Task Performance Benefits", *Human Factors*, vol. 47, *3*, pp. 574–590, 2005.

[7] M. Mulder, D. A. Abbink, and E. R. Boer, "The effect of haptic guidance on curve negotiation behavior of young, experienced drivers", *in Conference Proceedings - IEEE International Conference on Systems, Man and Cybernetics*, 2008, pp. 804–809, ISBN: 978-1-4244-2383-5.

[8] L. Marchal-Crespo, S. McHughen, S. C. Cramer, and D. J. Reinkensmeyer, "The effect of haptic guidance, aging, and initial skill level on motor learning of a steering task", *Experimental Brain Research*, vol. 201, *2*, pp. 209–220, 2010, ISSN: 00144819.

[9] M. Mulder, D. A. Abbink, and E. R. Boer, "Sharing control with haptics: Seamless driver support from manual to automatic control", *Human Factors*, vol. 54, *5*, pp. 786–798, 2012.

[10] Z. Wang, R. Zheng, T. Kaizuka, K. Shimono, and K. Nakano, "The effect of a haptic guidance steering system on fatigue-related driver behavior", *IEEE Transactions on Human-Machine Systems*, vol. 47, *5*, pp. 741–748, 2017, ISSN: 21682291.

[11] S. M. Petermeijer, D. A. Abbink, M. Mulder, and J. C. De Winter, "The Effect of Haptic Support Systems on Driver Performance: A Literature Survey", *IEEE Transactions on Haptics*, vol. 8, *4*, pp. 467–479, 2015, ISSN: 19391412.

[12] S. M. Petermeijer, D. A. Abbink, and J. C. De Winter, "Should drivers be operating within an automation-free bandwidth? Evaluating haptic steering support systems with different levels of authority", *Human Factors*, vol. 57, *1*, pp. 5–20, 2015, ISSN: 15478181.

[13] Z. Wang, T. Kaizuka, and K. Nakano, "Effect of Haptic Guidance Steering on Lane Following Performance by Taking Account of Driver Reliance on the Assistance System", *in Proceedings - 2018 IEEE International Conference on Systems, Man, and Cybernetics, SMC 2018*, 2018, ISBN: 9781538666500.

[14] M. Sivak, "The Information That Drivers Use: Is it Indeed 90% Visual?", *Perception*, vol. 25, *9*, pp. 1081–1089, 1996, PMID: 8983048.

[15] S. Y. De Nijs, M. Mulder, and D. A. Abbink, "The value of haptic feedback in lane keeping", *in Conference Proceedings - IEEE International Conference on Systems, Man and Cybernetics*, vol. 2014-Janua, Institute of Electrical and Electronics Engineers Inc., 2014, pp. 3599–3604.

[16] F. Mars, M. Deroo, and J.-M. Hoc, "Analysis of human-machine cooperation when driving with different degrees of haptic shared control", *IEEE Transactions on Haptics*, vol. 7, *3*, pp. 324–333, 2014, ISSN: 19391412.

[17] A. Ameyoe, P. Chevrel, E. Le-Carpentier, F. Mars, and H. Illy, "Identification of a Linear Parameter Varying Driver Model for the Detection of Distraction", *1st IFAC Workshop on Linear Parameter Varying Systems LPVS 2015*, vol. 48, *26*, pp. 37–42, 2015, ISSN: 2405-8963.

[18] F. Mars and P. Chevrel, "Modelling human control of steering for the design of advanced driver assistance systems", *Annual Reviews in Control*, vol. 44, *Supplement C*, pp. 292–302, 2017, ISSN: 13675788.

[19] M. Marcano, S. Diaz, J. Perez, and E. Irigoyen, "A Review of Shared Control for Automated Vehicles: Theory and Applications", *IEEE Transactions on Human-Machine Systems*, *September*, pp. 1–17, 2020, ISSN: 2168-2291.

[20] L. Saleh, P. Chevrel, F. Claveau, J. F. Lafay, and F. Mars, "Shared steering control between a driver and an automation: Stability in the presence of driver behavior uncertainty", *IEEE Transactions on Intelligent Transportation Systems*, vol. 14, pp. 974–983, 2013.

[21] M. Flad, L. Fröhlich, and S. Hohmann, "Cooperative Shared Control Driver Assistance Systems Based on Motion Primitives and Differential Games", *IEEE Transactions on Human-Machine Systems*, vol. 47, *5*, pp. 711–722, 2017.

[22] A. T. Nguyen, C. Sentouh, and J. C. Popieul, "Sensor Reduction for Driver-Automation Shared Steering Control via an Adaptive Authority Allocation Strategy", *IEEE/ASME Transactions on Mechatronics*, vol. 23, *1*, pp. 5–16, 2018, ISSN: 10834435.

[23] M. A. Benloucif, C. Sentouh, J. Floris, P. Simon, and J. C. Popieul, "Online adaptation of the Level of Haptic Authority in a lane keeping system considering the driver's state", *Transportation Research Part F: Traffic Psychology and Behaviour*, vol. 61, pp. 107–119, 2019, ISSN: 13698478.

[24] C. Sentouh, A. Nguyen, M. A. Benloucif, and J. Popieul, "Driver-Automation Cooperation Oriented Approach for Shared Control of Lane Keeping Assist Systems", *IEEE Transactions on Control Systems Technology*, vol. 27, *5*, pp. 1962–1978, 2019, ISSN: 1558-0865.

[25] X. Ji, K. Yang, X. Na, C. Lv, and Y. Liu, "Shared Steering Torque Control for Lane Change Assistance: A Stochastic Game-Theoretic Approach", *IEEE Transactions on Industrial Electronics*, vol. 66, *4*, pp. 3093–3105, 2019, ISSN: 1557-9948.

[26] B. Pano, P. Chevrel, and F. Claveau, "Anticipatory and compensatory e-assistance for haptic shared control of the steering wheel", *2019 18th European Control Conference, ECC 2019*, pp. 724–731, 2019.

[27] D. D. Salvucci and R. Gray, "A two-point visual control model of steering", *Perception*, vol. 33, *10*, pp. 1233–1248, 2004.

[28] E. Donges, "A Two-Level Model of Driver Steering Behavior", *Human Factors: The Journal of the Human Factors and Ergonomics Society*, vol. 20, *6*, pp. 691–707, Dec. 1978.

[29] M. Land and J. Horwood, "Which parts of the road guide steering?", *Nature*, vol. 377, *6547*, pp. 339–340, Sep. 1995, ISSN: 00280836.

[30] J. Steen, H. J. Damveld, R. Happee, M. M. Van Paassen, and M. Mulder, "A review of visual driver models for system identification purposes", *in Conference Proceedings - IEEE International Conference on Systems, Man and Cybernetics*, 2011, pp. 2093–2100, ISBN: 9781457706523.

[31] I. Frissen and F. Mars, "The Effect of Visual Degradation on Anticipatory and Compensatory Steering Control", *Quarterly Journal of Experimental Psychology*, vol. 67, *3*, pp. 499–507, Mar. 2014, ISSN: 1747-0218.

[32] G. Markkula and J. Engström, "A Steering Wheel Reversal Rate Metric for Assessing Effects of Visual and Cognitive Secondary Task Load", *in Proceedings of the 13th ITS World Congress.*, 2006, ISBN: 0000000302.

[33] L. Nilsson, N. Merat, H. Jamson, S. Mouta, J. Carvalhais, J. Santos, V. Anttila, H. Sandberg, J. Luoma, D. de Waard, K. Brookhuis, E. Johansson, J. Engström, T. Victor, J. Harbluk, W. Janssen, and R. Brouwer, *HASTE Deliverable 2: HMI and Safety-Related Driver Performance*, English, J. Östlund, O. Carsten, and S. Jamson, Eds. Belgium: European Commission EC, 2004, PNA: Harjula, Virpi.

[34] F. Mars, L. Saleh, P. Chevrel, F. Claveau, and J.-F. Lafay, "Modeling the visual and motor control of steering with an eye to shared-control automation", *in Human Factors and Ergonomics Society 55th Annual Meeting*, vol. 55, 2011, pp. 1422–1426.

[35] L. Saleh, P. Chevrel, F. Mars, J. F. Lafay, and F. Claveau, "Human-like cybernetic driver model for lane keeping", *in Proceedings of the 18th IFAC World Congress*, 2011, pp. 4368–4373, ISBN: 9783902661937.

[36] L. Ljung, *System Identification: Theory for the User*, 2nd ed., ser. Prentice Hall information and system sciences series. Prentice Hall PTR, 1999, ISBN: 9780136566953.

Chapter 8

Towards a Driver Model to Clarify Cooperation Between Drivers and Haptic Guidance Systems

Abstract

Understanding a driver's behavior in a steering task is essential to the development of haptic guidance systems. This paper aims to predict driver torque control, especially when haptic guidance is part of haptic feedback. A new cybernetic driver model with an improved neuromuscular system is proposed and identified. It is assumed that the driver converts a target steering-wheel angle into torque by both indirect and direct control. Indirect control refers to the adaptation of the parameters of an internal model of steering compliance as perceived by the driver. Direct control accounts for the driver's corrective action through direct haptic feedback. The parameters of the model were identified with data collected from experiments conducted with a driving simulator. The results of identification were satisfactory and led to good representation of the driver's action, with or without haptic guidance. The model accurately predicted driver torque output. It can be used to study driver adaptation to haptic guidance systems.

8.1 Introduction

To meet the design guidelines for human-automation interaction, a specific mode has been proposed, called "shared haptic control." Shared haptic control has attracted increasing research attention in recent years [1], [2]. Its application to vehicle steering control is generally referred to as a "haptic guidance system." The main functionality of the system is

to provide human drivers with continuous additional torque feedback through the steering wheel. Hence, the steering wheel is simultaneously controlled by the driver and the automated system so that it acts as an effective communication interface. The benefits of haptic guidance systems have been observed in lane-keeping performance [3]–[5].

To achieve sound cooperation between a driver and the haptic guidance system, it is essential to understand human behavior during a steering task. In several haptic guidance systems (e.g. see[6], [7]), a driver model is directly included to predict human driver behavior. A driver model can improve performance by minimizing the potential for conflict between the system and the driver. In addition, the model can analyze how drivers adapt their behavior when driving with the system.

A cybernetic driver model has been proposed in [8]–[10]. In this model, it is assumed that to steer the vehicle, the driver implicitly aims at a steering angle δ_d, which is determined from the visual scene (left part of Figure 8.1). This angle is then converted to a torque applied to the steering system through co-activation of the muscles by α- and γ- motor commands. The model has been successfully used in the synthesizing a haptic steering system [11] and in discriminating various types of distraction through analyzing parametric variations [10], [12], [13].

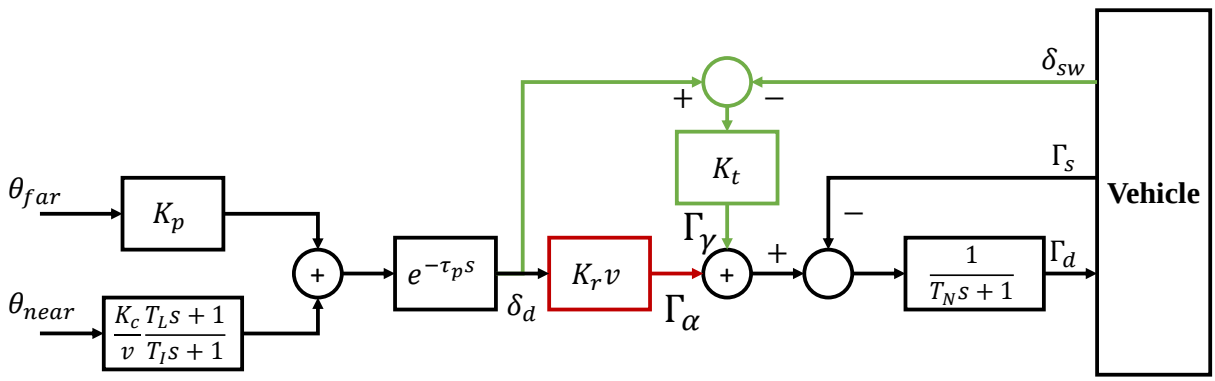

Figure 8.1 – Cybernetic driver model in [8]–[10].

However, the model has been designed and identified in situations where the human drives alone. It considers only the self-aligning torque as haptic feedback but does not take into account the influence of a haptic guidance system, which could be either parametric or structural. Generally, it is difficult for a driver to distinguish between self-aligning torque and haptic guidance torque because they act together on the steering wheel and are perceived through the same channel. Therefore, there is no reason to explicitly separate them in the driver model, and it is the combination that is called *haptic feedback*.

In addition, when analyzing the driver's neuromuscular behavior using the model, it becomes difficult to interpret the intermediate torque generated by the α- and γ- commands. Precisely, on the one hand, the co-activation of muscles must generate a torque that is

$$\Gamma_\alpha + \Gamma\gamma \approx \Gamma_s + \Gamma_d \tag{8.1}$$

as the time constant T_N is relatively small. On the other hand, the total torque applied on the steering system, ignoring the friction, is

$$\sum \Gamma \approx \Gamma_d - \Gamma_s \tag{8.2}$$

Substituting the Γ_d in (8.1) by the Γ_d in (8.2) gives

$$\Gamma_\alpha + \Gamma\gamma \approx 2\Gamma_s + \sum \Gamma \tag{8.3}$$

The above calculations imply that from the target steering-wheel angle δ_d, the intermediate torque generated by the α- and γ- commands is double the strength of the self-aligning torque. Such result has not been observed in any experiment yet.

To solve these issues, this article presents a new driver model with a reconsidered neuromuscular system (*NMS*). The system is designed taking into account the haptic feedback, which is the sum of self-aligning torque and assistance torque when driving with the haptic guidance system, or only the former if driving alone. The structure of the model is discussed in Section 8.2. The methods adopted for data collection and identification of the model parameters are presented in Section 8.3 and 8.4, respectively. The results are presented in Section 8.5. Finally, we provide conclusions about the results and propose future work in Section 8.6.

8.2 Driver Model with Haptic Feedback

The main contribution of this paper consists of the new driver model structure shown in Figure 8.2. The description of signals is listed in Table 8.1. This model decomposes the vehicle lateral-control task of driver into two steps: 1) generating a target steering-wheel angle by a two-point visual model; and 2) applying the target angle to limb-steering system by *NMS*, with the implicit and explicit involvement of haptic feedback, as shown by the dashed line and solid line from Γ_{fb}, respectively.

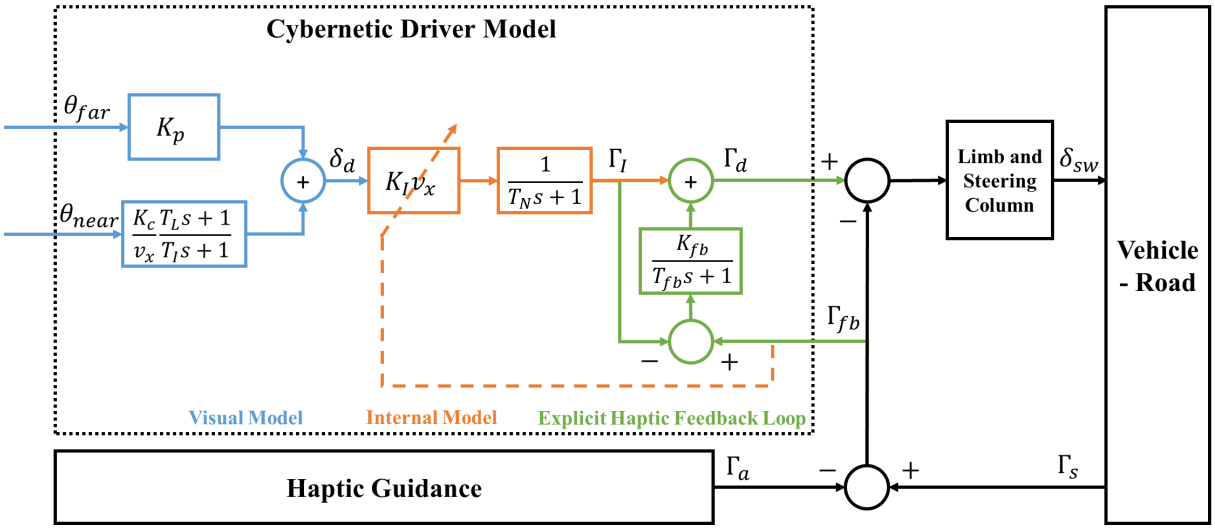

Figure 8.2 – Structure of the proposed cybernetic driver model. Blue: two-point visual model; Orange: driver internal model; Green: direct haptic feedback loop.

8.2.1 Two-point Visual Model

The two-point visual model is adopted as a starting point. As described in the literature [14], [15], the visual information that a human perceives while driving is extracted from both a distant and a near area. Two points within these zones, referred to as far and near points respectively, are a simplified representation of the visual inputs. The far point may be the tangent point of the inner edge of the road; it represents the anticipation of changes in the curvature of the road. The near point is a few meters ahead of the vehicle. It represents the visual perception of the lateral deviation of the vehicle used by the driver to keep the vehicle in the lane. The angle between the heading of the vehicle and these points, namely θ_{far} and θ_{near}, are used as input for the visual model.

8.2.2 Neuromuscular Action

Neuromuscular-system modeling aims to represent two fundamental mechanisms: 1) how muscles convert the target steering-wheel angle into steering torque and 2) how haptic feedback is involved in the driver's control[8]. It has been shown that humans can actually adapt to various types of haptic feedback laws but cannot drive without such feedback (i.e., with zero or inverted haptic feedback)[16]. In the proposed model, the *NMS* associated with the limb-steering system functionally acts as an angular servo system to ensure that the actual steering-wheel angle follows the target angle. The *NMS* may achieve

Table 8.1 – Description of signals in Figure 8.2

Signal	Description
θ_{far}	Far-point Angle
θ_{near}	Near-point Angle
δ_d	Target Steering-wheel Angle
δ_{SW}	Actual Steering-wheel Angle
Γ_I	Torque from Internal Model
Γ_d	Driver Steering Torque
Γ_{fb}	Haptic Feedback Torque
Γ_a	Haptic Guidance Torque
Γ_s	Self-aligning Torque

this by direct or indirect control. "Indirect control" here refers to parameter adaptation. Specifically, the parameter defines an internal model of the steering system, simply reduced to its stiffness. By contrast, "direct control" consists of torque feedback that compensates for errors of the internal model.

Driver Internal Model There is reason to believe that drivers adapt their behavior through their interactions with the steering wheel, by perceiving steering compliance and inversing it. This idea has been proposed and explored in neural science[17]. The internal model results from driver perception and prior knowledge of the steering system. During driving, the arm muscles and the steering wheel are combined to form a limb-steering system. The driver learns about the dynamics of the system and adapts to them by updating an internal model of steering system compliance. Ideally, if the estimate is accurate (i.e. if the internal model is equal to the inverse steering system), no additional information is needed for the driver to reach the target steering angle; the driver can accurately provide the necessary steering torque. However, it is likely that this estimate is only approximate and corresponds to a simple (low-order) internal model [18]. In this study, it is limited to a static gain $K_I v_x$, which depends on the longitudinal speed v_x of the vehicle.

An important characteristic of the internal model is that it can be learned by the driver through experience with the vehicle. The learning process can be rapid because an experienced driver can easily adapt to another vehicle with a different steering system.

The same is true when the extra guidance torque is applied to the steering system. From a driver's perspective, it appears that the dynamics of the steering system is modified, and the driver thus adapts to cooperate with the new steering dynamics. To represent this process in the model, the haptic feedback signal is used to update the internal model. The adaptation of the internal model to the haptic guidance system should occur at the start of the driving scenario. Analysis of the speed of adaptation is beyond the scope of this study; only the adjustment mechanism of the internal model is considered.

The torque from the internal model is passed through a first-order system with a time constant T_N to represent that muscles require time to produce the torque control Γ_I. The value of T_N is fixed at $0.23s$, which corresponds to the cut-off frequency of $0.7Hz$ for reflexive muscle activity previously proposed[19].

Explicit Haptic Feedback Loop As stated above, the internal model that the driver learned can hardly be equivalent to the inverse limb-steering dynamics. To compensate for the error between the internal model's output Γ_I and the driver steering torque Γ_d, a closed-loop control must be formed. This control uses signals perceived by the driver from the steering wheel. From the perspective of muscle anatomy and physiology, muscles contain two types of sensors that convert mechanical stimuli into neural activity. The first is the muscle spindle, which detects changes and the change rate of muscle length. The second is the Golgi tendon organ, which detects changes in muscle force. In other words, either the steering-wheel angle δ_{SW}, steering-wheel angular speed $\dot{\delta}_{SW}$ or the haptic feedback Γ_{fb} can be used to establish the closed-loop control.

In our model, an explicit haptic feedback loop is introduced based on the difference between the haptic feedback torque and the output torque of the internal model (i.e., $\Gamma_{fb} - \Gamma_I$). Other choices could have been $\delta_d - \delta_{SW}$ or $\dot{\delta}_d - \dot{\delta}_{SW}$. However, haptic feedback compensation is considered to be faster and more intuitive for the driver, while a minor error between the target steering angle and the actual steering angle would be more difficult to detect through muscle sensors and would likely be compensated for by visual information. For example, a small static error in the steering-wheel angle will gradually lead to a lane change and will eventually be corrected by the driver. In other words, the *NMS* is more likely to counterbalance the haptic feedback to stabilize the steering wheel than to achieve the exact target steering-wheel angle.

8.3 Data Acquisition

8.3.1 Apparatus

An experiment for acquiring data was performed using a fixed-base driving simulator powered by SCANeR Studio (Figure 8.3a). It simulates the interior environment of a family car, with a complete dashboard; a five-speed gear stick; gas, brake and clutch pedals; and a steering wheel connected to a TRW steering system. Sensors for measuring steering-wheel angle, speed and torque are mounted in the steering system. The visual scene is displayed on three LCD screens: a central one in front of the driver and two others oriented at 45° relative to the center. The screens cover a field of view of 25° high and 115° wide. In the experiment, a small family car, the Citroën C5, was chosen as the vehicle model.

(a) Fixed-base driving simulator.

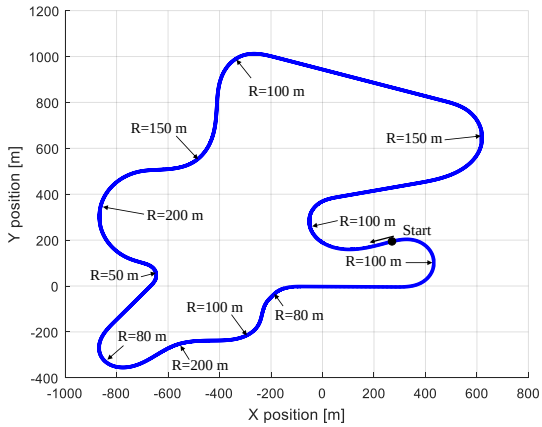

(b) Track used in the experiment.

Figure 8.3 – Experiment settings.

8.3.2 Haptic Guidance System

A haptic guidance system was implemented in the driving simulator using a controller designed in Simulink. The controller was previously developed[7] and its global architecture is shown in Figure 8.4. The final guidance Γ_a was a combination of anticipatory and compensatory assistance. The anticipatory assistance generates a reference trajectory (references for states, x_{ref}, and control input, u_{ref}, of vehicle-road model) from previewed

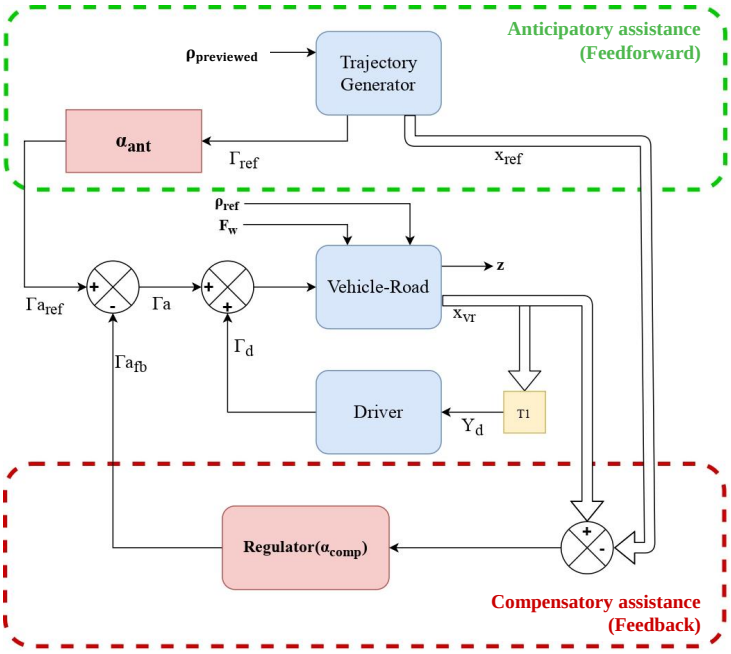

Figure 8.4 – Design strategy of the haptic guidance system.

road curvature, $\rho_{previewed}$,

$$\begin{pmatrix} \Gamma_{ref} \\ x_{ref} \end{pmatrix} = K_{FF}(p)\rho_{previewed} \tag{8.4}$$

where $K_{FF}(p)$ represents the transfer function of the trajectory generator. The applied anticipatory torque was then determined by accounting for the targeted sharing level: $\Gamma_{a_{ref}} = \alpha_{ant}\Gamma_{ref}$. The compensatory assistance adjusted the vehicle's position in the lane. It consisted of an H_2/H_∞ static output feedback that controlled the steering against disturbances and uncertainties:

$$\Gamma_{fb} = K_{FB}(x_{vr} - x_{ref}) \tag{8.5}$$

Similarly, the applied compensatory torque control was determined according to the sharing level, α_{comp}, of the compensatory part: $\Gamma_{a_{fb}} = \alpha_{comp}\Gamma_{fb}$.

In this study, both sharing levels were fixed at 50%. This configuration results in a system that delivers clear haptic guidance, although without any action from the human driver it will eventually leave the lane during some curves.

8.3.3 Participants

Five participants took part in the experiment. They were recruited from students and staff of the Laboratory of Digital Sciences in Nantes and Institute Mines-Télécom Atlantique Nantes. All participants possessed a valid driver's license with at least three years of driving experience. The participants had no known medical issues that could affect their driving skills. None of them had ever experienced a haptic guidance system.

8.3.4 Scenarios

The track used in the experiment is shown in Figure 8.3b). It was a two-lane road with a lane width of 3.5 m. All curves were Euler spirals with continuous changes in the curvature of the road. At the beginning of the experiment, all participants were provided with a brief introduction to the simulator, including the haptic guidance system. They were then instructed to drive in two different scenarios in random order: with and without the haptic guidance system. During the task, the vehicle longitudinal speed was fixed at 64 km/h (18 m/s) so that they only needed to control the steering wheel. They were asked to drive in the right-hand lane without making any lane changes for 10 min in each scenario, which equaled to almost two laps on the track.

8.4 Model Parameter Identification

It is difficult to identify the entire model directly, for the following reasons: 1) the target steering-wheel angle is not measurable; 2) the internal model is implicitly affected by the haptic feedback; 3) some parameters are weakly identifiable with the entire model. Thus, the model is separated into three parts that are identified one by one, sequentially. The data collected from the experiment are also equally divided into two parts, one for identification and another for validation.

8.4.1 Visual Model Identification

The visual model considered, shown in Figure 8.5, borrows from that in Figure 8.1. The main problem is that the target steering-wheel angle δ_d that the driver is supposed to derive from the visual angle is unknown. The only relevant signal measured was the actual angle of the steering wheel, δ_{SW}. Assuming that there is only a delay between the

two angles, it is possible to obtain the visual model with delay by identification using δ_{SW} as an output, which yields the desired parameters (K_p, K_c, T_I, T_L).

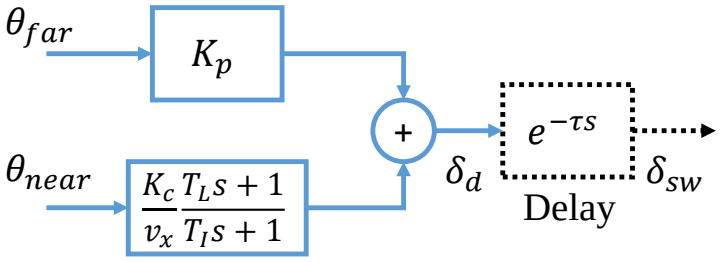

Figure 8.5 – Visual model with delay for identification.

One minimal realization of the visual model with delay (approximated by a first-order system) is written as follows:

$$\begin{cases} \dot{x} = Ax + Bu \\ y = Cx + Du \end{cases} \tag{8.6}$$

with

$$y = \delta_d \tag{8.7}$$

$$u = \begin{bmatrix} \theta_{far} & \theta_{near} \end{bmatrix}^T \tag{8.8}$$

$$A = \begin{bmatrix} -\frac{1}{T_I} & 0 \\ -\frac{1}{\tau}\frac{K_c}{v_x}(\frac{T_L}{T_I} - 1) & -\frac{1}{\tau} \end{bmatrix} \tag{8.9}$$

$$B = \begin{bmatrix} 0 & \frac{1}{T_I} \\ \frac{1}{\tau}K_p & \frac{1}{\tau}\frac{K_c}{v_x}\frac{T_L}{T_I} \end{bmatrix} \tag{8.10}$$

$$C = \begin{bmatrix} 0 & 1 \end{bmatrix} \tag{8.11}$$

$$D = \begin{bmatrix} 0 & 0 \end{bmatrix} \tag{8.12}$$

The input signals highlighted in Figure 8.6 were approximated as follows, with $D_{far} = 18m$ and $l_s = 5m$.

$$\theta_{far} \approx D_{far} \times \rho, \theta_{near} \approx -y_L/l_s \tag{8.13}$$

The identification was performed using the prediction error minimization (PEM)[20] method with data from the experiment. The system identification toolbox in MATLAB

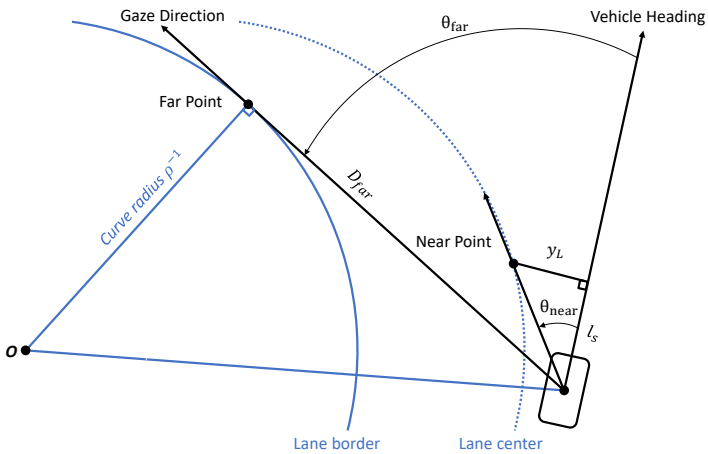

Figure 8.6 – Approximation of the far point angle and the near point angle.

was used to compute the identification results. The criterion was:

$$J = \sum_{k=1}^{N} e_v^2[k] \tag{8.14}$$

where $e_v[k]$ represents the difference between the measured output and predicted output of the model $\hat{\delta}_{SW}$:

$$e_v[k] = \delta_{SW}[k] - \hat{\delta}_{SW}[k] \tag{8.15}$$

A potential problem with using the actual steering-wheel angle to identify the visual model is that when a haptic guidance system is used for driving, the actual steering-wheel angle represents the joint effort of the human driver and the haptic guidance system. The identified visual model would in this case be a projection of the dynamics of the driver-automation system. To avoid this problem, it is necessary that the visual model of the human driver is invariant. For this purpose and for each participant, the visual model was identified from the data of the scenario without haptic guidance, and kept as-is in the scenario with haptic guidance to identify the rest of the driver model.

8.4.2 Driver Internal Model Identification

As the vehicle's longitudinal speed was fixed at 18 m/s in the experiment, only the static gain K_I needed to be identified in the driver internal model. This could be achieved by fixing the value of parameters in the visual model and minimizing the following criterion:

$$J = \sum_{k=1}^{N} e_I^2[k] \tag{8.16}$$

where

$$e_I[k] = \Gamma_d[k] - \hat{\Gamma}_I[k] \tag{8.17}$$

8.4.3 Explicit Haptic Feedback Loop Identification

Once the visual model and the driver internal model had been identified, the resulting parameter values could be used to identify the entire model by focusing on the explicit haptic feedback loop. One minimal realization of the entire model can be written as follows:

$$\begin{cases} \dot{x} = Ax + Bu \\ y = Cx + Du \end{cases} \tag{8.18}$$

with

$$y = \Gamma_d \tag{8.19}$$

$$u = \begin{bmatrix} \theta_{far} & \theta_{near} & \Gamma_{fb} \end{bmatrix}^T \tag{8.20}$$

$$A = \begin{bmatrix} -\frac{1}{T_I} & 0 & 0 \\ -K_I v_x \frac{1}{T_N} \frac{K_c}{v_x} (\frac{T_L}{T_I} - 1) & -\frac{1}{T_N} & 0 \\ 0 & -\frac{K_{fb}}{T_{fb}} & -\frac{1}{T_{fb}} \end{bmatrix} \tag{8.21}$$

$$B = \begin{bmatrix} 0 & \frac{1}{T_I} & 0 \\ K_I v_x \frac{1}{T_N} K_p & K_I v_x \frac{1}{T_N} \frac{K_c}{v_x} \frac{T_L}{T_I} & 0 \\ 0 & 0 & \frac{K_{fb}}{T_{fb}} \end{bmatrix} \tag{8.22}$$

$$C = \begin{bmatrix} 0 & 1 & 1 \end{bmatrix} \tag{8.23}$$

$$D = \begin{bmatrix} 0 & 0 & 0 \end{bmatrix} \tag{8.24}$$

Similar to the identification of the visual model, the results were also calculated using the *PEM* method implemented in the system identification toolbox of MATLAB. The only two parameters to be identified at this stage were K_{fb} and T_{fb}. The other parameters were

fixed at their nominal values, which were obtained at previous identification stages. The criterion was similar to (8.16), except the error was the difference between the measured driver steering torque and the predicted steering torque of the model:

$$J = \sum_{k=1}^{N} e_d^2[k], e_d[k] = \Gamma_d[k] - \hat{\Gamma}_d[k] \tag{8.25}$$

8.5 Results

8.5.1 Visual Model with Delay

As detailed in section 8.4.1, the visual model was identified first, based on the data recorded *ad hoc* when the participants were driving alone. The identified parameters of the model, including the time delay ,τ, are listed in Table 8.2. The FIT value, which

Table 8.2 – Identified visual model.

Participant	K_p	K_c	T_I	T_L	τ	$FIT(\%)$
P1	3.69	2.63	0.38	7.19	0.57	85.61
P2	3.82	3.69	0.45	5.80	0.56	79.45
P3	3.63	2.49	0.44	7.00	0.53	84.86
P4	3.67	2.15	0.70	6.47	0.61	82.70
P5	3.79	2.99	0.62	8.16	0.62	86.79

indicates the difference between the predicted model output and the measured output, is calculated as follows:

$$FIT = \left(1 - \frac{\|\delta_{SW} - \hat{\delta}_{SW}\|_2}{\|\delta_{SW} - m_{\delta_{SW}}\|_2}\right) \times 100\% \tag{8.26}$$

where $m_{\delta_{SW}}$ is the arithmetic mean of δ_{SW}.The identification results converged to almost the same ranges in value for all participants, with the model explaining on average 83.88% of the actual steering-wheel angle. No parameter showed an abnormal value. The variation of model parameters, especially for the near-point angle input, could imply different driving styles. In addition, the values of delay were close because they mainly represented the transport delay of the simulator (computation, graphics, sensors etc.)[8].

8.5.2 Driver Internal Model

The identified values of the driver internal gain, K_I, based on the data without and with the haptic guidance system, are listed in Table 8.3. These values enable a comparison of

Table 8.3 – Identified driver internal model.

	Without Haptic Guidance		With Haptic Guidance	
Participant	K_I	$FIT(\%)$	K_I	$FIT(\%)$
P1	0.214	83.46	0.128	51.09
P2	0.211	81.48	0.157	64.33
P3	0.217	85.42	0.129	59.51
P4	0.213	82.20	0.128	64.80
P5	0.210	82.42	0.156	51.18

the torque output predicted by the identified driver internal model, $\hat{\Gamma}_I$, and the measured driver steering torque, Γ_d, which is the FIT value shown in the table, calculated as follows:

$$FIT = \left(1 - \frac{\|\Gamma_d - \hat{\Gamma}_I\|_2}{\|\Gamma_d - m_{\Gamma_d}\|_2}\right) \times 100\% \tag{8.27}$$

where m_{Γ_d} is the arithmetic mean of Γ_d.

A significant decrease in the gain of the driver internal model was observed when the participants were driving with the haptic guidance. This was reasonable, as one of the main objectives of the haptic guidance system is to reduce the driver's effort in controlling the vehicle by providing additional torque. It also demonstrates that, as hypothesized, the participants adjusted their internal model to cooperate with the haptic guidance during the experiment. In fact, all five participants successfully completed the experiment without having any difficulty in maintaining the vehicle in the lane. For all participants, the reduction of the gain K_I was around 60% to 70%, which is related to the 50% sharing level chosen for the haptic guidance system in the experiment. The difference may suggest that participants did not fully rely on the system.

There was also a significant difference in the FIT values between the two conditions. Without the haptic guidance, the predicted torque output from the driver internal model was rather close to the measured driver steering torque. This was not the case with the haptic guidance. To investigate this difference, a residual analysis was performed. As an example, Figure 8.7 shows the residual of the driver internal model (i.e., $\Gamma_d - \hat{\Gamma}_I$) of

participant P1 in both conditions.

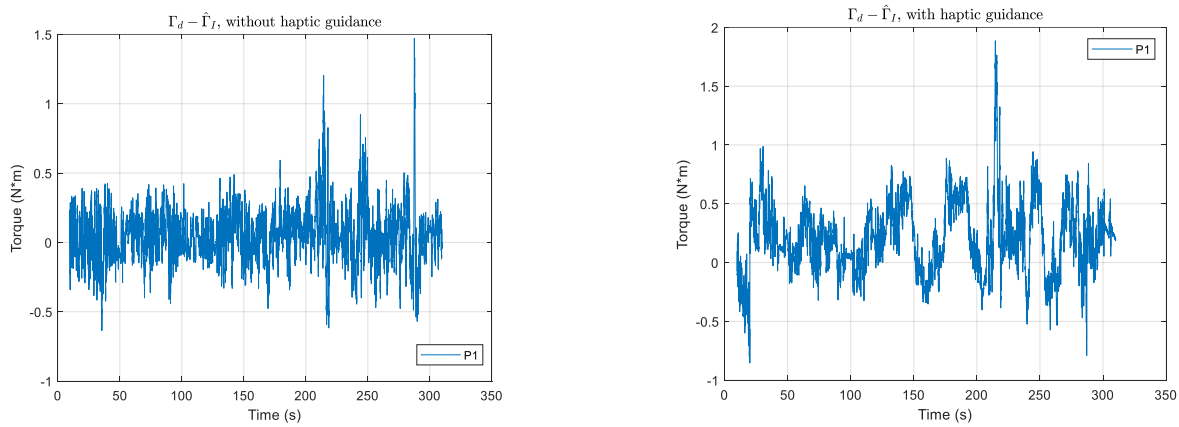

(a) Without haptic guidance.

(b) With haptic guidance.

Figure 8.7 – Residual of the driver internal model for P1.

Without haptic guidance, the residual was almost white noise—because in this situation the haptic feedback was merely self-aligning torque. The self-aligning torque is usually modeled as being approximately proportional to the steering-wheel angle[21]. Thus, a driver internal model in the form of a simple gain is almost accurate. However, this is not the case when the haptic guidance is part of the haptic feedback. In that case, the relationship between the haptic feedback and the steering wheel angle depends on the design strategy of the haptic guidance system and is difficult to predict only with the driver internal model. This leads to the difference between FIT values and the useful information left in the residual, which is explained by the explicit haptic feedback loop.

8.5.3 Explicit Haptic Feedback Loop

The identified explicit haptic feedback loop, without and with the haptic guidance system, is listed in Table 8.4. The FIT is calculated similarly as (8.26), where the predicted model output is $\hat{\Gamma}_d$ and the measured output is Γ_d.

The FIT values of the model with the explicit haptic feedback loop showed a close match between the predicted and measured driver steering torque, under both conditions (either with or without the haptic guidance). Compared with the results in Table 8.3, a distinct improvement is evident, especially when haptic guidance torque was part of the haptic feedback. These results indicate that this model structure was valid in both

Table 8.4 – Identified explicit haptic feedback model.

	Without Haptic Guidance			With Haptic Guidance		
Participant	K_{fb}	T_{fb}	$FIT(\%)$	K_{fb}	T_{fb}	$FIT(\%)$
P1	0.92	0.014	91.11	0.97	0.023	86.34
P2	0.90	0.012	91.83	0.90	0.028	88.97
P3	0.86	0.013	91.66	0.96	0.022	86.26
P4	0.92	0.014	91.79	0.91	0.027	85.38
P5	0.89	0.016	91.36	0.97	0.027	88.34

situations, although with haptic guidance there was still a substantial loss of around 3% to 5%. This point could be investigated in future research.

A similar gain between the two experimental conditions was obtained for the explicit haptic feedback loop. The time constant was almost doubled in the case of haptic guidance but remained smaller than the neuromuscular time constant fixed, T_N, which was 0.23 s. The difference between T_{fb} and T_N could correspond to the fact that control by spinal feedback pathways (30-40 ms for the arm muscles) is more efficient and faster than control by supraspinal pathways (i.e. the visual system)[22]. It should be noted, however, that the T_{fb} value could also be artificially increased or decreased by potential delays in the dynamics of the torque sensors. The difference in T_{fb} between the two conditions is probably related to the predictive property of the haptic guidance system. As part of its design strategy, the system anticipates changes in road curvature and can generate guidance torque even before the driver does. The haptic feedback that includes the assistance torque therefore occurs before the haptic feedback includes only the self-aligning torque, allowing the human driver more time to react.

Once each part of the model was identified, validation of the entire model using experimental data was performed to verify the model prediction. As an example, Figure 8.8 shows the results of the validation of participant P1 under both conditions. The figure shows that the driver model output predicts well the driver steering torque measured in the validation data, whether driving without or with the haptic guidance system.

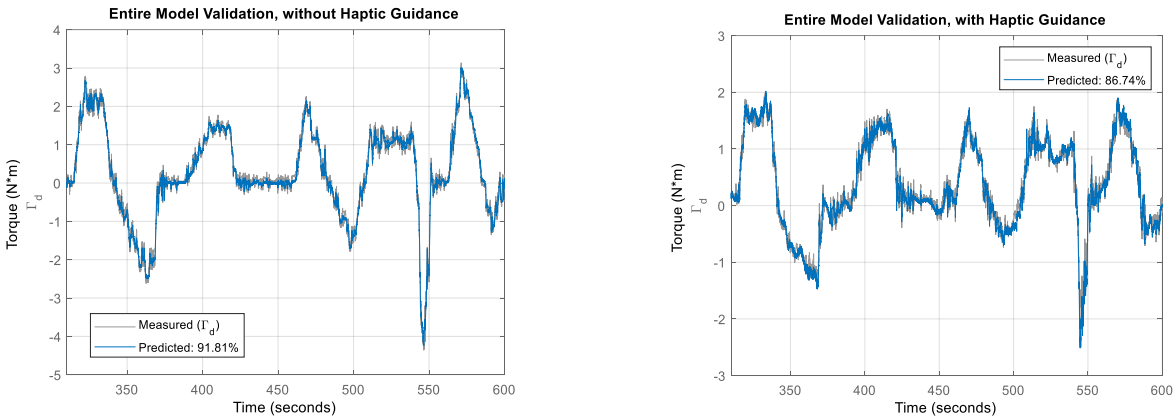

(a) Without haptic guidance.

(b) With haptic guidance.

Figure 8.8 – Validation of the entire driver model for P1.

8.6 Conclusion

In this article, a new cybernetic model of the driver in the steering task is proposed, with a reconsidered neuromuscular sub-model. The objective is to model the driver's steering control behavior, especially when a haptic guidance system is active. The haptic feedback signal, which includes both guidance and self-aligning torque, is used as a key input to the new model. It intervenes in the steering control, both by adapting the gain of the internal model to the compliance of the steering system (implicit feedback) and by explicit feedback after comparison with the target torque derived from the visual system. The results from our identification study show a good fit between the predicted and measured steering torque by the driver. Future work will focus on the model with different haptic steering systems set at different split levels. Additional tests involving more drivers will be conducted to examine how the proposed model can help to further understand how drivers interact with haptic guidance systems.

Acknowledgment

This work was supported by RFI Atlanstic 2020, funded by Région Pays de la Loire.

8.7 References

[1] M. Steele and R. B. Gillespie, "Shared Control between Human and Machine: Using a Haptic Steering Wheel to Aid in Land Vehicle Guidance", *Proceedings of the Human Factors and Ergonomics Society Annual Meeting*, vol. 45, *23*, pp. 1671–1675, 2001.

[2] D. A. Abbink and M. Mulder, "Exploring the dimensions of haptic feedback support in manual control", *Journal of Computing and Information Science in Engineering*, vol. 9, *1*, pp. 1–9, 2009.

[3] P. G. Griffiths and R. B. Gillespie, "Sharing Control Between Humans and Automation Using Haptic Interface: Primary and Secondary Task Performance Benefits", *Human Factors*, vol. 47, *3*, pp. 574–590, 2005.

[4] M. Mulder, D. A. Abbink, and E. R. Boer, "Sharing control with haptics: Seamless driver support from manual to automatic control", *Human Factors*, vol. 54, *5*, pp. 786–798, 2012.

[5] Z. Wang, R. Zheng, T. Kaizuka, K. Shimono, and K. Nakano, "The effect of a haptic guidance steering system on fatigue-related driver behavior", *IEEE Transactions on Human-Machine Systems*, vol. 47, *5*, pp. 741–748, 2017, ISSN: 21682291.

[6] L. Saleh, P. Chevrel, F. Claveau, J. F. Lafay, and F. Mars, "Shared steering control between a driver and an automation: Stability in the presence of driver behavior uncertainty", *IEEE Transactions on Intelligent Transportation Systems*, vol. 14, pp. 974–983, 2013.

[7] B. Pano, P. Chevrel, and F. Claveau, "Anticipatory and compensatory e-assistance for haptic shared control of the steering wheel", *2019 18th European Control Conference, ECC 2019*, pp. 724–731, 2019.

[8] F. Mars, L. Saleh, P. Chevrel, F. Claveau, and J.-F. Lafay, "Modeling the visual and motor control of steering with an eye to shared-control automation", *in Human Factors and Ergonomics Society 55th Annual Meeting*, vol. 55, 2011, pp. 1422–1426.

[9] L. Saleh, P. Chevrel, F. Mars, J. F. Lafay, and F. Claveau, "Human-like cybernetic driver model for lane keeping", *in Proceedings of the 18th IFAC World Congress*, 2011, pp. 4368–4373, ISBN: 9783902661937.

[10] F. Mars and P. Chevrel, "Modelling human control of steering for the design of advanced driver assistance systems", *Annual Reviews in Control*, vol. 44, *Supplement C*, pp. 292–302, 2017, ISSN: 13675788.

[11] L. Saleh, "Contrôle Latéral Partagé d'un Véhicule Automobile", Ph.D. dissertation, Ecole Centrale de Nantes (ECN), Apr. 2012.

[12] P. Hermannstädter and B. Yang, "Driver Distraction Assessment Using Driver Modeling", *in 2013 IEEE International Conference on Systems, Man, and Cybernetics*, Oct. 2013, pp. 3693–3698.

[13] A. Ameyoe, P. Chevrel, E. Le-Carpentier, F. Mars, and H. Illy, "Identification of a Linear Parameter Varying Driver Model for the Detection of Distraction", *1st IFAC Workshop on Linear Parameter Varying Systems LPVS 2015*, vol. 48, *26*, pp. 37–42, 2015, ISSN: 2405-8963.

[14] E. Donges, "A Two-Level Model of Driver Steering Behavior", *Human Factors: The Journal of the Human Factors and Ergonomics Society*, vol. 20, *6*, pp. 691–707, Dec. 1978.

[15] D. D. Salvucci and R. Gray, "A two-point visual control model of steering", *Perception*, vol. 33, *10*, pp. 1233–1248, 2004.

[16] D. Toffin, G. Reymond, A. Kemeny, and J. Droulez, "Role of steering wheel feedback on driver performance: driving simulator and modeling analysis", *Vehicle System Dynamics*, vol. 45, *4*, pp. 375–388, 2007.

[17] E. R. Kandel, J. H. (H. Schwartz, T. M. Jessell, S. Siegelbaum, A. J. Hudspeth, and S. Mack, *Principles of neural science*, 5th ed. McGraw-Hill Education / Medical, 2013, p. 1709, ISBN: 0071810013.

[18] A. Pick, "Neuromuscular dynamics and the vehicle steering task", Ph.D. dissertation, University of Cambridge, 2004.

[19] D. A. Abbink, M. Mulder, and M. M. Van Paassen, "Measurements of muscle use during steering wheel manipulation", *in Conference Proceedings - IEEE International Conference on Systems, Man and Cybernetics*, 2011, pp. 1652–1657, ISBN: 9781457706523.

[20] L. Ljung, *System Identification: Theory for the User*, 2nd ed., ser. Prentice Hall information and system sciences series. Prentice Hall PTR, 1999, ISBN: 9780136566953.

[21] N. Minoiu Enache, "Assistance préventive à la sortie de voie", Theses, Université d'Evry-Val d'Essonne, Nov. 2008.

[22] E. De Vlugt, "Identification of Spinal Reflexes", Ph.D. dissertation, Delft University of Technology, 2004, ISBN: 9077595422.

Chapter 9

Driver Model Validation through Interaction with Varying Levels of Haptic Guidance

Abstract

Driver modeling is essential in the development of haptic guidance systems. A new cybernetic driver model designed to account for the cooperation between the driver and haptic guidance systems has recently been proposed. This paper aims to validate this model in situations of interaction with different levels of haptic guidance on a driving simulator. Two experiments have been performed for this purpose. The first experiment consisted of implementing the driver model in the driving simulator and evaluating its lateral control performance when interacting with a haptic guidance system. The results reveal that the model can be adapted to different sharing levels by adjusting only the gain of an internal model of the steering wheel compliance. The second experiment consisted of estimating the evolution of the gain of this internal model using the unscented Kalman filter. The results reveal consistency between the evolution of the identified parameter and the level of sharing of the haptic guidance system. The driver model represents the process of human driver adaptation to variations in the level of sharing in haptic guidance systems.

9.1 Introduction

In line with the increasing interest in research on advanced driver assistance systems, a mode of interaction between humans and automation called haptic shared control[1], [2] has been intensively studied. Haptic shared control proposes that the human driver

and automation simultaneously apply a control action on an interface. In this case, the driver receives continuous haptic feedback and is aware of the action performed by the automation. Haptic shared control is considered an efficient method to achieve smooth human-machine cooperation, especially in automotive applications[3]. It has proven to be safer in emergency situations than traditional modes[4]–[6]. When haptic shared control is applied to the steering control task, the assistance system is generally referred to as a haptic guidance system. Figure 9.1 illustrates how the steering task is performed in cooperation between the driver and the system.

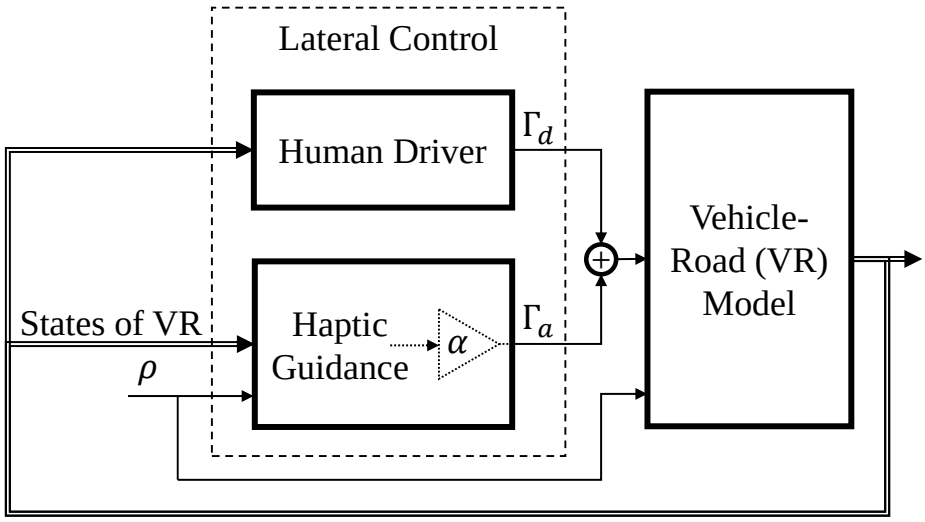

Figure 9.1 – Shared control between the human driver and haptic guidance system. ρ: road curvature; α: sharing level; Γ_d: driver steering torque; Γ_a: haptic guidance torque.

To minimize the potential conflicts between drivers and haptic guidance systems, understanding and predicting driver behavior is essential. For the development of some systems, a driver model was included in the design strategy to predict the output torque of the human driver [7], [8]. In a recent study[9], a new cybernetic driver model was proposed. The advantage of this model is that it uses the haptic torque feedback as input to account for the cooperation between the driver and haptic guidance system. The model was identified under two conditions: manual driving and driving with a haptic guidance system whose sharing level was set at 50% (i.e., the system produced 50% of the total guidance torque, see Section 9.3.2). Under both conditions, the model's prediction of steering torque control was accurate.

This article is a follow-up to our previous study. It aims to answer two questions related to the validation of the driver model: 1) Is the behavior of the model close to that

of a human driver regardless of the level of sharing? 2) How can the model account for the driver's adaptation to variations in the level of sharing over the course of driving? Two experiments were conducted to answer these questions.

This article is organized as follows: Section 9.2 briefly reviews the driver model. Section 9.3 introduces the driving simulator and haptic guidance system used in the experiments of this study. Sections 9.4 and 9.5 present the realization of the two experiments for validating the driver model: one by implementing the driver model in a driving simulator to evaluate its lateral control performance and another by continuously identifying model parameters. Finally, Section 9.6 concludes the results and proposes our future work.

9.2 Cybernetic Driver Model

9.2.1 Structure of the Proposed Cybernetic Model

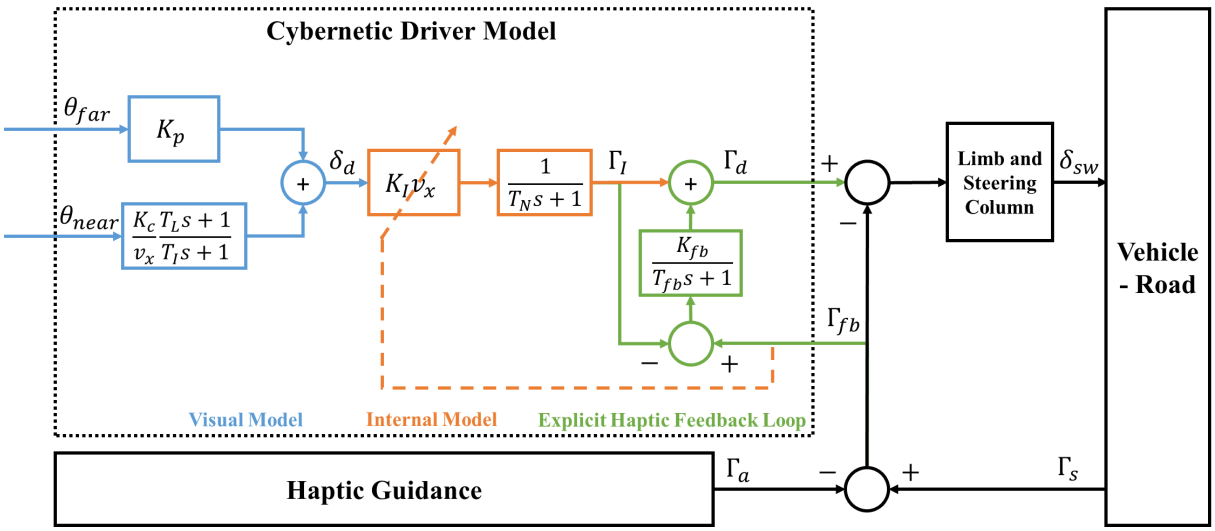

Figure 9.2 – Structure of the proposed cybernetic driver model. Blue: two-point visual model; Orange: driver internal model; Green: direct haptic feedback loop.

The proposed model structure is depicted in Figure 9.2 with the description of signals listed in Table 9.1. The basic hypothesis of the model is that, in steering control, the driver implicitly aims at a steering angle determined from the visual scene and then applies it to the steering wheel through the activation of muscles. The model structure reflects these two steps: 1) generating a target steering-wheel angle δ_d using a two-point visual model (the blue part) and 2) applying the target angle to a combination of limbs and

Table 9.1 – Description of signals in Figure 9.2.

Signal	Description
θ_{far}	Far-point Angle
θ_{near}	Near-point Angle
δ_d	Target Steering-wheel Angle
δ_{SW}	Actual Steering-wheel Angle
Γ_I	Torque from Internal Model
Γ_d	Driver Steering Torque
Γ_{fb}	Haptic Feedback Torque
Γ_a	Haptic Guidance Torque
Γ_s	Self-aligning Torque

the steering system through the neuromuscular system (NMS) and outputting a torque control (the orange and green parts). The two-point visual model takes two angles, a far-point angle and a near-point angle, as input to represent the visual information that the driver references. The haptic feedback torque Γ_{fb}, which is the combination of the haptic guidance torque and the self-aligning torque, is the key input to the neuromuscular model. It intervenes in the model in two ways. First, it implicitly influences an internal model of steering wheel compliance (dotted orange line). Second, it forms an explicit feedback loop (solid green line). One minimal realization of the model could be written as follows:

$$\begin{cases} \dot{x}(t) = Ax(t) + Bu(t) \\ y(t) = Cx(t) + Du(t) \end{cases} \tag{9.1}$$

with

$$y(t) = \Gamma_d \tag{9.2}$$

$$u(t) = \begin{bmatrix} \theta_{far} & \theta_{near} & \Gamma_{fb} \end{bmatrix}^T, \tag{9.3}$$

$$A = \begin{bmatrix} -\dfrac{1}{T_I} & 0 & 0 \\ -K_I v_x \dfrac{1}{T_N} \dfrac{K_c}{v_x}(\dfrac{T_L}{T_I} - 1) & -\dfrac{1}{T_N} & 0 \\ 0 & -\dfrac{K_{fb}}{T_{fb}} & -\dfrac{1}{T_{fb}} \end{bmatrix} \tag{9.4}$$

$$B = \begin{bmatrix} 0 & \frac{1}{T_I} & 0 \\ K_I v_x \frac{1}{T_N} K_p & K_I v_x \frac{1}{T_N} \frac{K_c}{v_x} \frac{T_L}{T_I} & 0 \\ 0 & 0 & \frac{K_{fb}}{T_{fb}} \end{bmatrix} \tag{9.5}$$

$$C = \begin{bmatrix} 0 & 1 & 1 \end{bmatrix} \tag{9.6}$$

$$D = \begin{bmatrix} 0 & 0 & 0 \end{bmatrix} \tag{9.7}$$

9.2.2 Internal Model

The internal model consists of a gain K_I and a time constant T_N. In neural science, it is believed that the nervous system uses models of the physical world to exercise control and prediction to achieve skilled motor performance[10]. In the case of steering control, the driver uses an internal model to convert the target steering-wheel angle to torque. This internal model results from driver perception and prior knowledge of the steering system. During driving, the driver learns about the dynamics of the system and adapts to it by updating the internal model of steering system compliance. It is likely that this estimation is approximate and corresponds to a simple (low-order) model, which is represented by the gain K_I. From the driver's viewpoint, the dynamics of the steering system are assessed through the haptic feedback. The haptic feedback torque thus affects the internal model, which is represented by the dashed line in Figure 9.2. The time constant T_N represents the fact that the muscles need time to output the torque control.

9.2.3 Explicit Haptic Feedback Loop

To achieve the target steering-wheel angle and stable control of the steering wheel, an open-loop control through the internal model is not sufficient, as it is not able to compensate for any perturbations that arise during the movement. A closed-loop control using sensory feedback is indispensable. The explicit haptic feedback loop is a first-order system that outputs a complementary torque based on the error between the torque output of the internal model and the haptic feedback. This compensation through haptic feedback torque is considered faster and more intuitive for the driver than through the actual steering-wheel angle because small errors between the target and actual steering-wheel angle are more likely to be observed via visual information, and the compensation is therefore much longer. In other words, the *NMS* is more likely to counterbalance the haptic

feedback to stabilize the steering wheel than to achieve the exact target steering-wheel angle.

9.3 Experiment Setting

9.3.1 Apparatus

The experiments in this study were all performed on a fixed-base driving simulator powered by SCANeR Studio (Figure 9.3, left). The simulator is equipped with a complete dashboard; a five-speed gear stick; gas, brake, and clutch pedals; and a steering wheel connected to a TRW steering system. Sensors for measuring the steering-wheel angle, speed, and torque are mounted in the steering system. The visual scene is displayed on three liquid crystal display (LCD) screens: a central one in front of the driver and two others oriented at 45° relative to the center. The screens cover a field of view of 25° high and 115° wide. The software allows a compilation and implementation of controllers developed in Simulink to control either the steering wheel or the vehicle. In all the experiments, a small family car, the Citroën C5, was chosen as the vehicle model, with the longitudinal speed fixed at 18 m/s.

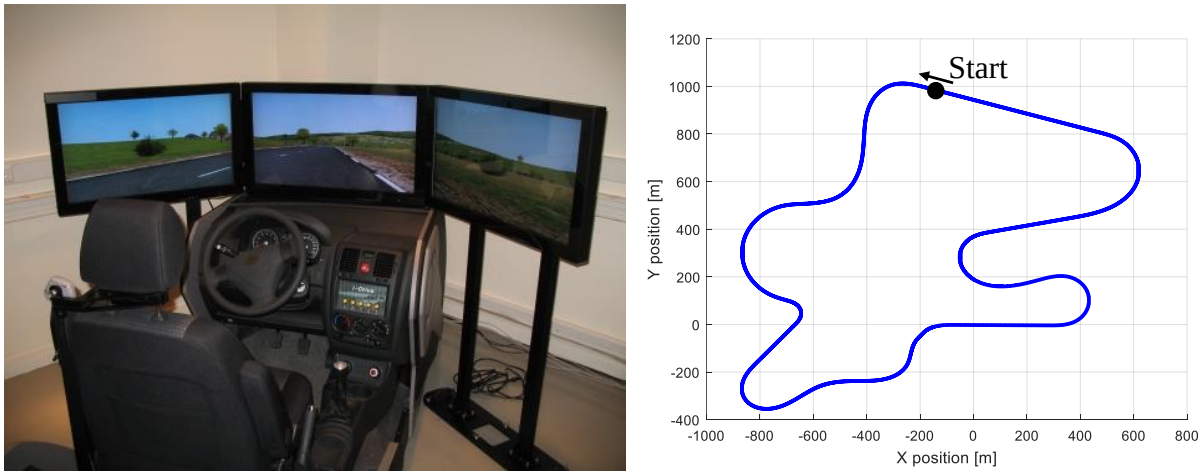

Figure 9.3 – Left: fixed-base driving simulator; Right: track used in the first experiment.

9.3.2 Haptic Guidance System

A haptic guidance system was implemented in the driving simulator using a controller designed in Simulink. The controller was previously developed[8]. The final guidance torque

Γ_a was a combination of an anticipatory and compensatory assistance torque depending on a factor α called the *sharing level*:

$$\Gamma_a = \alpha \times \Gamma_{ant} + \Gamma_{comp}(\alpha) \tag{9.8}$$

where Γ_{ant} and Γ_{comp} are the torque generated by the anticipatory and compensatory assistance, respectively. The anticipatory assistance generates a reference trajectory from the previewed road curvature. The compensatory assistance consists of an H_2/H_∞ static output feedback that controls the steering against disturbances and uncertainties. The sharing level determines how much guidance torque is finally applied on the steering wheel, and its value could vary from 0% (completely manual driving) to 100% (completely automatic driving).

9.4 Validation I: Driver Model Simulation

9.4.1 Objective

In a previous study[9], the parameters of the driver model were sequentially estimated using the prediction error minimization method[11] with driving data from five participants. Two sets of parameters were obtained under two experimental conditions: one for fully manual driving and one for driving with a haptic guidance system with a 50% sharing level. The model was validated under both conditions with a good prediction quality of driver torque control (FIT between 85% and 92%). The comparison between the two sets of parameters implies that the *NMS*, in particular, the internal gain K_I of the model, accounts for the driver's adaptation to the intervention of the haptic guidance system. This observation corresponds to the expected role of the internal model in the model. Further, whether the driver's model can cooperate effectively with a haptic guidance system as soon as the gain of the internal model corresponds to the chosen sharing level remains to be verified.

9.4.2 Experiment

Figure 9.4 illustrates how the experiment was conducted. Instead of a human driver, the driver model was implemented as a controller in the driving simulator to control the vehicle in cooperation with the haptic guidance system. Two independent variables were

manipulated in this experiment: the sharing level of the haptic guidance system, α, and the internal model gain, K_I. Four values for the sharing level were chosen: 0%, 30%, 50%, and 80%. The corresponding values of the internal model gain are 0.23, 0.17, 0.13, and 0.04. The other parameters in the driver model were fixed at their nominal values (Table 9.2). The combination of the two independent variables provides 16 different experimental scenarios. Each scenario lasted for about 5 min. A normal track with the Euler spiral turns and straight lines was chosen for this experiment (Figure 9.3, right). The vehicle trajectory was recorded and used to evaluate the lateral control performance.

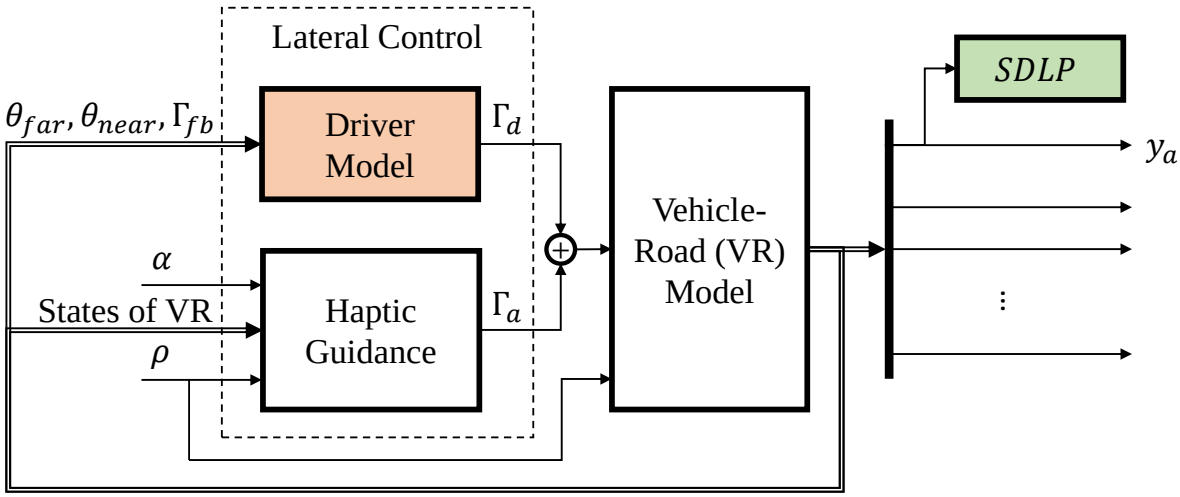

Figure 9.4 – Driver model validation with the implemented driver model.

Table 9.2 – Nominal parameter values used in validation I.

Parameter	Description	Value
K_p	Anticipatory Gain	3.7
K_c	Compensatory Gain	2.6
T_I	Compensation Time Constant	0.4
T_L	Compensation Rate	7.2
T_N	Neuromuscular Time Constant	0.23
K_{fb}	Haptic Feedback Loop Gain	0.97
T_{fb}	Haptic Feedback Loop Time Constant	0.023
v_x	Vehicle Longitudinal Speed	18 (m/s)

9.4.3 Results

The standard deviation of the lateral position (SDLP) from the lane center was chosen as the metric in this experiment to present the validation results. It is calculated using the lateral position deviation signal y_a, which is the distance from the center of gravity of the vehicle to the lane center (in meters). A relatively large *SDLP* indicates poor lane-keeping performance.

The *SDLP* values for all 16 scenarios are listed in Table 9.3. Each *SDLP* value on the diagonal is the lowest in its row and column. This implies that, when the sharing level and internal model gain match each other, the driver model and haptic guidance system reach a relatively stable cooperation with only a small variation in the lateral position. Note that the *SDLP* is slightly higher for $\alpha = 0$ than in the other three cases because the driver model in manual mode tends to cut corners, while the haptic guidance system tends to follow the center of the lane. For a given sharing level, either a larger or smaller value of the internal model gain results in a higher *SDLP*. In these situations, the torque output from the internal model is either too large or too small. Such bias on the internal model, which represents the compliance of the steering system, cannot entirely be compensated for by the explicit haptic feedback loop, which eventually leads to a difference between the target and actual steering-wheel angle. Therefore, the vehicle position oscillates between the left and right border (or even outside) of the lane.

Table 9.3 – Standard deviation of the lateral position of all 16 scenarios.

	$K_I = 0.23$	$K_I = 0.17$	$K_I = 0.13$	$K_I = 0.04$
$\alpha = 0\%$	*0.51*	2.39	5.47	33.03*
$\alpha = 30\%$	0.69	*0.23*	0.46	1.75
$\alpha = 50\%$	0.91	0.48	*0.20*	0.85
$\alpha = 80\%$	1.14	0.81	0.55	*0.20*

* The scenario ended exceptionally due to the vehicle left completely the lane without return.

In conclusion, the results indicate that the adjustment of the internal model gain through the haptic feedback is imperative when the driver model interacts with the haptic guidance system at different sharing levels. This adjustment is sufficient for a significant improvement in lateral control performance.

9.5 Validation II: Driver Model Identification

9.5.1 Objective

The previous validation experience has shown that the adjustment of the internal model gain accounts for the adaptation of the driver model to various levels of sharing. The second experimental validation seeks to capture the adaptation of the human driver to the haptic guidance system through online identification of the internal model gain. This is done in a situation in which the sharing level varies during driving from 0% to 100%. The assumption is that the gain of the internal model varies homogeneously with the sharing level.

9.5.2 Experiment

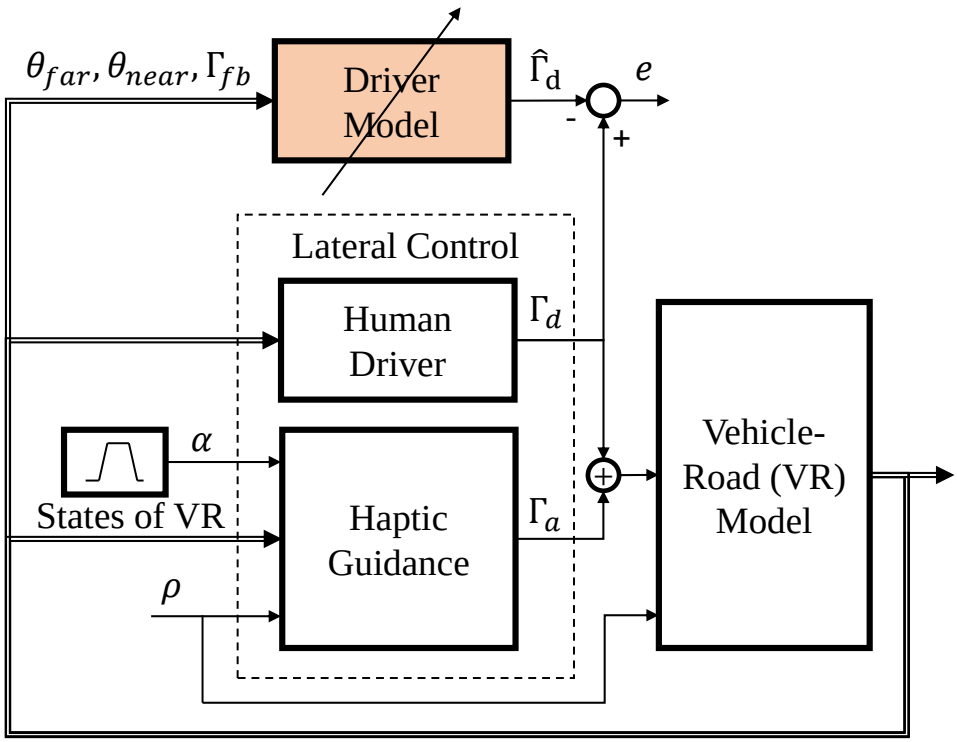

Figure 9.5 – Driver model validation with the identified driver model.

Figure 9.5 illustrates how the second experiment was conducted. The driver was instructed to steer the vehicle in cooperation with the haptic guidance system on the track

shown in Figure 9.6, a road consisting only of Euler spiral bends with a radius of curvature varying between 75 m and 95 m. The experiment started in manual driving ($\alpha = 0$). After the vehicle passed P1, the sharing level started to increase from 0% to 100% in 50 s. The transition was indicated on the simulator screen by a progress bar. When driving was fully automated, the driver was required to remove the driver's hands from the steering wheel. When the vehicle passed P2 on the road, a takeover request was issued and the sharing level began to decrease from 100% to 0% in 50 s. The driving session lasted approximately 4 min. The signals used to calculate the inputs and outputs of the driver model were recorded throughout the drive at 100 Hz.

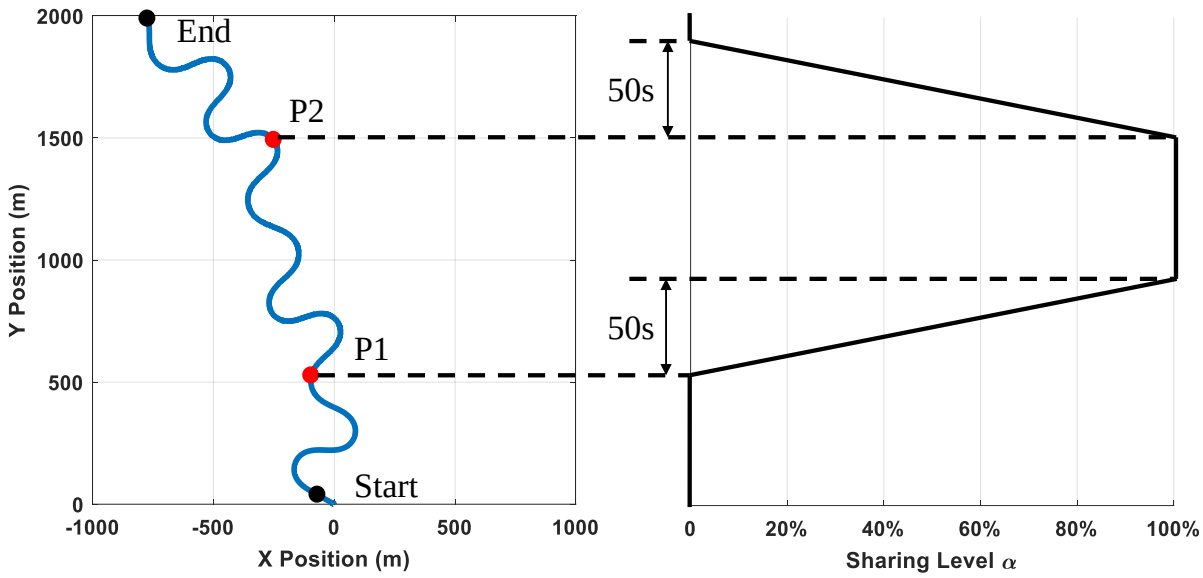

Figure 9.6 – Left: track used in the validation II; Right: variation of the sharing level in the experiment.

A group of 11 males and six females aged 24 to 53 (mean = 31 years, standard deviation = 8.2 years) participated in the experiment. All participants had a valid driver's license and drove regularly (12550 km per year on average). The participants had no known medical conditions that could affect their driving skills and had normal or corrected vision. None of them had ever experienced a haptic guidance system.

9.5.3 Parameter Identification

For each participant, the driver model identification was performed in two steps: 1) identification of the complete driver model using the data from the first manual driving phase

(i.e., when $\alpha = 0$ from the start of the experiment) and 2) estimation of the variation of the internal model gain K_I using all the data in the experiment. The goal of the first step was to obtain an initial value for K_I and a nominal value for the other parameters, which were needed in the second step. The identification method in the first step was the same as in [9]: the visual model, internal model, and explicit haptic feedback loop were identified sequentially by the prediction error minimization method. In the second step, as the value of K_I may change continuously, a linear time-varying system identification method was used. The method was developed and validated in [12].

With the hypothesis that the variation of the internal model gain $K_I(t)$ can be modeled as a Wiener process and that it is slower than the variation of the system states, the system can be augmented with K_I and then can be discretized using the Euler method. The augmented system derived from (9.1) in discrete time is written as follows:

$$\begin{cases} x_a[k+1] = f_d(x_a[k], u[k]) + w_{a,d}[k] \\ y[k] = g_d(x_a[k], u[k]) + v[k] \end{cases} \tag{9.9}$$

with

$$x_a[k] = \begin{bmatrix} x[k] \\ K_I[k] \end{bmatrix} = \begin{bmatrix} x(kT_s) \\ K_I(kT_s) \end{bmatrix} \tag{9.10}$$

$$u[k] = u(kT_s) \tag{9.11}$$

$$y[k] = y(kT_s) \tag{9.12}$$

$$f_d(x_a[k], u[k]) = \begin{bmatrix} \big(T_s A(K_I[k]) + I\big)x[k] + T_s B(K_I[k])u[k] \\ K_I[k] \end{bmatrix} \tag{9.13}$$

$$g_d(x_a[k], u[k]) = Cx[k] + Du[k] \tag{9.14}$$

where $w_{a,d}[k]$ and $v[k]$ are the discretized augmented process noise and measurement noise, with the covariance matrices denoted as $Q_{a,d}$ and R_d, respectively. The T_s is the sampling time, which was 0.01 s in this experiment. The I in (9.13) is an identity matrix that is the same size as the matrix A. Note that the matrices A and B are all functions of K_I in this case; thus in (9.13) the values evaluated at $K_I[k]$ are used.

The unscented Kalman filter (UKF) is applied to estimate the augmented system

states $x_a[k]$ recursively by minimizing the following cost function:

$$\begin{aligned} J(\hat{x}_a[k]) = \hat{x}_a^T[0]P_a^{-1}[0]\hat{x}_a[0] \\ + T_s \sum_{k=0}^{N-1} \hat{w}_{a,d}^T[k]Q_{a,d}^{-1}\hat{w}_{a,d}[k] \\ + T_s \sum_{k=0}^{N-1} \hat{v}_d^T[k]R_d^{-1}\hat{v}_d[k] \end{aligned} \tag{9.15}$$

where $P_a[0]$ is the initial covariance matrix of the augmented states and

$$\hat{w}_{a,d}[k] = \hat{x}_a[k+1] - f_d(\hat{x}_a[k], u[k]) \tag{9.16}$$

$$\hat{v}_d[k] = y[k] - g_d(\hat{x}_a[k], u[k]) \tag{9.17}$$

The calculation steps of *UKF* are listed in Algorithm 9.1.

The tuning methodology proposed by [12] was adopted to configure the filter, especially the value of the matrices $Q_{a,d}$ and R_d. The configuration of the filter demands a compromise between the rapidity and the precision (noise sensitivity) in the process of the estimation. A multi-model *UKF* approach was finally applied to estimate simultaneously the steady-state value of K_I and detect fast parametric variation with one relatively slow and another relatively fast filter.

9.5.4 Results

The FIT values were first obtained from the results of *UKF* to verify the prediction of the driver torque. The calculation is as follows:

$$FIT = \left(1 - \frac{\|\Gamma_d - \hat{\Gamma}_d\|_2}{\|\Gamma_d - mean(\Gamma_d)\|_2}\right) \times 100\% \tag{9.25}$$

where Γ_d is the measured driver torque, and $\hat{\Gamma}_d$ is the prediction. For the slow *UKF*, the mean value of FIT for all participants is 91.5% with a standard deviation of 0.3%. For the fast *UKF*, the mean value of FIT is 92.1% with a standard deviation of 0.4%. These values confirm the validity of the identified driver model. As an example, Figure 9.7 (left) compares the prediction results of the Participant 1. Note that, during the completely automatic driving phase (around 110 s to 150 s), the driver torque was not exactly zero even though the participants did not touch the steering wheel. This was probably caused

Algorithm 9.1 Estimation of $x_a[k]$ with the unscented Kalman filter.

Step 1: Initialization
At time step $k = 0$, configure $x_a[0]$, $P_a[0]$, $Q_{a,d}$ and R_d:
Step 2: Calculation of the output prediction
At time step $k > 0$, estimate the output prediction using the unscented transformation (UT)[13]:

$$(\hat{y}[k|k-1], C'_{yy}[k], C_{xy}[k]) = UT(g_d, \hat{x}_a[k|k-1], P_a[k|k-1]) \tag{9.18}$$

$$C_{yy}[k] = C'_{yy}[k] + R_d \tag{9.19}$$

Step 3: Correction with measurements
At time step k, correct the values and the covariance of the augmented states with the measurements:

$$L[k] = C_{xy}[k]C_{yy}^{-1}[k] \tag{9.20}$$

$$\hat{x}_a[k|k] = \hat{x}_a[k|k-1] + L[k]\Big(y[k] - \hat{y}[k|k-1]\Big) \tag{9.21}$$

$$P_a[k|k] = P_a[k|k-1] - L[k]C_{xy}^T[k] \tag{9.22}$$

Step 4: States prediction for the next time step
At time step k, predict the augmented states value and covariance for the next time step $k+1$ using UT:

$$(\hat{x}_a[k+1|k], P'_a[k+1|k]) = UT(f_d, \hat{x}_a[k|k], P_a[k|k]) \tag{9.23}$$

$$P_a[k+1|k] = P'_a[k+1|k] + Q_{a,d} \tag{9.24}$$

Step 5: $k \leftarrow k+1$, repeat step 2 to 4 until $k = N$.

by the friction in the steering system that was measured by the torque sensor.

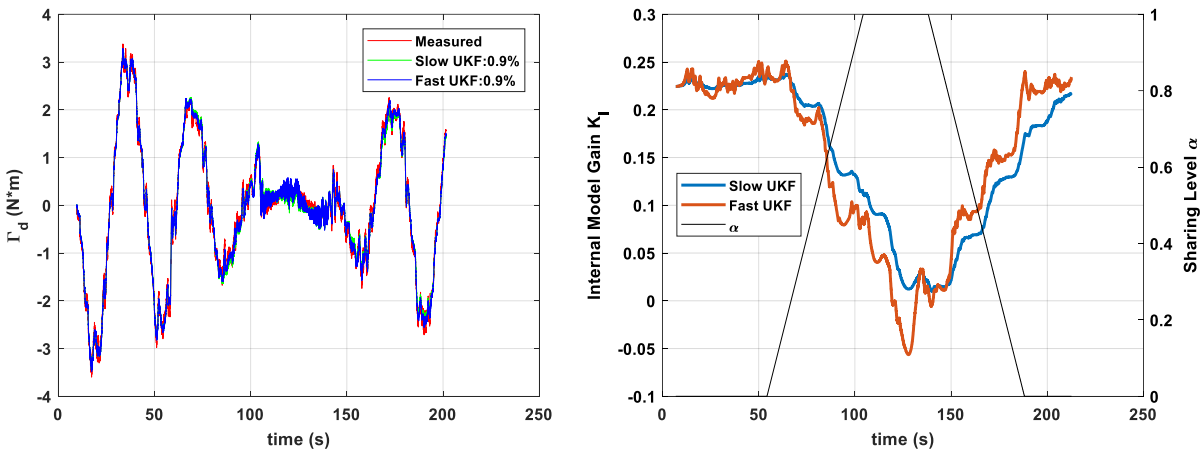

Figure 9.7 – Left: measured vs. predicted driver torque of Participant 1; Right: estimated K_I variation of Participant 5.

Second, the variation of K_I was analyzed. Figure 9.7 (right) presents the results of Participant 5 as an example. To check whether the variation of all participants is similar, the results were synchronized so that all participants passed Point P1 at the same time (after the synchronization, they passed the Point P2 with a time difference of less than 0.5 s, which could be ignored). Figure 9.8 reveals two curves for the variation of mean K_I with a three-sigma (three standard deviations) band of all participants, one estimated using the slow filter and another using the fast filter. The mean and standard deviation values were calculated with the estimated K_I of all participants at each sampling instance using the synchronized results. The figure reveals that both the slow and fast filters exhibit a similar variation trend. For all participants, the internal model gain decreases when the sharing level increases, and vice versa. The K_I is nearly zero during completely automatic driving. In addition, a delay of about 10 s occurs between the change in the sharing level and the variation of the internal model gain. During the experiment, human drivers adapted to the change of sharing level by delivering more or less torque on the steering wheel. This adaptation is captured very well by the variation of the internal model gain. In conclusion, the results demonstrated that the internal model gain of the driver model is directly related to the sharing level of the haptic guidance system. By adjusting this parameter, the prediction of the driver model in cooperation with the haptic guidance system is always valid when the sharing level changes.

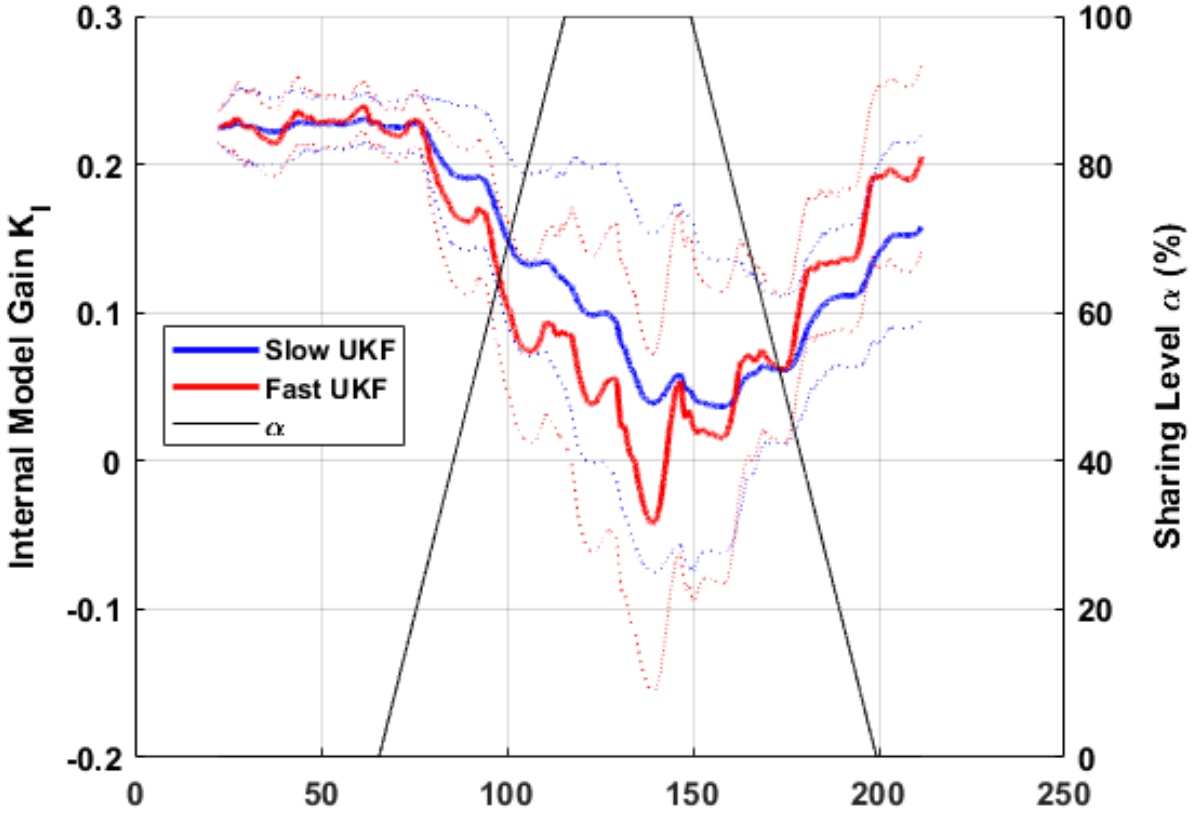

Figure 9.8 – Mean K_I variation with the three-sigma band of all participants. Blue: results of slow unscented Kalman filter(UKF); Red: results of fast *UKF*; Black: sharing level α; Sold line: mean K_I; Dotted line: three-sigma band.

9.6 Conclusion

The driver model proposed in [9] was developed to account for the cooperation between a driver and haptic guidance system. This paper aims to validate this model when the level of sharing between the two agents changes. Two experiments were conducted consecutively. The first experiment consisted of implementing the driver model in a driving simulator so that it could perform the steering task itself. The results indicated that the model that was identified for a given sharing level was no longer able to drive the simulator in cooperation with the haptic guidance system when the level of sharing changed. This implies that an adaptation of the model must occur either by changing the values of the parameters in the model or by changing the structure of the model.

The experiment demonstrates that this adaptation can be achieved by varying only the value of the gain of the internal model of the steering system compliance. As a corollary, this result validated the meaning attributed to the model parameters: the visual model is not affected by haptic guidance, and the neuromuscular time constant is invariant, as indicated in the literature [14]. Moreover, the explicit haptic feedback cannot perform the adaptation by itself. Ultimately, the adaptation of the internal model gain is imperative because, from the driver's viewpoint, the haptic guidance system modifies the dynamics of the steering wheel.

Based on these results, the second experiment validated the driver model with all possible sharing-level values. This time, the value of the internal model gain was identified using a *UKF* method with driving data from human drivers who were experiencing slow transitions between manual and autonomous driving. This was achieved by gradually varying the sharing level. The results indicated that the variation in the internal model gain is directly related to the sharing level. This suggests that driver adaptation to the haptic guidance system is mostly achieved by updating the internal model. The driver model captures this adaptation process successfully.

Similar adaptation situations can be envisioned, such as when the driver discovers a new vehicle with a steering wheel that is more or less difficult to turn than expected. During the first few curves, lane control may be inaccurate and then improves as the next curves are negotiated. This adaptation would likely be done by adjusting the gain of the internal model; thus, the model would be able to account for it. This issue will be investigated in future studies.

Acknowledgment

This work was supported by RFI Atlanstic 2020, funded by Région Pays de la Loire, and AutoConduct research program funded by the French ANR "Agence Nationale de la Recherche" (grant ANR-16-CE22-0007-05).

9.7 References

[1] M. Steele and R. B. Gillespie, "Shared Control between Human and Machine: Using a Haptic Steering Wheel to Aid in Land Vehicle Guidance", *Proceedings of the*

Human Factors and Ergonomics Society Annual Meeting, vol. 45, *23*, pp. 1671–1675, 2001.

[2] D. A. Abbink and M. Mulder, "Exploring the dimensions of haptic feedback support in manual control", *Journal of Computing and Information Science in Engineering*, vol. 9, *1*, pp. 1–9, 2009.

[3] D. A. Abbink, M. Mulder, and E. R. Boer, "Haptic shared control: Smoothly shifting control authority?", *Cognition, Technology and Work*, vol. 14, *1*, pp. 19–28, 2012, ISSN: 14355558.

[4] M. Mulder, D. A. Abbink, and E. R. Boer, "Sharing control with haptics: Seamless driver support from manual to automatic control", *Human Factors*, vol. 54, *5*, pp. 786–798, 2012.

[5] P. G. Griffiths and R. B. Gillespie, "Sharing Control Between Humans and Automation Using Haptic Interface: Primary and Secondary Task Performance Benefits", *Human Factors*, vol. 47, *3*, pp. 574–590, 2005.

[6] Z. Wang, R. Zheng, T. Kaizuka, K. Shimono, and K. Nakano, "The effect of a haptic guidance steering system on fatigue-related driver behavior", *IEEE Transactions on Human-Machine Systems*, vol. 47, *5*, pp. 741–748, 2017, ISSN: 21682291.

[7] L. Saleh, P. Chevrel, F. Claveau, J. F. Lafay, and F. Mars, "Shared steering control between a driver and an automation: Stability in the presence of driver behavior uncertainty", *IEEE Transactions on Intelligent Transportation Systems*, vol. 14, pp. 974–983, 2013.

[8] B. Pano, P. Chevrel, and F. Claveau, "Anticipatory and compensatory e-assistance for haptic shared control of the steering wheel", *2019 18th European Control Conference, ECC 2019*, pp. 724–731, 2019.

[9] Y. Zhao, P. Chevrel, F. Claveau, and F. Mars, "Towards a Driver Model to Clarify Cooperation Between Drivers and Haptic Guidance Systems", *in 2020 IEEE International Conference on Systems, Man, and Cybernetics (SMC)*, 2020, pp. 1731–1737.

[10] E. R. Kandel, J. H. (H. Schwartz, T. M. Jessell, S. Siegelbaum, A. J. Hudspeth, and S. Mack, *Principles of neural science*, 5th ed. McGraw-Hill Education / Medical, 2013, p. 1709, ISBN: 0071810013.

[11] L. Ljung, *System Identification: Theory for the User*, 2nd ed., ser. Prentice Hall information and system sciences series. Prentice Hall PTR, 1999, ISBN: 9780136566953.

[12] Y. Zhao, P. Chevrel, F. Claveau, and F. Mars, "Continuous Identification of Driver Model Parameters via the Unscented Kalman Filter", *IFAC-PapersOnLine*, vol. 52, *28*, pp. 126–133, 2019, 3rd IFAC Workshop on Linear Parameter Varying Systems LPVS 2019, ISSN: 2405-8963.

[13] S. J. Julier and J. K. Uhlmann, "New extension of the Kalman filter to nonlinear systems", *in Proc. SPIE 3068,Signal Processing, Sensor Fusion, and Target Recognition VI*, 1997.

[14] L. Saleh, P. Chevrel, F. Mars, J. F. Lafay, and F. Claveau, "Human-like cybernetic driver model for lane keeping", *in Proceedings of the 18th IFAC World Congress*, 2011, pp. 4368–4373, ISBN: 9783902661937.

Part IV

Conclusion and Perspective

Chapter 10

General Conclusion and Perspectives

10.1 General Discussion

This thesis was conducted as a step in the development of haptic shared control driving assistance systems (i.e., haptic guidance systems). It focused on understanding and predicting driver's adaptation to haptic guidance systems during interaction with the system at varying levels.

The crucial element in this study was cybernetic driver steering model. The work consisted of two main parts around this element: mathematical tools for identifying the model and experimental investigations performed with the model. The PEM and UKF method, especially their practical use in this context, were considered for identifying time-invariant and time-variant systems, respectively. A model-based analysis method was introduced and improved in the experimental investigation. This method proposed to capture the adaptive behavior of driver through the cybernetic driver model, and in particular, the variation over time of model parameters. With this method, the improvement of the model and the study of the adaptation could be carried out. In the end, a new cybernetic driver model capable of predicting the driver's adaptation to the haptic guidance system at varying levels was obtained.

Results of this thesis could contribute to the design of haptic guidance system for minimizing potential conflicts between drivers and the system. Besides, it showed a successful application of the new cybernetic driver model in the study of adaptation, with the help of time-varying system identification tools. Meanwhile, it demonstrated the potential of the new cybernetics theory invoked in the literature[1].

10.2 Synthesis of Experimental Investigations

The literature about the effect of haptic guidance systems on driver steering control performance was dominated by behavioral analysis. Cybernetic driver steering models are copies of driver steering behavior, thus a "good" model should react to the haptic guidance systems and reproduce human adaptive behavior. Moreover, driver models including learning and adaptation process have benefits in the realization of haptic guidance systems as well. This requirement is, however, beyond the scope of most of current models. This gap motivated the application of model-based analysis in experimental investigations. A series of experiments aiming at understanding and modeling the adaptation of the human-machine interaction were carried out sequentially, as presented in three papers in Chapter 7, 8 and 9, respectively.

The starting point to this research was to investigate the effectiveness of the model-based analysis with a simple (in the sense of structure and comprehensiveness) and robust model. In the first experiment in Chapter 7, we chose to study the interactive effect of the visibility condition and the haptic guidance system which had already been studied in several previous researches [2], [3]. The aim of repeating a similar experiment was to understand the behavior of the human-machine system by projecting it onto the visual steering model and verifying parametric variations. In the end, the validity of the model to account for the effect of the manipulated variables, but also its limitations, were revealed. The model validation and parameter uncertainties were particularly considered when performing the model-based analysis to ensure the validity and generality of identified model. The anticipatory gain was sensible to any changes made to the followed trajectory and the compensatory gain was sensible to reduction in the variability of lateral position deviation. This corresponds to the meaning attributed to each parameter. However, this model cannot independently distinguish between the actions of the human driver and those of the haptic guidance systems on the steering wheel, because the steering-wheel angle is the joint effort of the two agents. Therefore, it would be hardly possible to use such a model in the study of driver's adaptation to the haptic guidance system.

The simplistic nature of the two-point steering model encouraged us to continue the investigation with advanced models incorporating a NMS. Attempts made with the model developed in previous study [4] failed because the model became invalid when the haptic guidance torque was applied. This issue led to the reconsideration of model structure in Chapter 8 by accounting for the driver's ability to incorporate the action of hap-

tic guidance into steering wheel control. The cybernetic driver model that we proposed regards human driver as a time-variant and adaptive controller. This is different from traditional cybernetics theory, which usually describes human driver as (quasi-) linear, time-invariant (LTI) feedback systems. However, it focuses on the adaptive characteristics of human control behavior in realistic control scenarios. In fact, both learning and adaptation behavior should have been considered at once as they usually decide together the switch of control strategy. Yet, the knowledge in the learning process would demand dedicated experiments to better understand it. Another assumption is underlying in the adaptive cybernetic model about how drivers perform a steering task. It was assumed that they achieved this in two steps: first by setting a target angle of the steering wheel from environmental perception, and then by aiming it through neuromuscular actions on the steering system. This is a basic assumption commonly adopted in previous models [5]–[7] but never verified.

The modeling of NMS was a challenge. The difficulty was knowing how to correctly represent this human-machine (driver-steering) system , which partly combines driver and steering system dynamics. The NMS in the developed model mainly converts the target steering-wheel angle aimed for, to torque control accounting for haptic feedback torque. The angle-torque conversion process was represented by the internal model inspired from neural science. Unlike the model proposed in [8], it was clarified that in most cases driver could not distinguish between the haptic guidance torque and the self-aligning torque. Therefore, the haptic feedback within the framework of this thesis referred to the combination of both torques. The involvement of haptic feedback was represented by an indirect and direct feedback loop. The indirect loop refers to the adaptation of the parameters of an internal model and the direct loop accounts for the driver's corrective action through direct haptic feedback. The role of the indirect loop has been studied in depth, while the direct feedback loop still needs to be further understood.

The driver model was validated as a "virtual driver" on the driving simulator in the third paper in Chapter 9. The experiment proved the fact that the haptic feedback torque could indeed affect the internal model, as shown in [9]. Furthermore, the adjustment of the internal model according to changes in the haptic feedback is imperative to avoid unrealistic variations of vehicle position in lane. This is actually coherent with scenarios in real life, and the proposed driver model is able to reproduce satisfactorily this phenomenon. At the end, using *ad hoc* time-variant system identification method, the adaptation of human driver to haptic guidance system with varying levels was successfully captured,

through the variation of what is called the internal model gain. Results indicated that when the effort provided by haptic guidance systems changes, human drivers adjust their internal representation of the steering system in order to reach a stable cooperation. In general, it is highly probable that such an adaptation is not limited only to modification of the haptic feedback, but also to any modification of the steering system stiffness.

10.3 Review of Methodology

10.3.1 Model-based Analysis

The model-based analysis is not new. In researches such as [4], [10], [11], different driver distraction modalities were successfully discriminated through the parametric analysis of a driver model. This method assumes that the sensitivity of model parameters is significant with regard to experimental conditions, as discussed in Chapter 6. Therefore, the effectiveness of model-based analysis largely depends on the model structure and parametrization chosen. Complementing previous works, this way of doing was further formalized and developed during the experimental investigation of this thesis. The model validation and the parameter uncertainties were studied in more depth in order to clarify two fundamental questions: the validity of driver model in different scenarios and the representativeness of the parametric difference.

One challenge for parameterized model-based analysis is the consideration of well suited parameters for system identification. In the current study, we benefited from the physiological and psychological knowledge included in the cybernetic driver models through *ad hoc* parameters. Driver model simulation was also helpful for confirming the potential parameters, as the first validation experiment in Chapter 9. The parameters that we selected were the most essential with regard to the stages of our investigation process and the experimental conditions. In Chapter 7, the anticipatory and compensatory gain were identified when driving in degraded visibility conditions; in Chapter 8 and 9, the internal model gain was focused when the sharing level of haptic guidance torque was varying. Generally, if there is only limited or no *a priori* knowledge, all parameters are supposed be considered as sensitive to experimental conditions and estimated in the first place. It is then possible to analyze the sensitivity of parameters and perform further investigations on the most sensitive ones.

10.3.2 System Identification

Two system identification algorithms were adopted in this thesis as tools for the model-based analysis. They were employed according to the hypothesis of the driver model for identification. For a linear time-invariant system, the PEM method was applied while the UKF method was chosen when considering linear time-variant assumptions. Their practical use to meet the need for our study was emphasized. Due to the stochastic nature of data and algorithms, it is necessary to examine the parameter uncertainties before comparing the identified parameter values, so as to ensure that the difference is significant statistically. For the UKF method, a tuning strategy and a multi-observator approach were proposed because a compromise between rapidity and noise sensitivity of estimation was inevitable. The configuration of the filter relies on *a prior* knowledge and assumptions about the dynamic of parameters to be identified, as discussed in Chapter 5. The application of multi-UKF in the identification of the internal model gain was successful. However, it is worth noting that the quality of estimated parameters also depends on the data. The weak identifiability issue was observed in the parameter identification in Chapter 5 and 9 when driving on straight lines or curves with constant curvature. For identifying a driver steering model, there must be a sufficiently informative excitation signal on the steering system of vehicle. This requirement demands intentional road design with bends of various length and curvature.

10.3.3 Driving Simulator

There are several advantages of using driving simulators compared to real vehicles for performing experiments. The most important one is the safety. Simulators can offer a virtual environment with potential dangerous driving tasks without actually putting drivers at risk [12]. The experiment in Chapter 7 with degraded visibility is an example. Another important benefit of using simulator is that currently there are seldom commercial vehicles including haptic guidance systems. It is more cost-effective and convenient to develop and implement haptic guidance systems using a driving simulator. Finally, simulators offer the possibility of manipulating almost every detail in the driving scenario and vehicle dynamics as well, and facilitate the acquisition of experimental data in a reproducible way.

There are also disadvantages with simulators. One problem is whether human drivers produce the same behavior when driving in simulators as in real vehicles or not. Low-

fidelity simulators may evoke unrealistic driving behavior and therefore produce invalid research outcomes[12]. When drivers realize that their behavior will not lead to fatal consequences, their concentration level and control accuracy may decrease. Simulators may also cause discomfort to human drivers. Nevertheless, these issues were seldom observed in our experiments because of the relatively simple driving task with respect to vehicle speed and road profile. The fixed-base driving simulator was able to provide high behavioral fidelity. In the scenarios with degraded visibility, almost all of the participants accomplished the experiments without leaving the lane or using emergency brake. Only one driver felt dizzy and abandoned the test due to 3D motion sickness and was excluded from the analysis. In the scenarios with haptic guidance at varying levels, all participants were able to cooperate with the system without evident conflicts on the steering wheel. Results of analysis demonstrated reasonable and realistic driving behavior as well.

10.4 Proposition of Future Works

The experimental investigations in this thesis could lead to future co-adaptation studies. The conclusions provide an idea how to improve the design of haptic guidance system in order to meet the common design guidelines for human-automation system and realize satisfactory interaction. For example, the driver steering model used in the current design of haptic guidance system was obtained from manual driving scenarios[7] (see [13]). This model could now be replaced by the adaptive driver model proposed. In that situation. on the one hand, human drivers will deliver less effort when they feel the haptic feedback on the steering wheel. On the other hand, the haptic guidance system will adjust the output torque by taking into consideration how much torque drivers will generate during cooperation. We define this process as “co-adaptation”, because both human driver and the system are trying to adapt to each other. Our hypothesis is that this process is iterative and in a short time human driver and the haptic guidance system will converge to a stable state, leading to a minimum of conflicts between the control effort from the two agents. Specifically, this state may correspond to a limit value of the internal model gain (with a small variance due to the human control). We further assumed that for different sharing levels, there is always such a stable state correspondingly. A function, or a mapping from sharing levels to internal model gains could be obtained through repeated experiments for a certain amount of sharing levels. In each experiment, the stable state could be found by designing the haptic guidance system and identifying the driver model repeatedly

until the identified parameter becomes invariant. We have obtained preliminary results in this direction. In the end, we imagine that this mapping could serve as an indispensable knowledge in the design of haptic guidance system so that the system can understand the intention of human driver. Therefore, the system can continuously follow the driver's behavior and realize perfect cooperation with human.

This thesis also offers a number of possible directions for researches on driver modeling. As stated in Chapter 8, the NMS in the proposed driver model chose to form a direct haptic feedback loop on the basis of torque difference measured by the force sensor in muscle, the Golgi tendon organs. However, as a position and velocity sensor, the muscle spindle can also initiate and regulate movements. In that case, it is the spinal reflex which forms a feedback path to allow closed loop control of the muscle's length. This path starts from the muscle spindle to the spinal cord and back to the muscle. Literature usually includes the spinal reflex in the NMS model[5], [7], [14], but it is worth noting that firstly, it is difficult to separate intrinsic mechanical responses of the limb and muscles from those generated by reflex feedback[5] and secondly, it demands a special measuring technique, the electromyography (EMG), and dedicated experimental scenarios to observe the spinal reflex characteristics. In our study, it was not possible to identify such a behavior. Our hypothesis is that the spinal reflex must be involved in the steering control of human driver. It is mainly activated when initializing a movement (a dynamic mode), while the direct haptic feedback loop takes charge afterwards for maintaining the gesture and rejecting disturbance (a static mode). Human driver could easily switch between these two modes, or mix them to generate force. In fact, during subsequent simulations of the proposed driver model, it has been observed that the introduction of a reflexive loop based on the angle and angular velocity difference as [5] can indeed reduce the standard deviation of lateral position. This phenomenon could be addressed in future studies to verify our hypothesis in order to further complete the model structure.

Finally, this thesis contributes to the development of new cybernetics theory in driver modeling. It demonstrated with the new driver model that, a linear time-variant driver steering model and a time-variant system identification algorithm were essential in the understanding of driver's transitional behavior. For the next step, the learning process could also be considered and modeled to investigate the learning-adaptation loop in human control.

10.5 References

[1] M. Mulder, D. M. Pool, D. A. Abbink, E. R. Boer, P. M. Zaal, F. M. Drop, K. Van Der El, and M. M. Van Paassen, "Manual Control Cybernetics: State-of-the-Art and Current Trends", *IEEE Transactions on Human-Machine Systems*, vol. 48, *5*, pp. 468–485, 2018, ISSN: 21682291.

[2] S. Y. De Nijs, M. Mulder, and D. A. Abbink, "The value of haptic feedback in lane keeping", *in Conference Proceedings - IEEE International Conference on Systems, Man and Cybernetics*, vol. 2014-Janua, Institute of Electrical and Electronics Engineers Inc., 2014, pp. 3599–3604.

[3] F. Mars, M. Deroo, and J.-M. Hoc, "Analysis of human-machine cooperation when driving with different degrees of haptic shared control", *IEEE Transactions on Haptics*, vol. 7, *3*, pp. 324–333, 2014, ISSN: 19391412.

[4] F. Mars and P. Chevrel, "Modelling human control of steering for the design of advanced driver assistance systems", *Annual Reviews in Control*, vol. 44, *Supplement C*, pp. 292–302, 2017, ISSN: 13675788.

[5] A. Pick, "Neuromuscular dynamics and the vehicle steering task", Ph.D. dissertation, University of Cambridge, 2004.

[6] C. Sentouh, P. Chevrel, F. Mars, and F. Claveau, "A sensorimotor driver model for steering control", *Conference Proceedings - IEEE International Conference on Systems, Man and Cybernetics*, *October*, pp. 2462–2467, 2009, ISSN: 1062922X.

[7] L. Saleh, P. Chevrel, F. Mars, J. F. Lafay, and F. Claveau, "Human-like cybernetic driver model for lane keeping", *in Proceedings of the 18th IFAC World Congress*, 2011, pp. 4368–4373, ISBN: 9783902661937.

[8] Z. Wang, T. Kaizuka, and K. Nakano, "Effect of Haptic Guidance Steering on Lane Following Performance by Taking Account of Driver Reliance on the Assistance System", *in Proceedings - 2018 IEEE International Conference on Systems, Man, and Cybernetics, SMC 2018*, 2018, ISBN: 9781538666500.

[9] F. Mars, M. Deroo, and C. Charron, "Driver adaptation to haptic shared control of the steering wheel", *in 2014 IEEE International Conference on Systems, Man, and Cybernetics (SMC)*, 2014, pp. 1505–1509.

[10] P. Hermannstädter and B. Yang, "Driver Distraction Assessment Using Driver Modeling", *in 2013 IEEE International Conference on Systems, Man, and Cybernetics*, Oct. 2013, pp. 3693–3698.

[11] A. Ameyoe, "Estimation de la distraction fondée sur un modèle dynamique de conducteur : principes et algorithmes", Theses, Ecole des Mines de Nantes, 2016.

[12] J. C. F. de Winter, P. M. van Leeuwen, and R. Happee, "Advantages and Disadvantages of Driving Simulators: A Discussion", *Proceedings of the Measuring Behavior Conference*, *January*, pp. 47–50, 2012.

[13] B. Pano, P. Chevrel, and F. Claveau, "Anticipatory and compensatory e-assistance for haptic shared control of the steering wheel", *2019 18th European Control Conference, ECC 2019*, pp. 724–731, 2019.

[14] E. De Vlugt, "Identification of Spinal Reflexes", Ph.D. dissertation, Delft University of Technology, 2004, ISBN: 9077595422.

UNIVERSITE BRETAGNE LOIRE / MATHSTIC

IMT Atlantique
Bretagne-Pays de la Loire
École Mines-Télécom

Titre : Modélisation cybernétique du conducteur pour la réalisation d'un contrôle haptique partagé du volant et l'adaptation du système homme-machine

Mot clés : Contrôle partagé, Adaptation, Modèle de conducteur, Identification.

Résumé : L'amélioration des systèmes d'assistance à la conduite (ADAS) des voitures passe par la minimisation des conflits entre conducteur et le système d'assistance. Le contrôle latéral partagé notamment, fait l'objet de nombreuses études ces dernières années. Il s'agit de partager l'action exercé sur le volant par voie haptique. La conception d'assistances évoluées de ce type suppose qu'un modèle dynamique du conducteur est disponible. Sur ce thème de la modélisation du conducteur, cette thèse s'attaque à comprendre et modéliser le processus d'adaptation réciproque du conducteur et de l'assistance au fil de l'usage. Au-delà de l'analyse comportementale souvent adoptée dans la littérature, l'utilisation de la théorie de l'estimation (identification, observateurs) et la mise en situation choisie de cohortes de conducteurs a permis d'enrichir les modèles de conducteur existants. Le comportement adaptatif du conducteur a pu être formalisé au travers de sa réaction haptique au couple produit sur le volant par l'assistance, mais aussi d'une évolution paramétrique de ce que nous avons convenu d'appeler son modèle interne. Les résultats obtenus montrent l'intérêt du modèle cybernétique proposé. Ils pourront à l'avenir être mis à profit pour le développement de nouveaux systèmes de contrôle latéral.

Title: Cybernetic driver modeling for the realization of haptic shared control and the adaptation of the human-machine system

Keywords: Haptic shared control, Adaptation, Driver steering model, System identification.

Abstract: Improving the advanced driver assistance systems (ADAS) involves minimizing conflicts between the driver and the system. The shared lateral control has been the subject of numerous studies in recent years. It refers to sharing the action exerted on the steering wheel through haptics. The design of such advanced assistances assumes that a dynamic driver model is available. Around this theme of driver modeling, this thesis focuses on understanding and modeling the process of reciprocal adaptation of the driver and the assistance through usage. Beyond the behavioral analysis often adopted in the literature, the implementation of estimation theory (identification, observers) and chosen scenario with cohorts of drivers made it possible to enrich the existing driver models. The drivers' adaptive behavior has been formalized not only through their haptic reaction to the torque produced on the steering wheel by the assistance, but also through a parametric evolution of what we called "internal model". The results obtained show the interest of the proposed cybernetic model. They can be used in the future for the development of new lateral control systems.